Supporting Information

Targeting the Hemopexin Domain of proMMP-9 with a Small Molecule Inhibitor Prevents Formation of Focal Adhesion Junctions

Vincent M. Alford,[1,3] Anushree Kamath,[2] Xiaodong Ren,[2] Kunal Kumar,[2] Qianwen Gan,[2] Monaf Awwa,[2] Michael Tong,[1] Markus A. Seeliger,[1,4] Jian Cao,[3] Iwao Ojima,[2,4] Nicole S. Sampson [2,4*]

[1]*Department of Molecular and Cellular Pharmacology, Stony Brook University, Stony Brook, NY, USA*
[2]*Department of Chemistry, Stony Brook University, Stony Brook, NY, USA*
[3]*Department of Medicine, Stony Brook University, Stony Brook, NY, USA*
[4]*Institute of Chemical Biology & Drug Discovery, Stony Brook, NY, USA*

Table of Contents

EXPERIMENTAL METHODS

Saturated Transfer Difference NMR. Saturation transfer difference (STD) experiments were acquired on a Bruker Avance III 700 MHz spectrometer equipped with a TCI cryoprobe. NMR samples were prepared in buffer containing: 20 mM Tris pH 8, 300 mM NaCl, 10 mM $CaCl_2$, 7 % DMSO-d6, and 10% D_2O. The ratio of Compound **3c**:MMP2 and/or :MMP9 was 38:1 (300 μM:8 μM). Spectra were collected at 4 °C to ensure sample stability throughout acquisition. Data were acquired in an interleaved manner using 128 scans in total, with a spectral width of 13.9 ppm, 32K data points, and 3 s relaxation delay. A 50 ms gaussian-shaped pulse was used for selective saturation, with 1 ms delay between the pulses. This pulse was applied for a total saturation time of 2.5 s. An attenuation of 40-dB was used for the selective saturation pulse. The proteins were irradiated with on and off resonance frequencies that were set to 783.26 Hz (1.12ppm), and -50000.00 Hz (-71.43 ppm) respectively, and the spin-lock time was set to 80 ms. The standard Bruker pulse sequence stddiffesgp.3 was implemented for STD experiments and uses excitation sculpting for water suppression. All spectra were processed using topspin.

Cellular Adhesion Assay. Collagen type I (3 mg/mL; BD Bioscience Discovery Labware) and fibronectin (1 mg/mL; Sigma-Aldrich) stock solutions were diluted in 1X PBS (pH 7.4) to a desired working concentration of 5 μg/mL. 96-welled plated were coated with 50 μL of each respective working stock solution of substrate overnight at 4 °C. The next day the excess substrate was removed by inverting the multiwall plate over a plastic reservoir and tapping gently. Wells were washed 3 times with cold 1X PBS and the 96-welled plate was inverted to remove liquid contents between each wash. HT1080 fibrosarcoma cells were then pre-treated in various conditions (DMSO (0.1% final), 50 μM **1f**, 50 μM **1a**, 50 μM **3c**, 80 nM Marimastat) for 30 min at 37 °C before being seeded at a density of 15,000 cells/100 μL complete DMEM medium per well. Cells were allowed to adhere and attach to either substrate under the various treatment conditions for 30 min at 37 °C. After the 30 min time allotment, the 96-well plate was inverted to remove DMEM media containing cells unable to adhere to the substrate-coated surface and wells were again washed 3 times with cold PBS before being fixed in 4% paraformaldehyde/PBS for 30 min at room temperature. Cell nuclei were then stained with DAPI nuclear dye (1:2000; Invitrogen) before 4x images were captured of each well containing a different substrate/treatment combination using a Nikon Eclipse TE2000-S (Tokyo, Japan) equipped with a Sutter Instruments SmartShutter System (Novato, CA) and a QiClick QImaging camera (Surrey, BC, Canada). Images were quantified for the number of cells attached by counting individual nuclei using automated computer software included in the Nikon Elements Basic Research Software analysis tools.

Supplemental Table 1. PEX-9 Inhibitor Structures and in vivo Efficacy

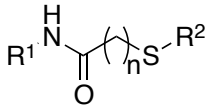

Inhibitor	R^1	n	R^2	cLogP	Kd (μM)	% Inhibition of proMMP9-Mediated Migration at 50 μM
1a	4-difluoromethoxyphenyl	1	4-oxo-6-propyl-1,4-dihydropyrimidin-2-yl	3.1 ± 0.7	1.3 ± 0.3	51 ± 2
1b	phenyl	1	4-oxo-6-propyl-1,4-dihydropyrimidin-2-yl	3.0 ± 0.7	4.5 ± 0.6	12 ± 3
1c	4-fluorophenyl	1	4-oxo-6-propyl-1,4-dihydropyrimidin-2-yl	3.3 ± 0.7	3.8 ± 0.6	29 ± 4
1d	benzimidazol-2-yl	1	4-oxo-6-propyl-1,4-dihydropyrimidin-2-yl	2.9 ± 0.7	1.2 ± 0.2	61 ± 2
1f	phenyl-(N-Me)	1	4-oxo-6-propyl-1,4-dihydropyrimidin-2-yl	2.2 ± 0.6	N/A	2 ± 6
2a	4-difluoromethoxyphenyl	3	4-oxo-6-propyl-1,4-dihydropyrimidin-2-yl	4.0 ± 0.7	1.0 ± 0.2	63 ± 4
2c	4-fluorophenyl	3	4-oxo-6-propyl-1,4-dihydropyrimidin-2-yl	3.7 ± 0.7	0.91 ± 0.1	68 ± 3
3a	4-difluoromethoxyphenyl	3	5,6,7,8-tetrahydro-4(1H)-quinazolinon-2-yl	3.5 ± 0.7	0.6 ± 0.1	74 ± 2
3b	phenyl	3	5,6,7,8-tetrahydro-4(1H)-quinazolinon-2-yl	3.3 ± 0.6	0.5 ± 0.1	76 ± 1
3c	4-fluorophenyl	3	5,6,7,8-tetrahydro-4(1H)-quinazolinon-2-yl	3.7 ± 0.7	0.32 ± 0.05	90 ± 2
3d	benzimidazol-2-yl	3	5,6,7,8-tetrahydro-4(1H)-quinazolinon-2-yl	3.2 ± 0.7	0.5 ± 0.2	77 ± 2
4a	4-difluoromethoxyphenyl	3	4-quinazolinon-2-yl	3.3 ± 0.7	0.5 ± 0.1	78 ± 3
4b	phenyl	3	4-quinazolinon-2-yl	3.1 ± 0.6	0.8 ± 0.1	64 ± 4
4c	4-fluorophenyl	3	4-quinazolinon-2-yl	3.5 ± 0.7	0.64 ± 0.06	73 ± 2
4d	benzimidazol-2-yl	3	4-quinazolinon-2-yl	3.1 ± 0.7	0.3 ± 0.1	81 ± 3
4e	*n*-hexyl	3	4-quinazolinon-2-yl	3.1 ± 0.7	0.9 ± 0.3	56 ± 1

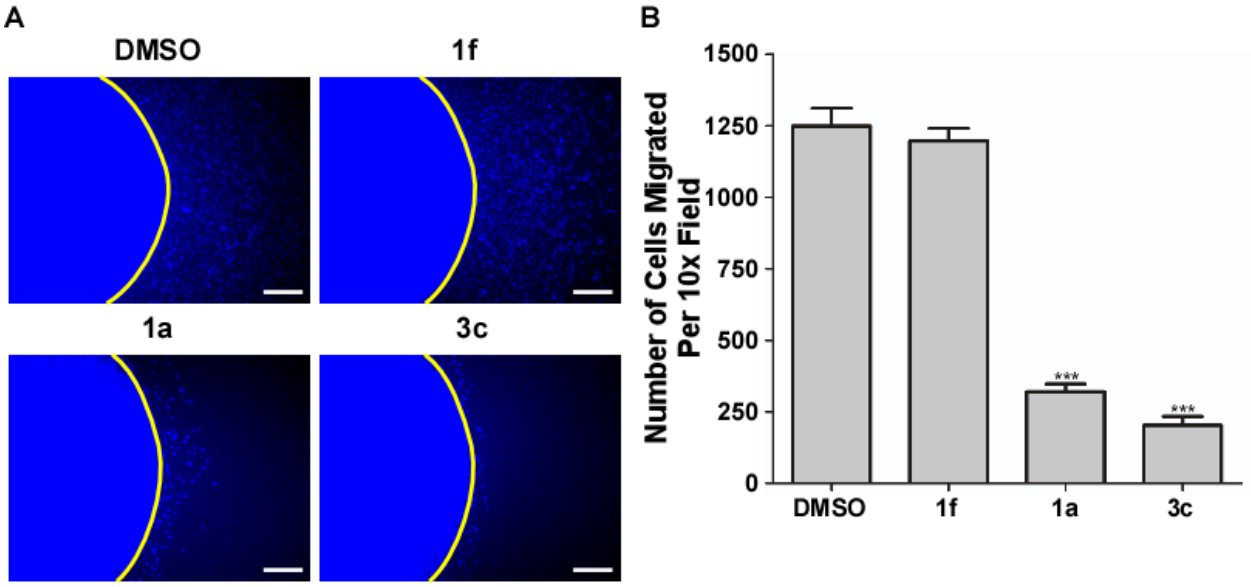

Supplemental Figure 1. Treatment with compound **3c** inhibits migration in endogenous MMP-9 expressing cells. (A) Representative 10x magnification DAPI images of HT1080 cells in a two-dimensional migration assay after treatment with 50 µM of compound **1a**, **1f**, or **3c** and (B) Quantitative analysis of the number of migrated cells per treatment condition. Scale bar = 250 µm.

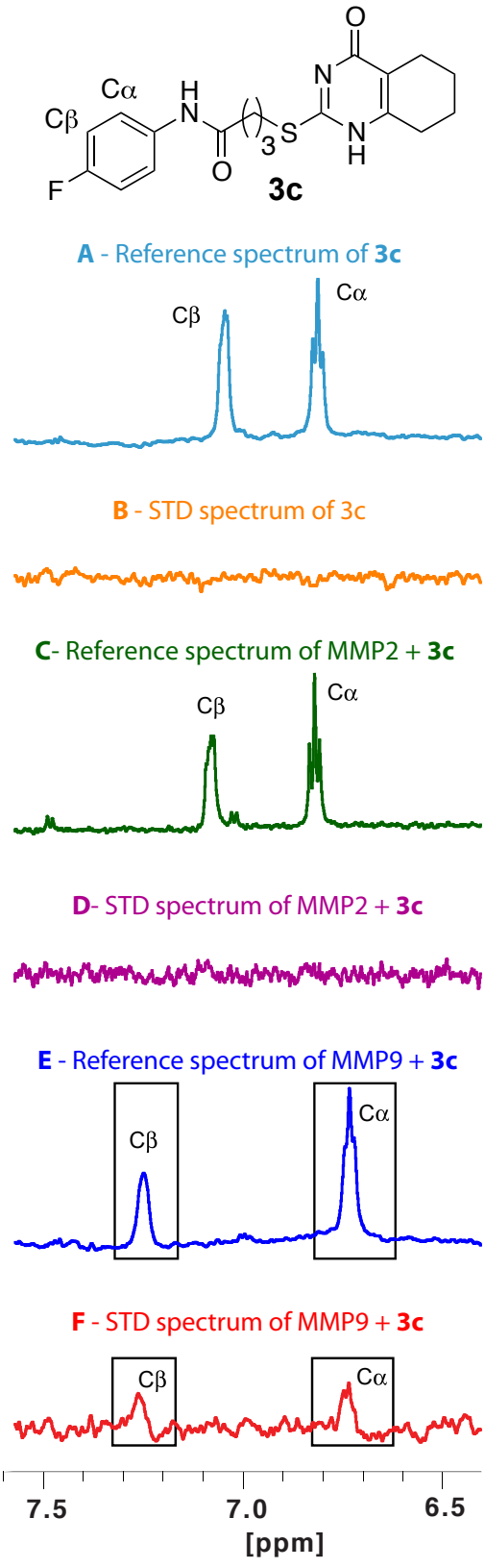

Supplemental Figure 2. Compound **3c** binds specifically to target protein proMMP-9. A 1D STD ^{1}H NMR experiment was performed with 300 µM compound **3c** and 8 µM protein. A) Reference ^{1}H NMR spectrum of **3c**. B) STD control spectrum of **3c** with selective saturation at 1.12 ppm. C) Reference ^{1}H NMR spectrum of **3c** and proMMP-2. D) STD NMR spectrum of **3c** and proMMP-2 with selective saturation at 1.12 ppm. E) Reference ^{1}H NMR spectrum of **3c** and proMMP-9. F) STD NMR spectrum of **3c** and proMMP-9 with selective saturation at 1.12 ppm.

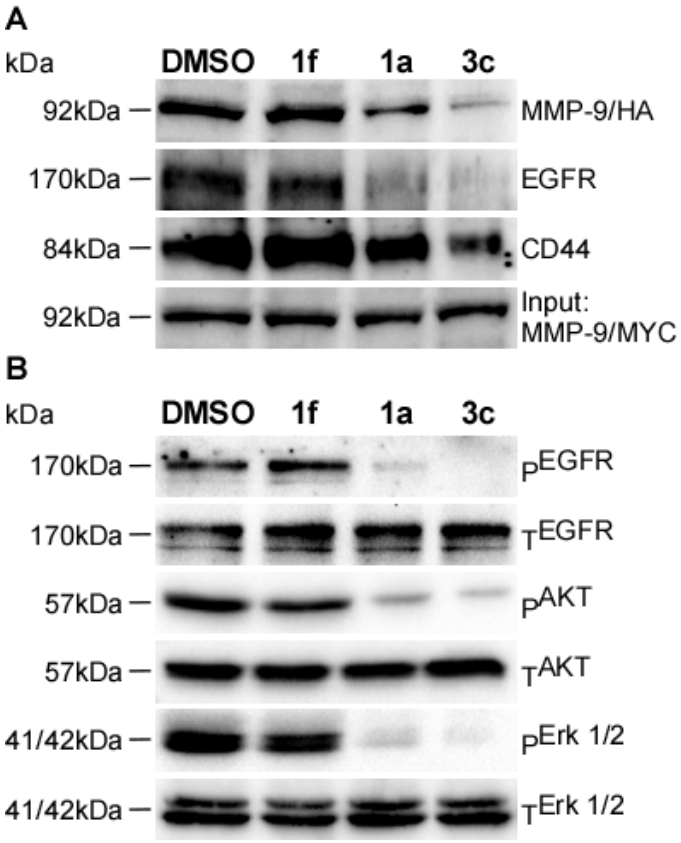

Supplemental Figure 3. Treatment with PEX-9 inhibitor prevents MMP-9 homodimerization and results in decreased EGFR-CD44 downstream signaling. (A) HT1080 cells co-transfected with MMP-9/MYC and MMP-9/HA cDNAs were treated with 50 μM of either compound **1a**, **1f**, or **3c**, the cells lysed and an anti-Myc (MMP-9) antibody used for immunoprecipitation. The precipitates were analyzed with an anti-HA (MMP-9), anti-EGFR or anti-CD44 antibody in the immunoblot. (B) The same cells as in (A) were treated with 50 μM of either compound **1a**, **1f**, or **3c**, the cells lysed and an anti-Myc (MMP-9) antibody used for immunoprecipitation. The precipitates were analyzed with antibody to the indicated antigen in the immunoblot.

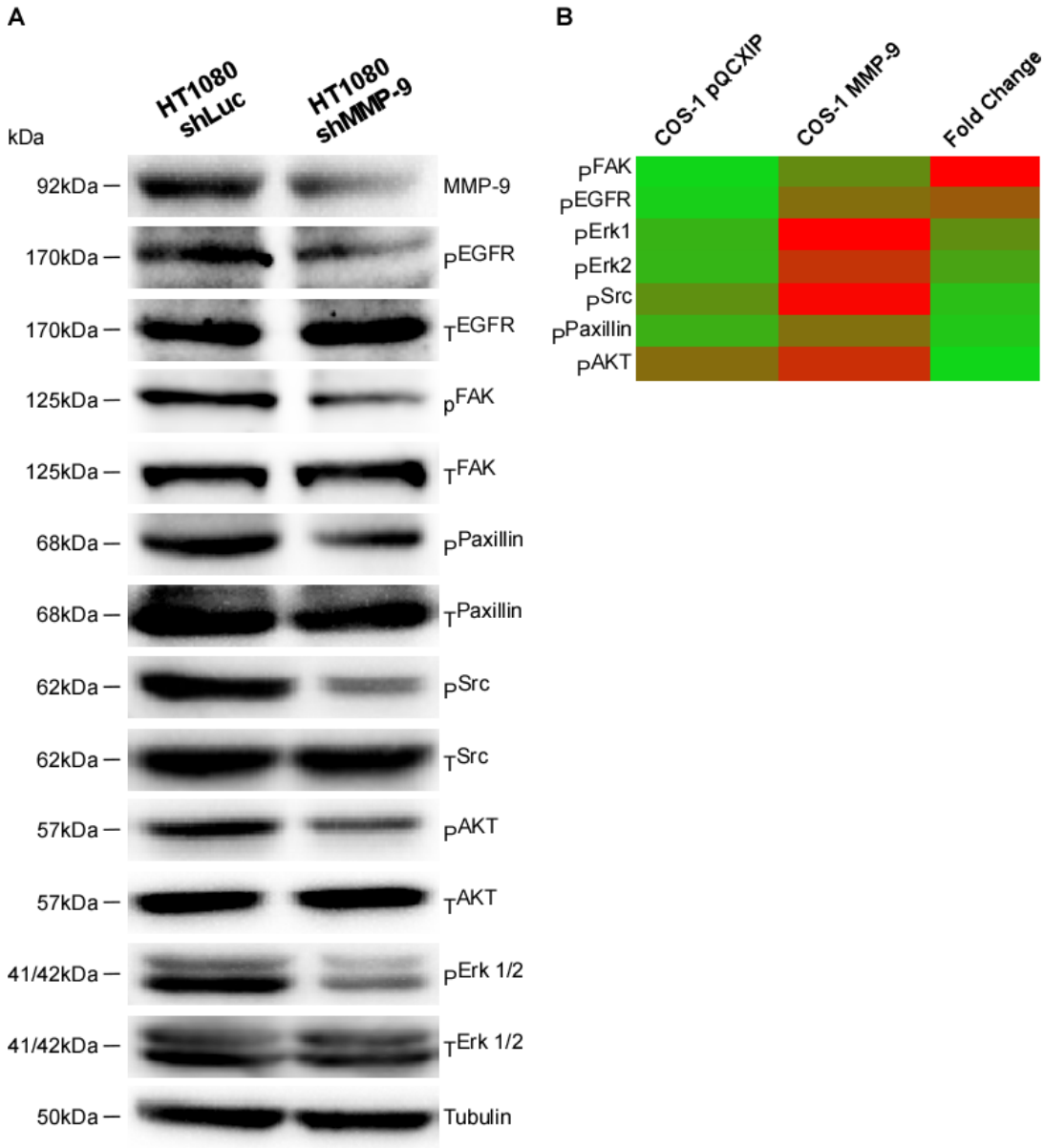

Supplemental Figure 4. proMMP-9 expression coincides with activation of both EGFR-CD44 and α4β1 integrin downstream signaling cascades. (A) HT1080 cells were transiently transfected with either shControl or shMMP-9 cDNA vectors. Cells were then lysed, and the lysates analyzed on an immunoblot which probed downstream targets involved in proMMP9-mediated migration. (B) Heatmap depicting protein levels in COS-1 cells engineered to stably express either vector control or proMMP-9 cDNAs using an antibody microarray and protein phosphorylation assay (KinexTM Antibody Microarray KAM-1.2 and Phospho-Site 1.3 Kinetworks Screen). Increased protein phosphorylation (red); decreased or baseline protein phosphorylation (green).

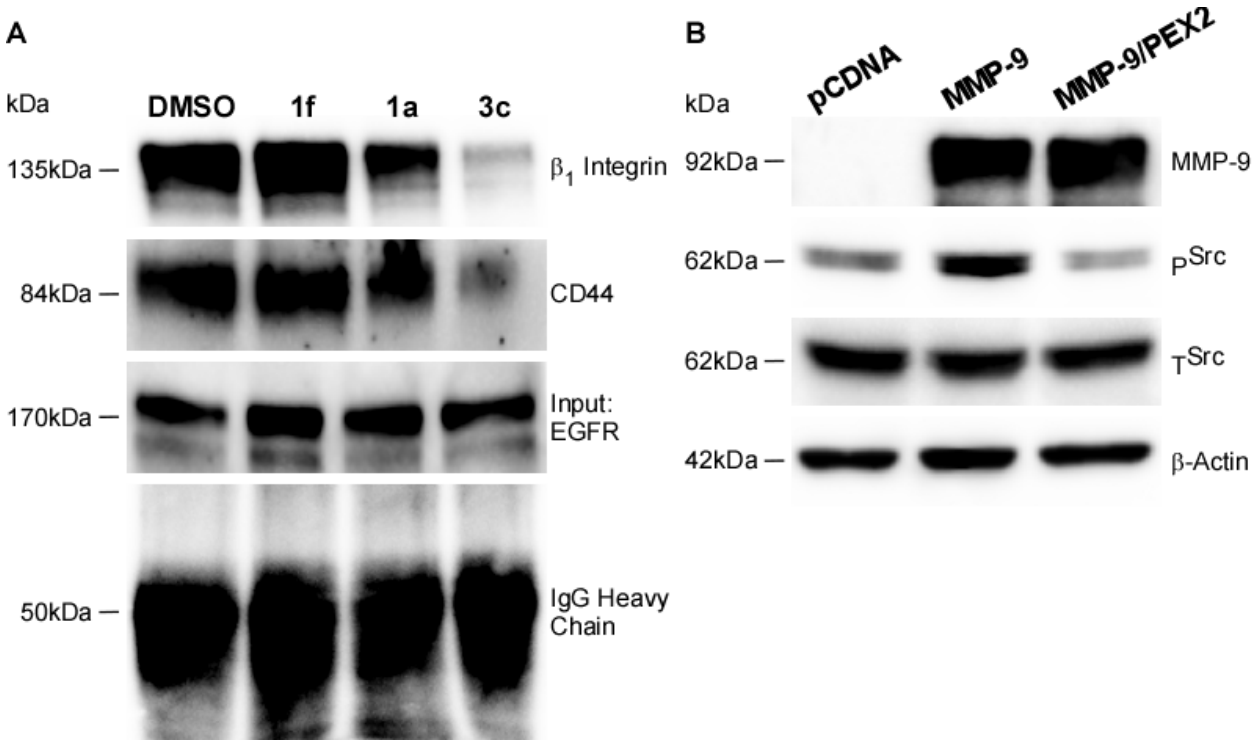

Supplemental Figure 5. proMMP-9 is a scaffold for focal adhesion induced Src signaling (A) Treatment with PEX-9 inhibitor results in decreased β1 integrin-EGFR-CD44 interaction at the cell surface. HT1080 cells were treated with 50 μM of either compound **1a**, **1f**, or **3c**, the cells lysed and an anti-EGFR antibody used for immunoprecipitation. The precipitates were analyzed with antibody to the indicated antigen in the immunoblot. (B) proMMP-9 is required for Src phosphorylation. non-MMP-9 expressing MCF-7 breast cancer cells were transiently transfected with either vector control, proMMP-9, or chimera proMMP-9/MMP-2PEX cDNAs. The cells were lysed and probed for p-SrcTyr418 by immunoblot.

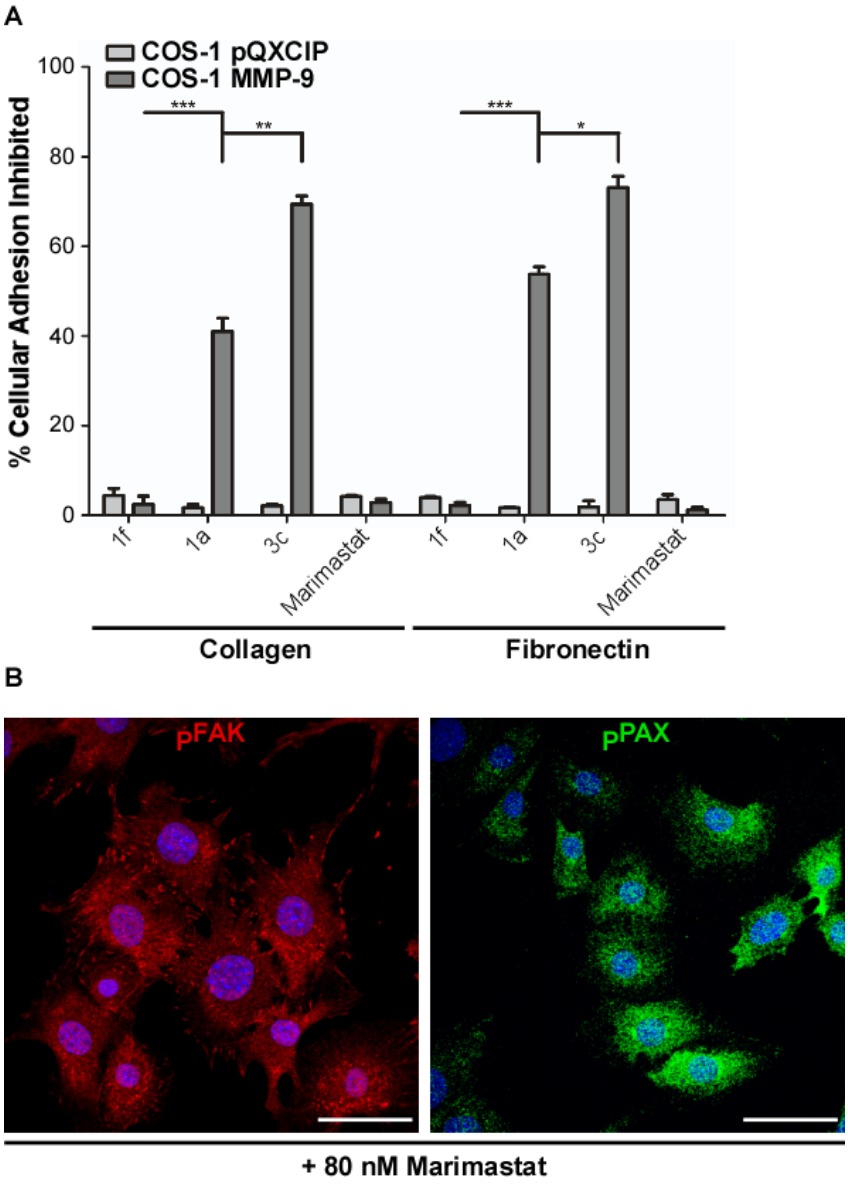

Supplemental Figure 6. proMMP9-mediated adhesion is independent of catalytic activity. (A) COS-1 cells engineered to overexpress either vector control or proMMP-9 cDNAs were seeded into individual wells (96-welled plate) coated with various ECM substrates (collagen or fibronectin) in addition to being treated with either a PEX-9 inhibitor (50 μM) or broad-spectrum MMP catalytic inhibitor Marimastat (80 nM). Cells were incubated for 30 min at 37 °C. After washing, attached cells were then fixed with a 4% paraformaldehyde/PBS solution and stained with DAPI nuclear dye. The number of adherent cells were quantified for each condition using nuclear staining and normalized to control cells treated with DMSO. (B) Immunofluorescence against p-FAKTyr 576/577 (red) and p-PAXTyr118 (green) was performed with HT1080 cells after treatment with Marimastat (80 nM). 60x magnification. Scale bars = 100 μm.

^{1}H NMR of compound 1a

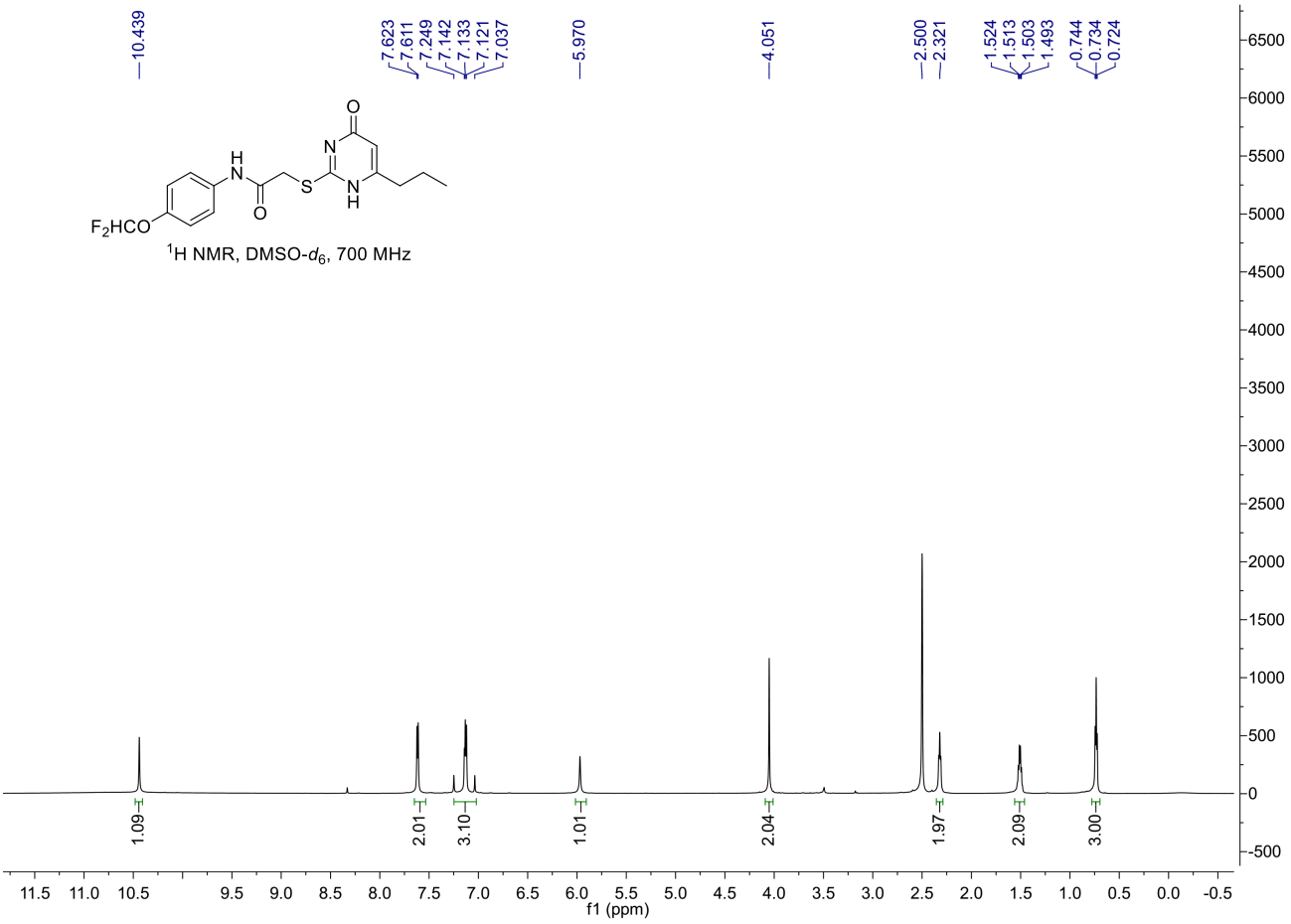

^{13}C NMR of compound 1a

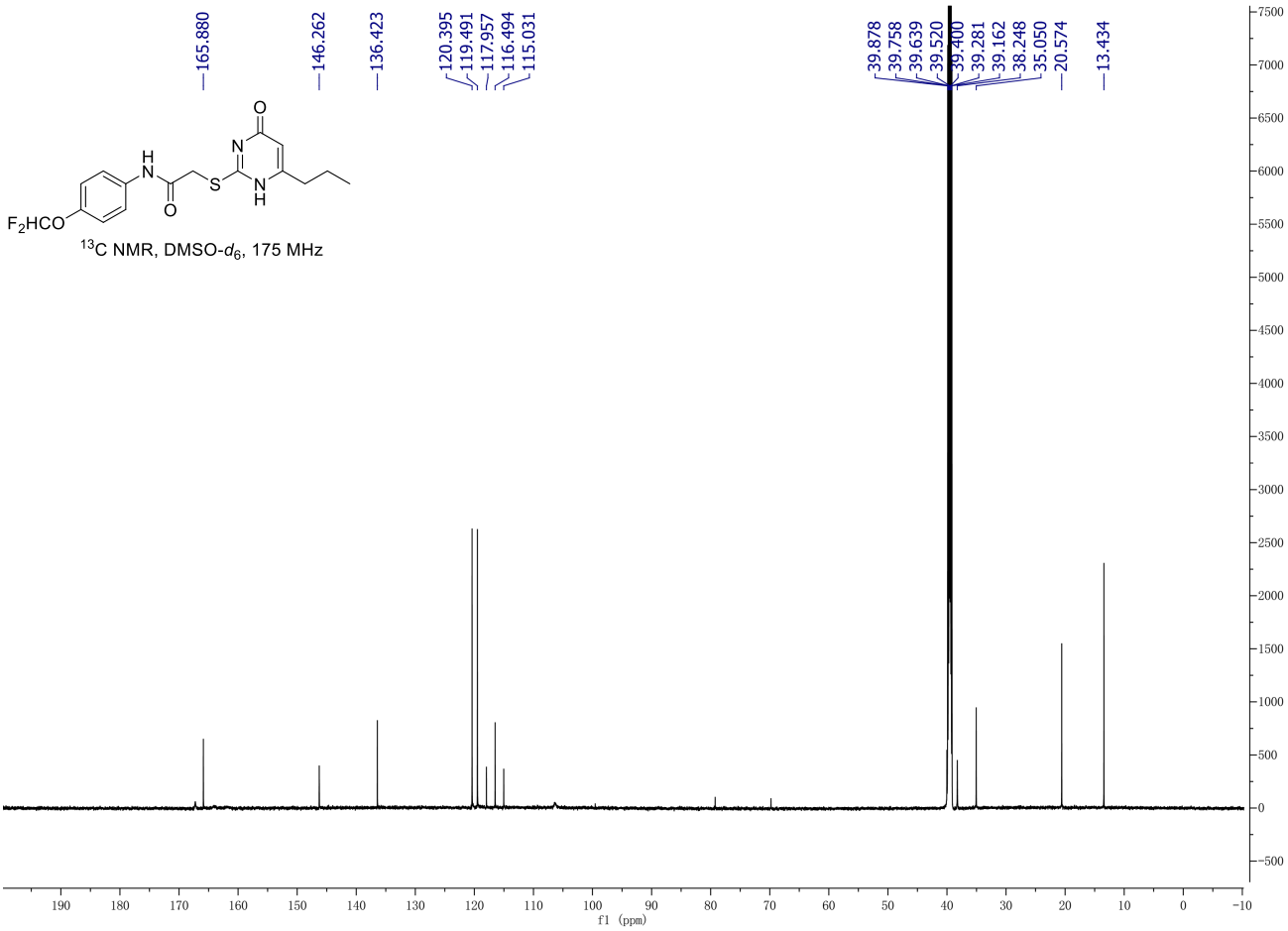

^{19}F NMR of compound 1a

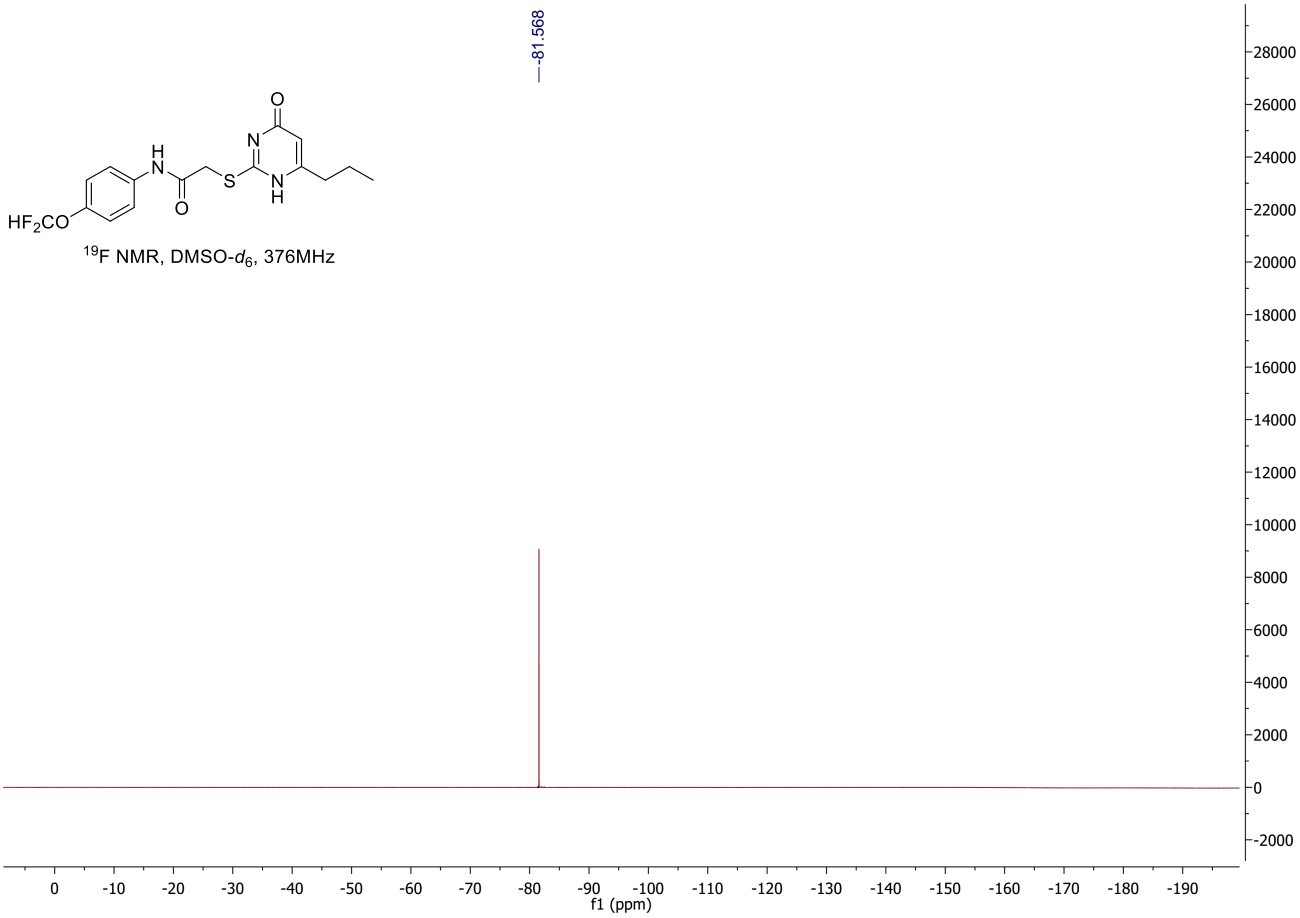

^{1}H NMR of compound 1b

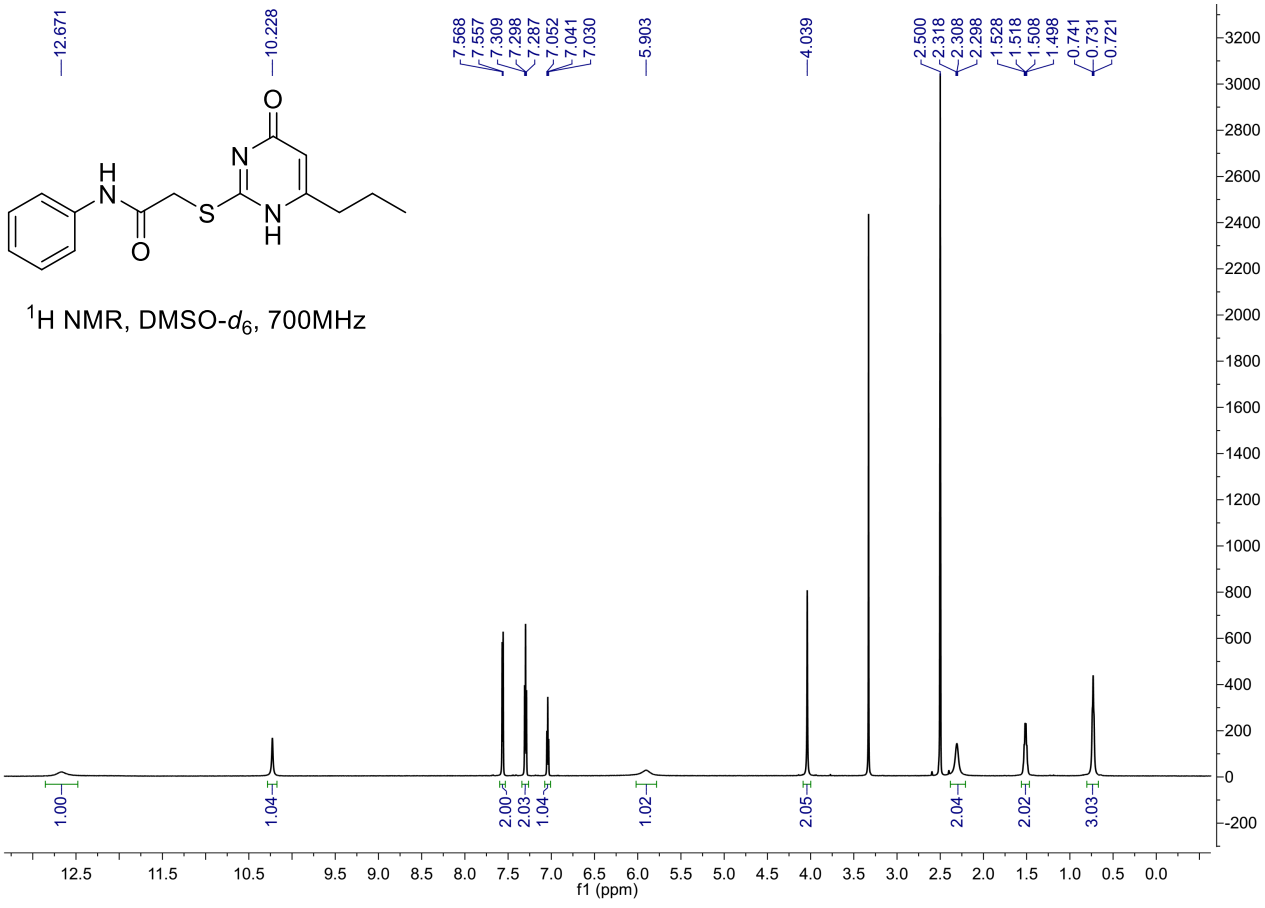

^{13}C NMR of compound 1b

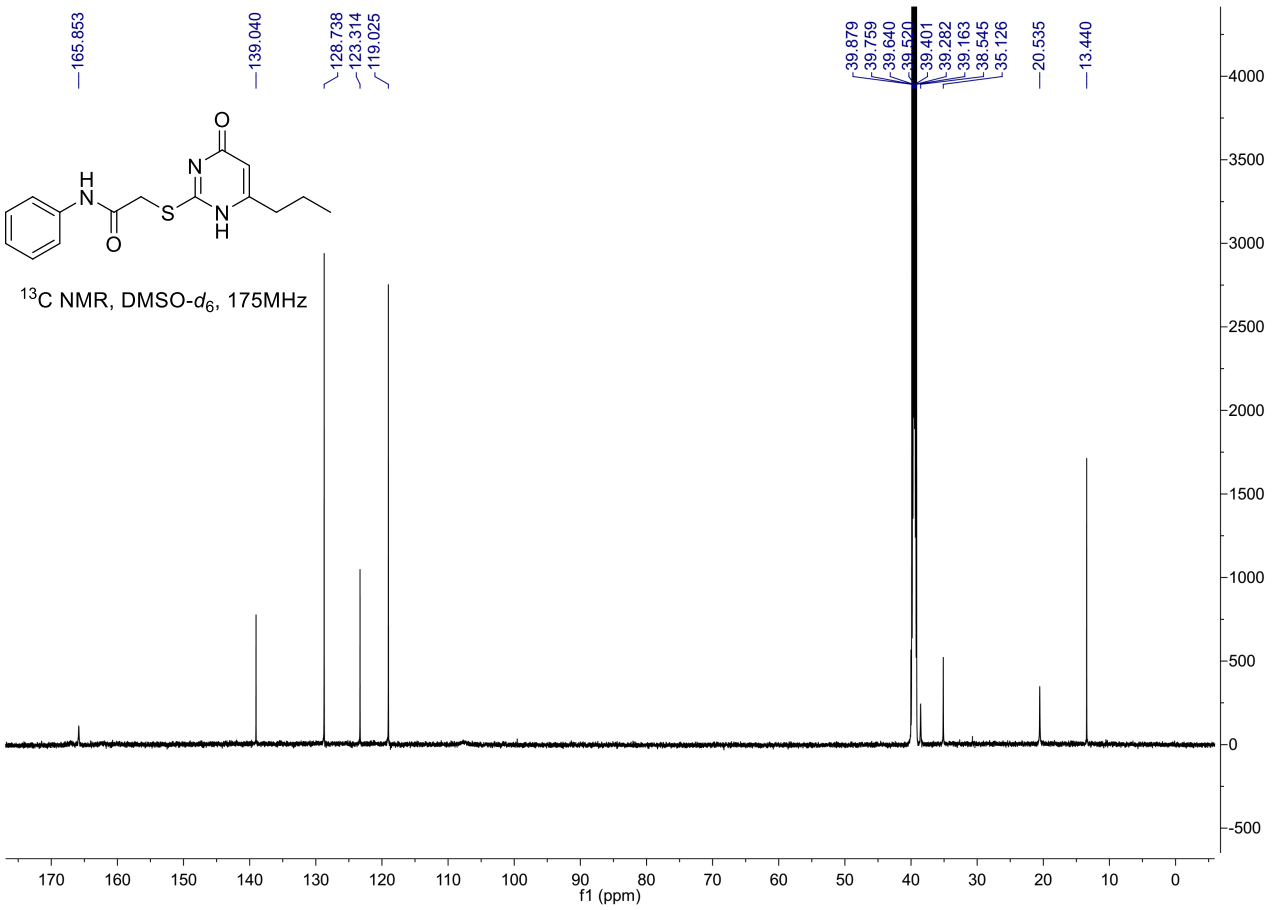

^{1}H NMR of compound 1c

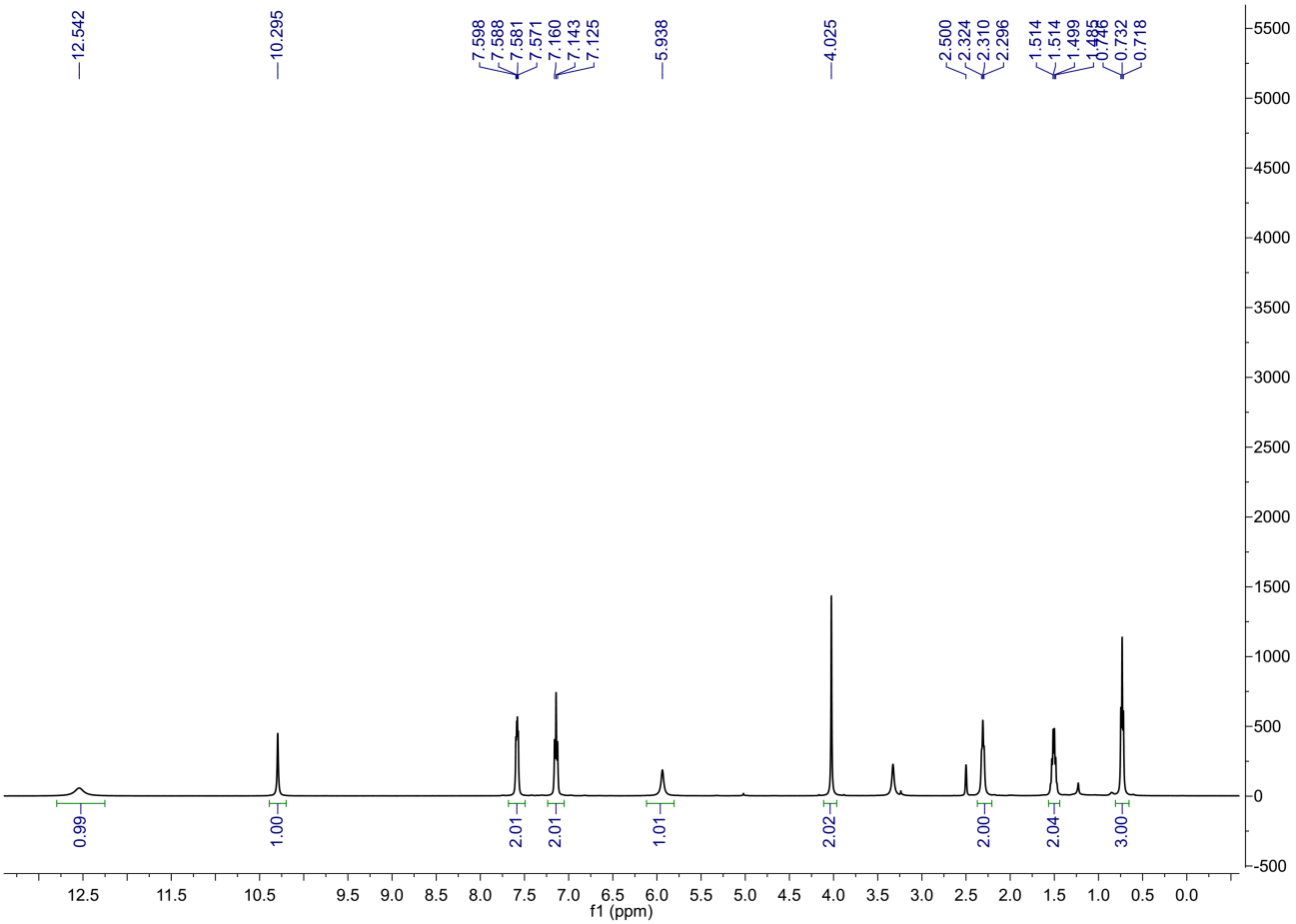

^{13}C NMR of compound 1c

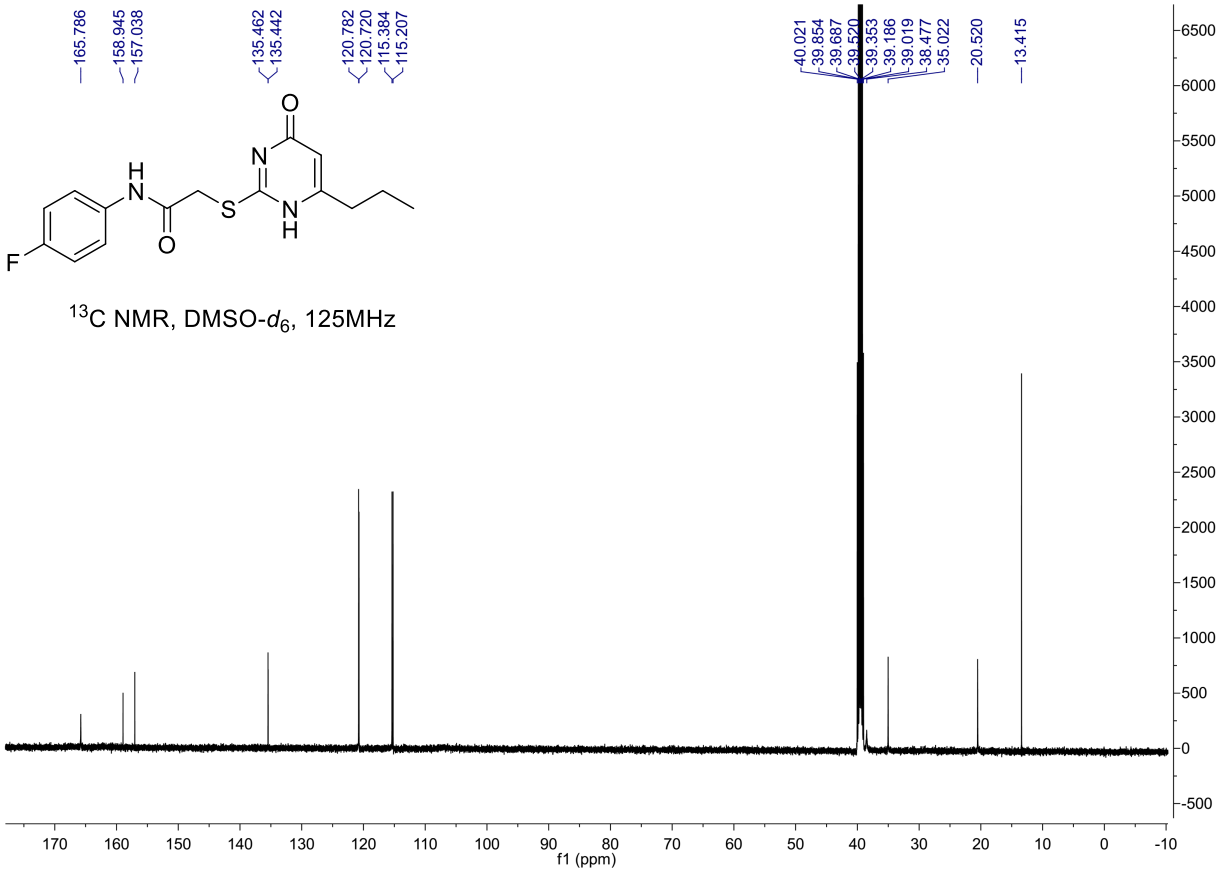

^{13}C NMR, DMSO-d_6, 125MHz

^{19}F NMR of compound 1c

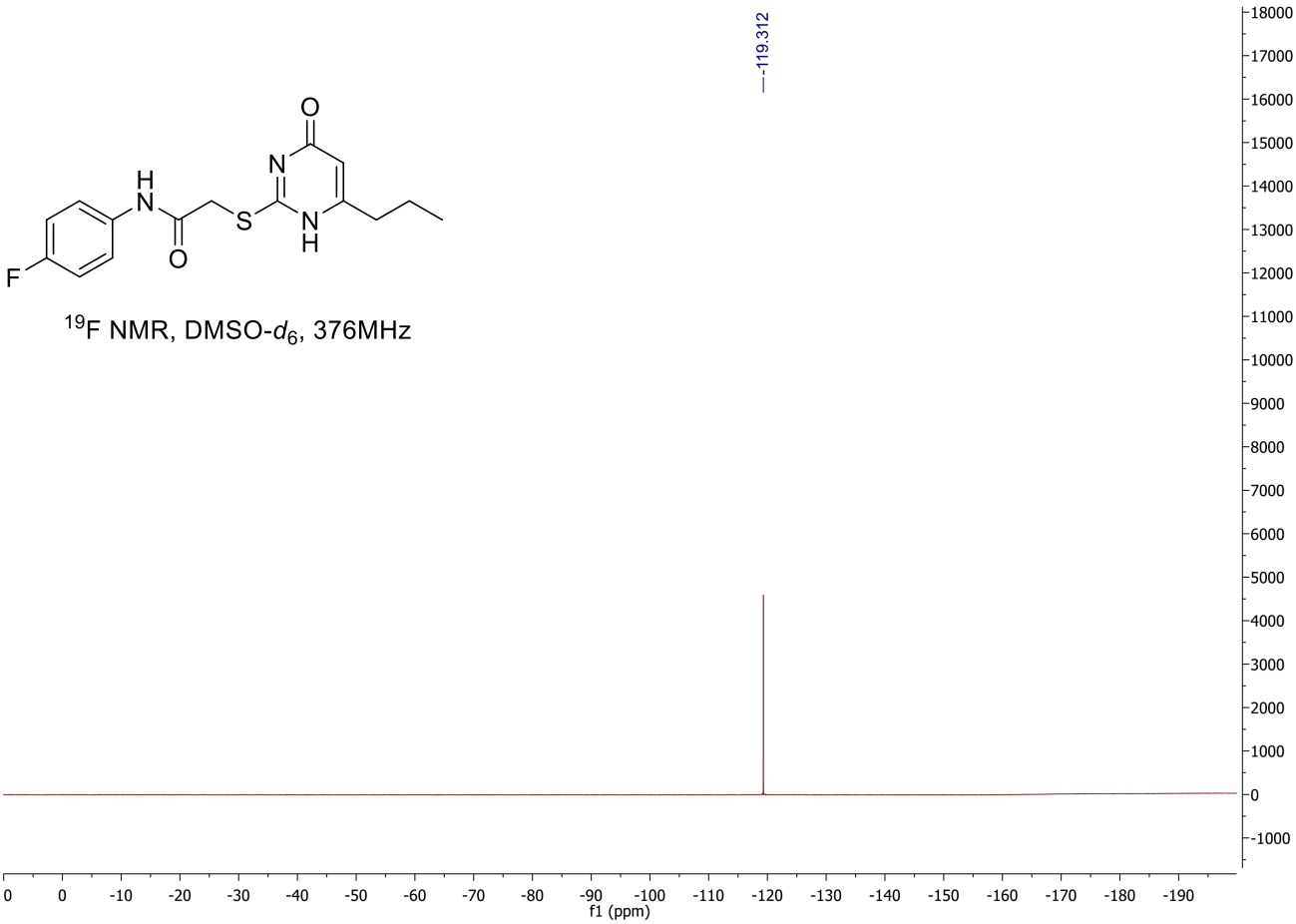

^{19}F NMR, DMSO-d_6, 376MHz

^{1}H NMR of ethyl 2-(4-oxo-6-propyl-1,4-dihydropyrimidin-2-ylthio)acetate

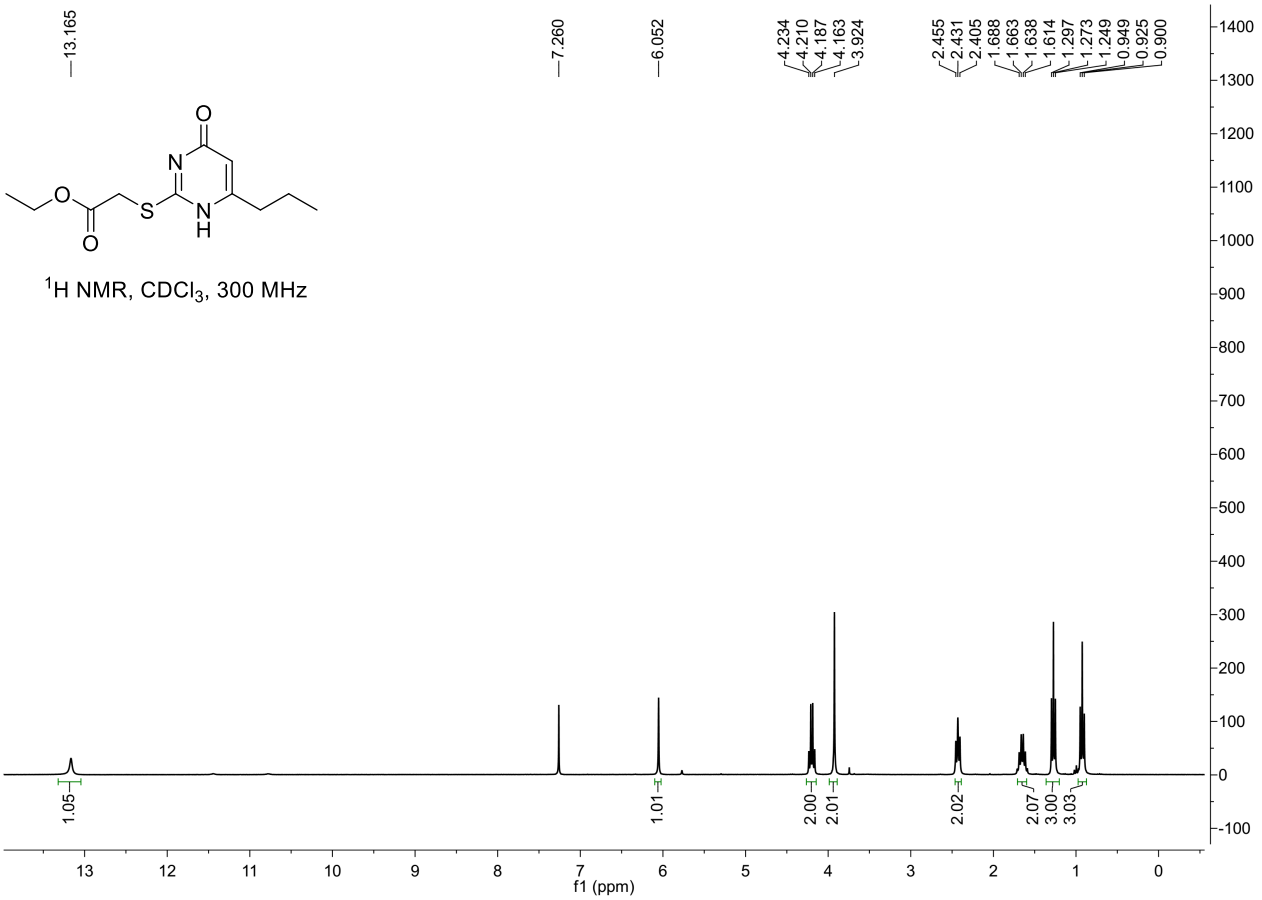

^{1}H NMR, $CDCl_3$, 300 MHz

^{13}C NMR of ethyl 2-(4-oxo-6-propyl-1,4-dihydropyrimidin-2-ylthio)acetate

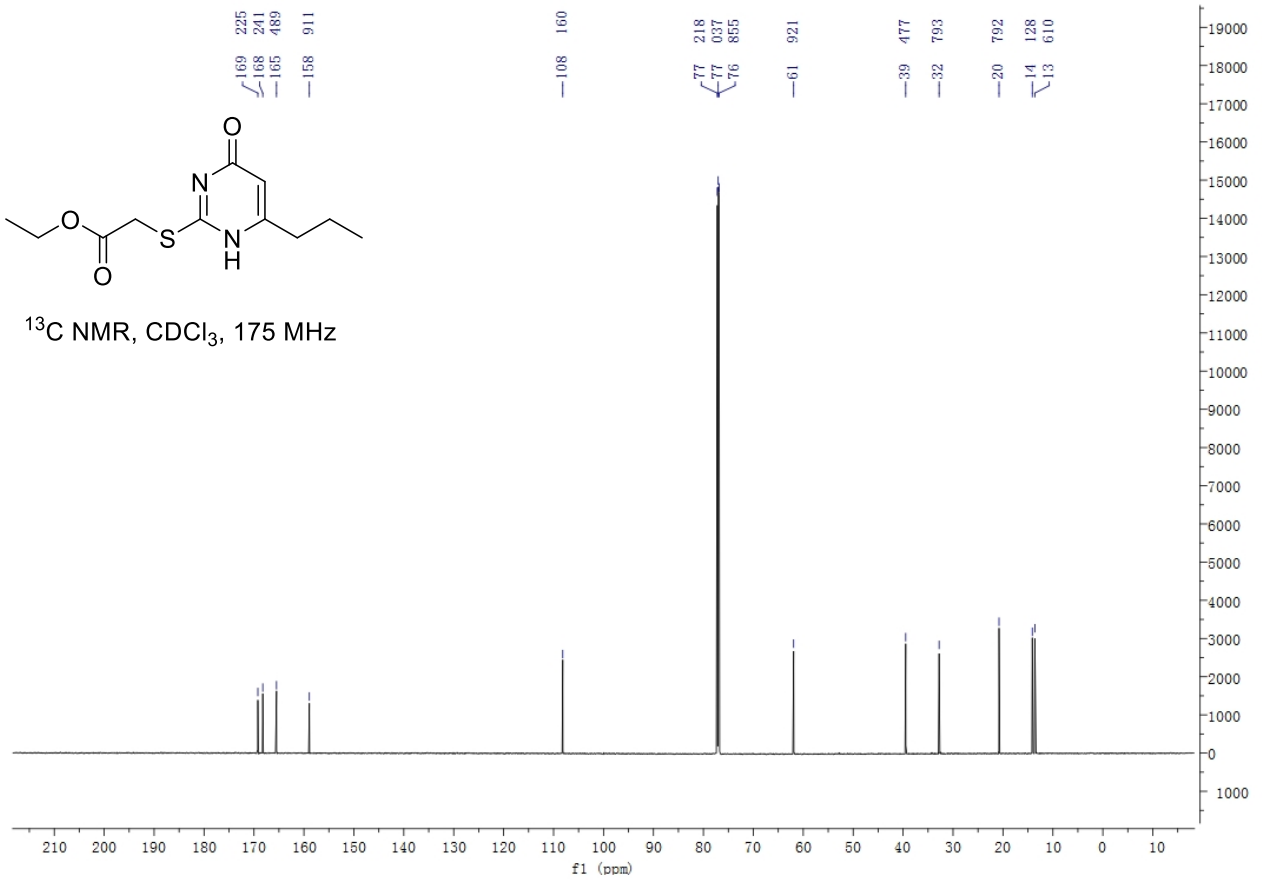

^{13}C NMR, $CDCl_3$, 175 MHz

^{1}H NMR of compound 8

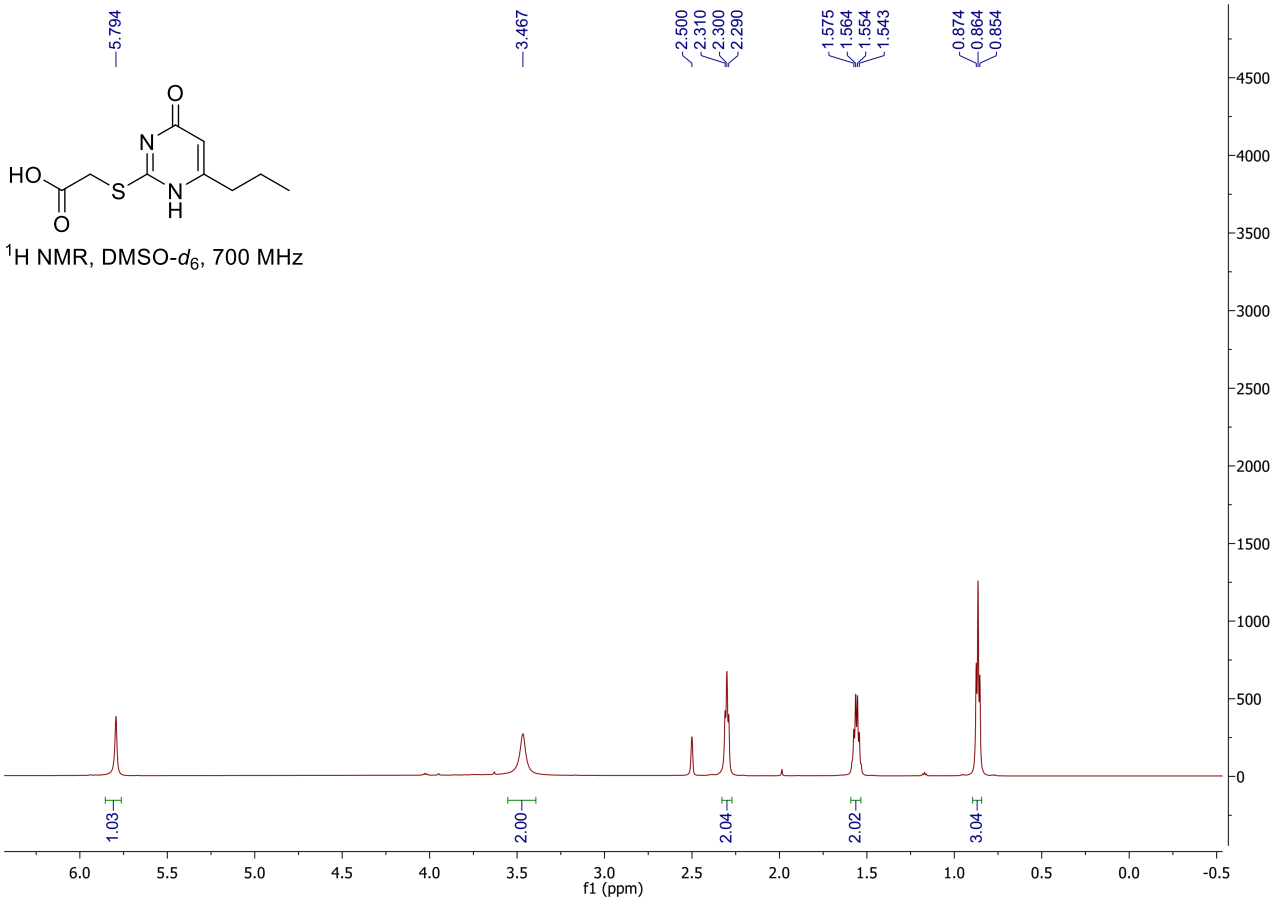

^{1}H NMR, DMSO-d_6, 700 MHz

^{13}C NMR of compound 8

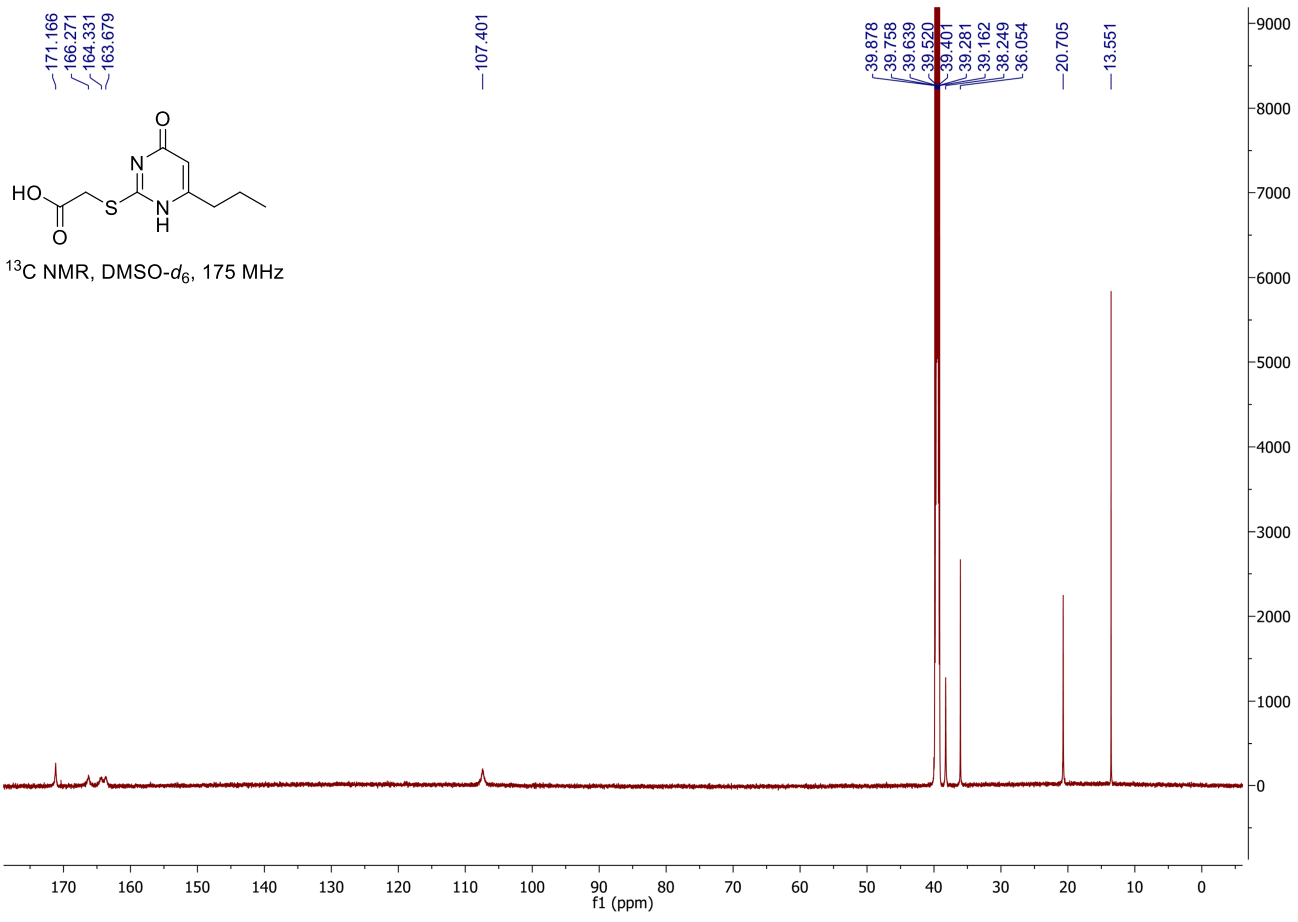

^{13}C NMR, DMSO-d_6, 175 MHz

^{1}H NMR of compound 1d

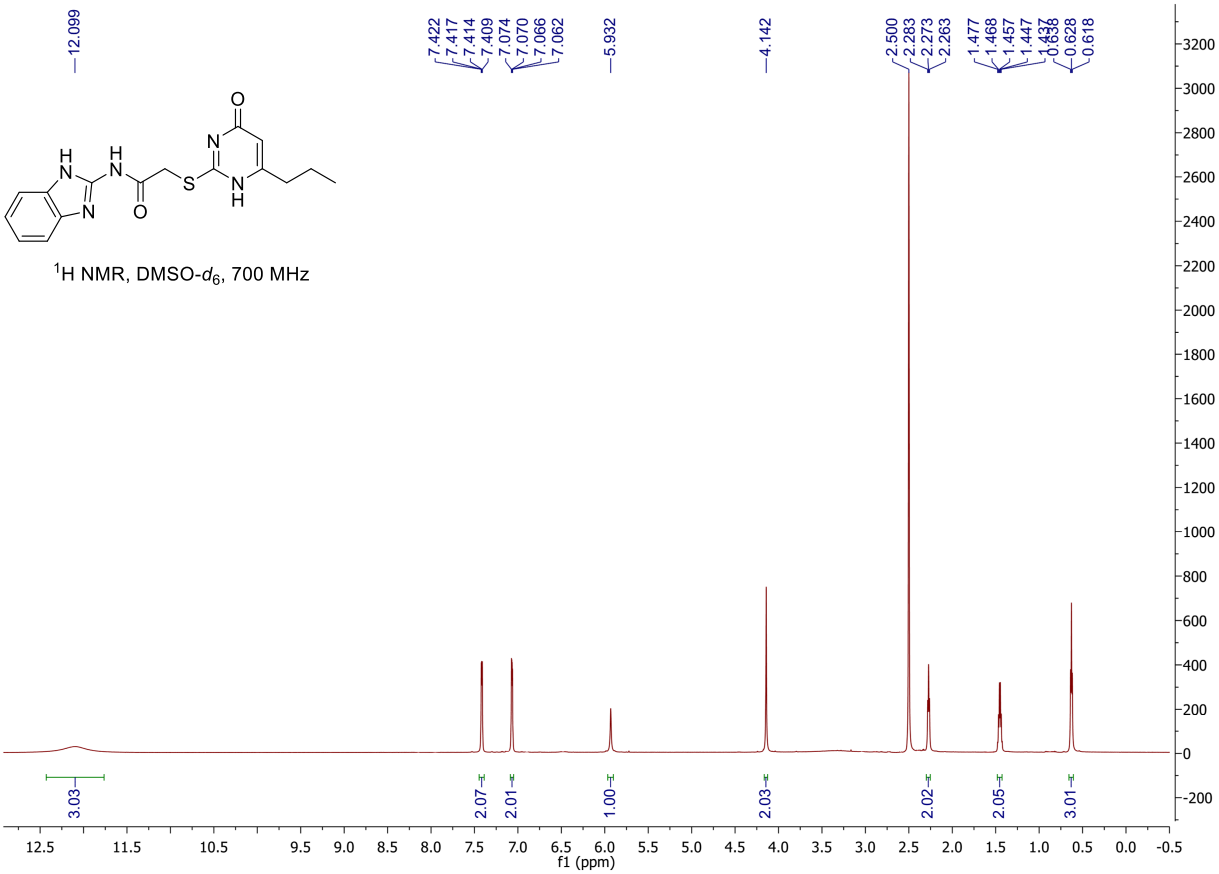

^{1}H NMR, DMSO-d_6, 700 MHz

^{13}C NMR of compound 1d

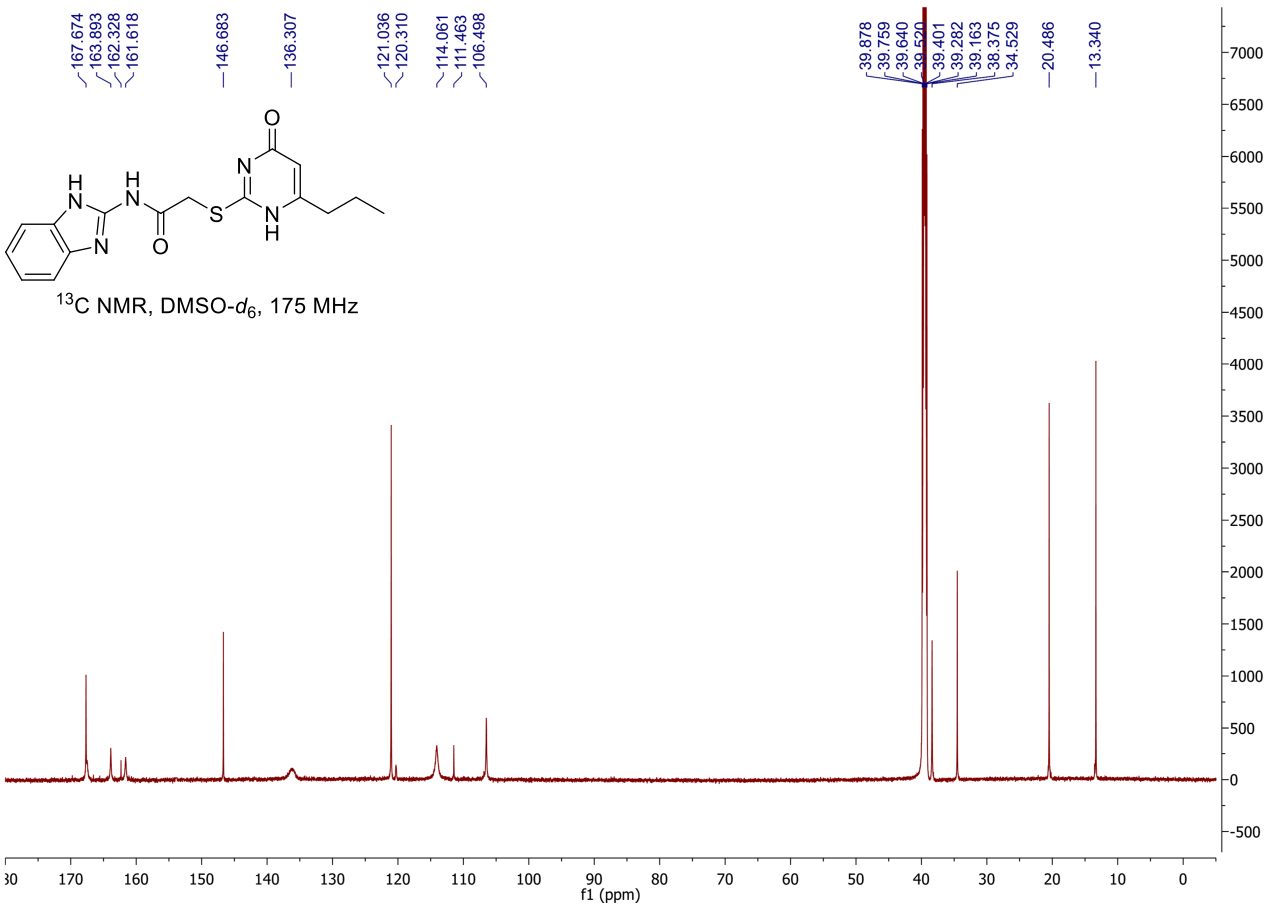

^{13}C NMR, DMSO-d_6, 175 MHz

^{1}H NMR of compound methyl 4-(4-oxo-6-propyl-1,4-dihydropyrimidin-2-ylthio)butanoate

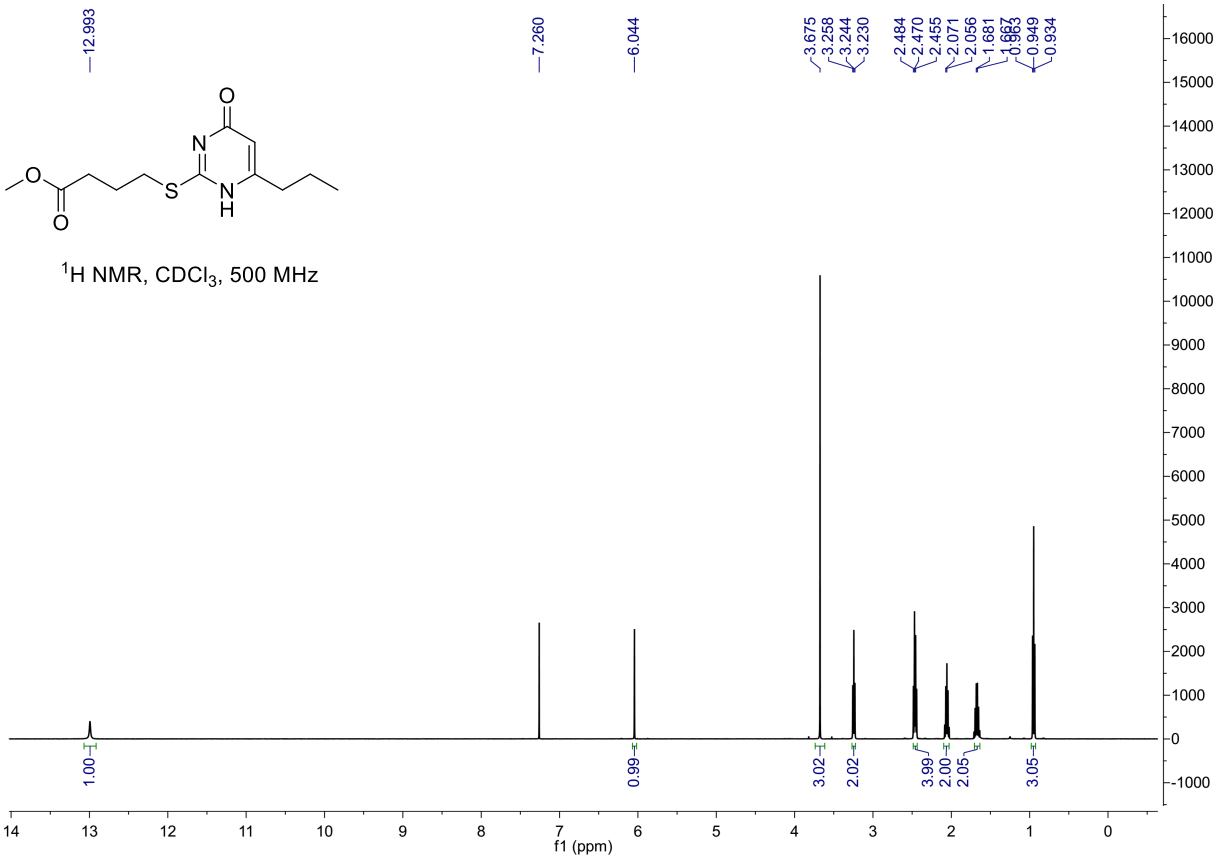

^{1}H NMR, $CDCl_3$, 500 MHz

^{13}C NMR of compound methyl 4-(4-oxo-6-propyl-1,4-dihydropyrimidin-2-ylthio)butanoate

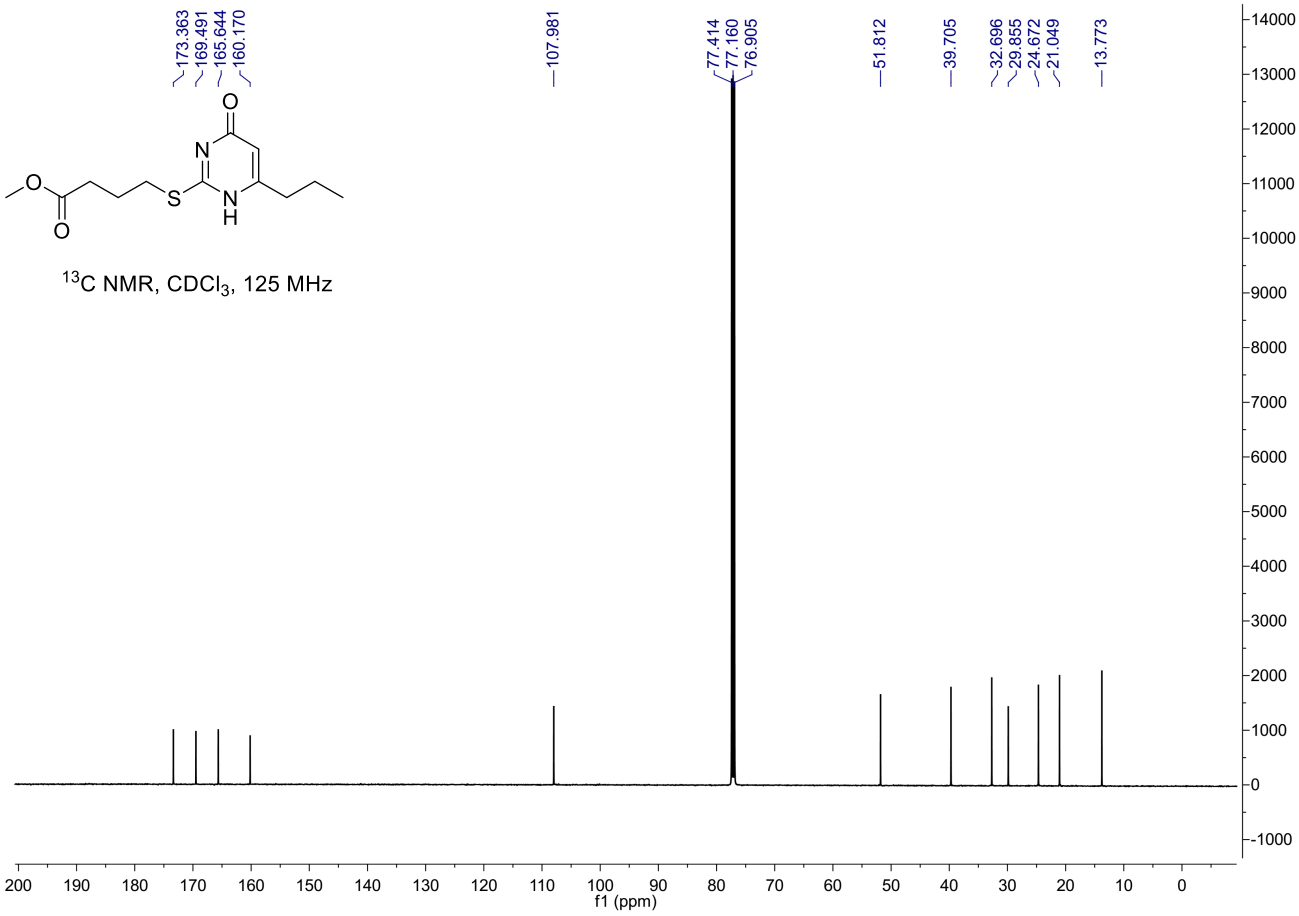

^{13}C NMR, $CDCl_3$, 125 MHz

^{1}H NMR of compound 9

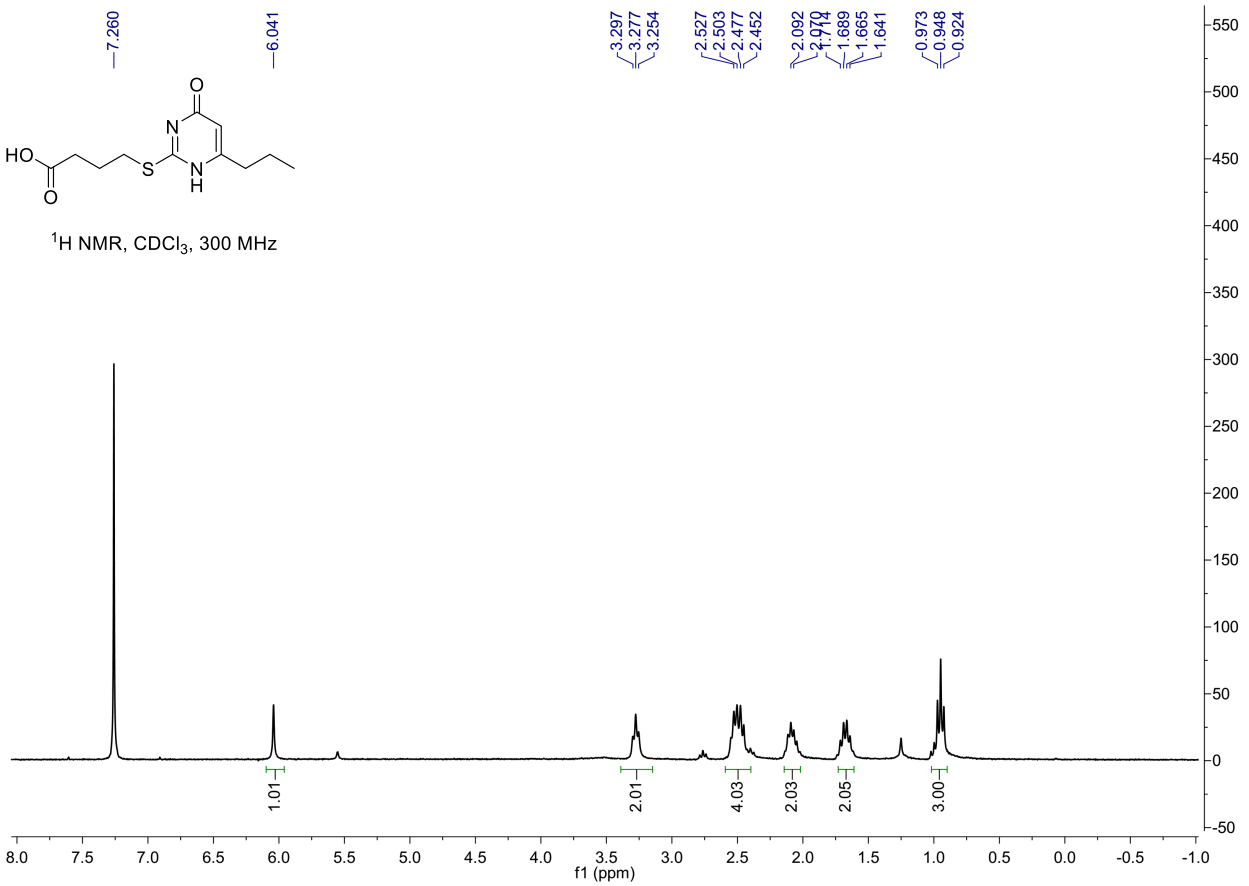

^{1}H NMR, $CDCl_3$, 300 MHz

^{13}C NMR of compound 9

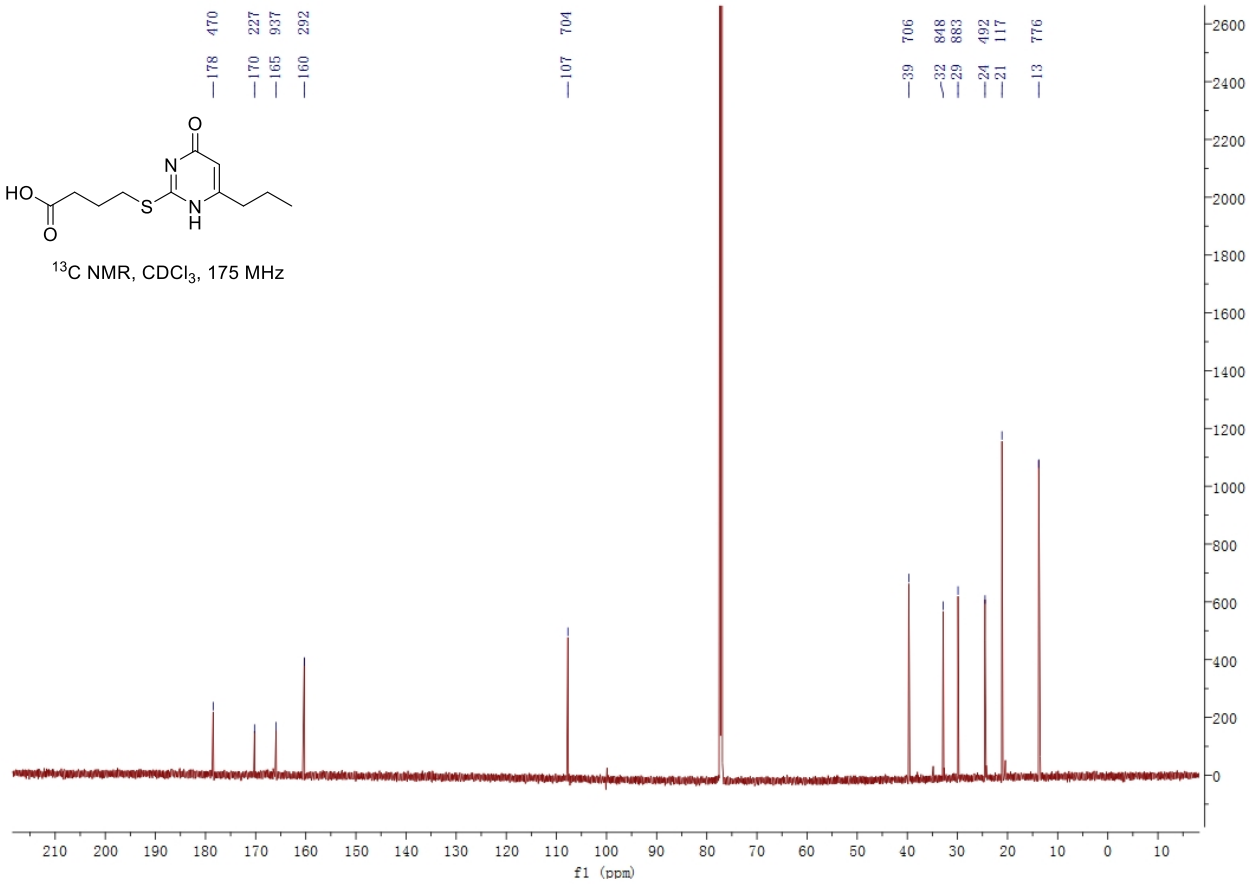

^{13}C NMR, $CDCl_3$, 175 MHz

^{1}H NMR of compound 2a

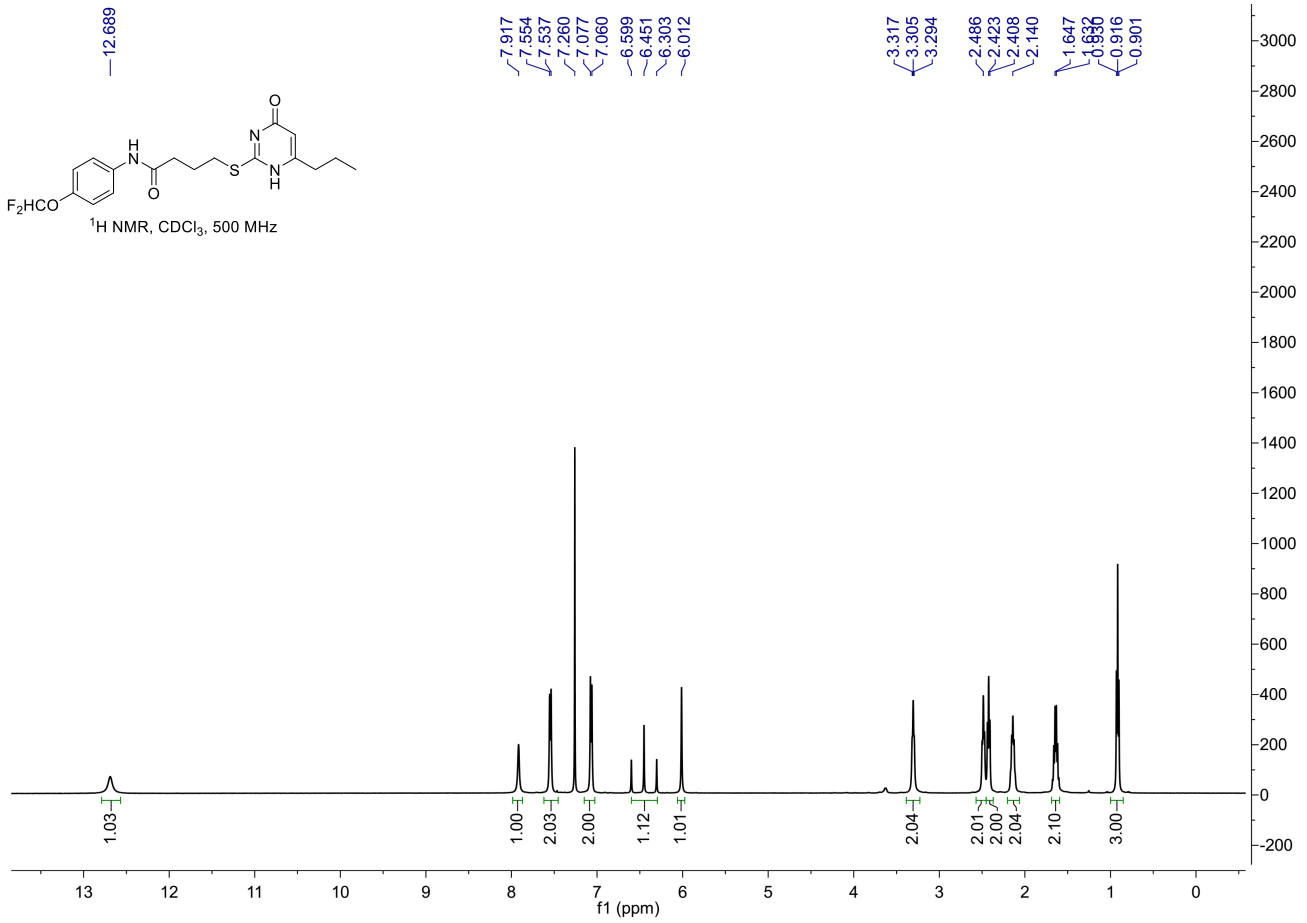

^{13}C NMR of compound 2a

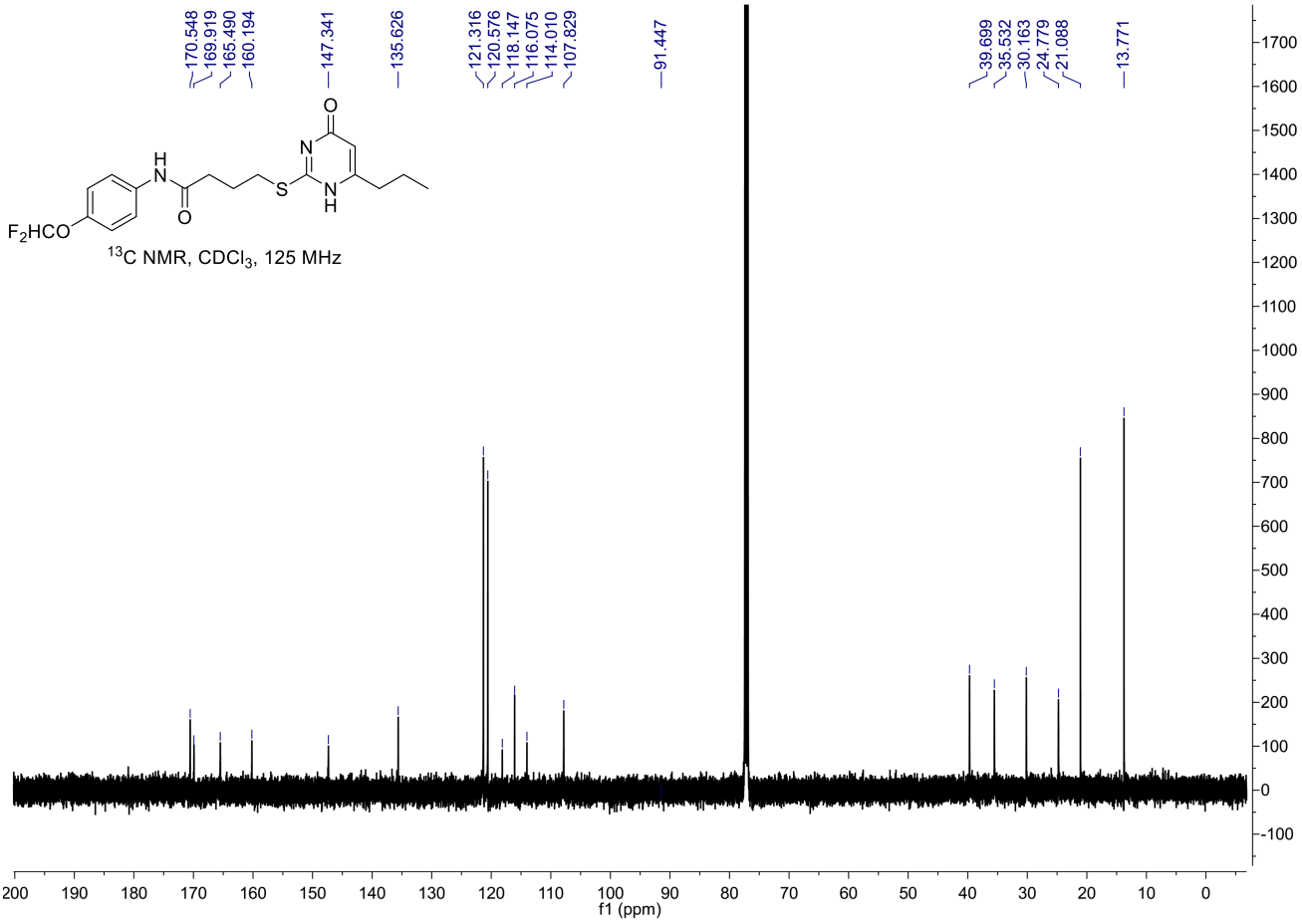

^{19}F NMR of compound 2a

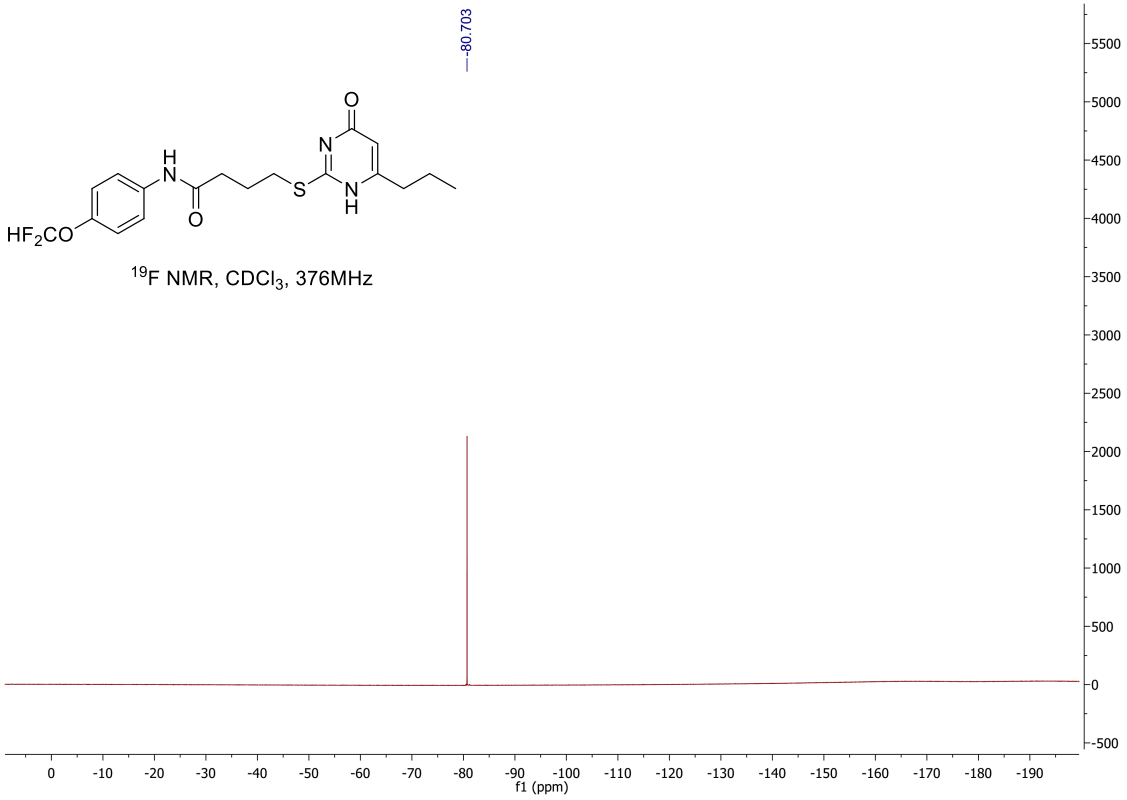

^{1}H NMR of compound 2c

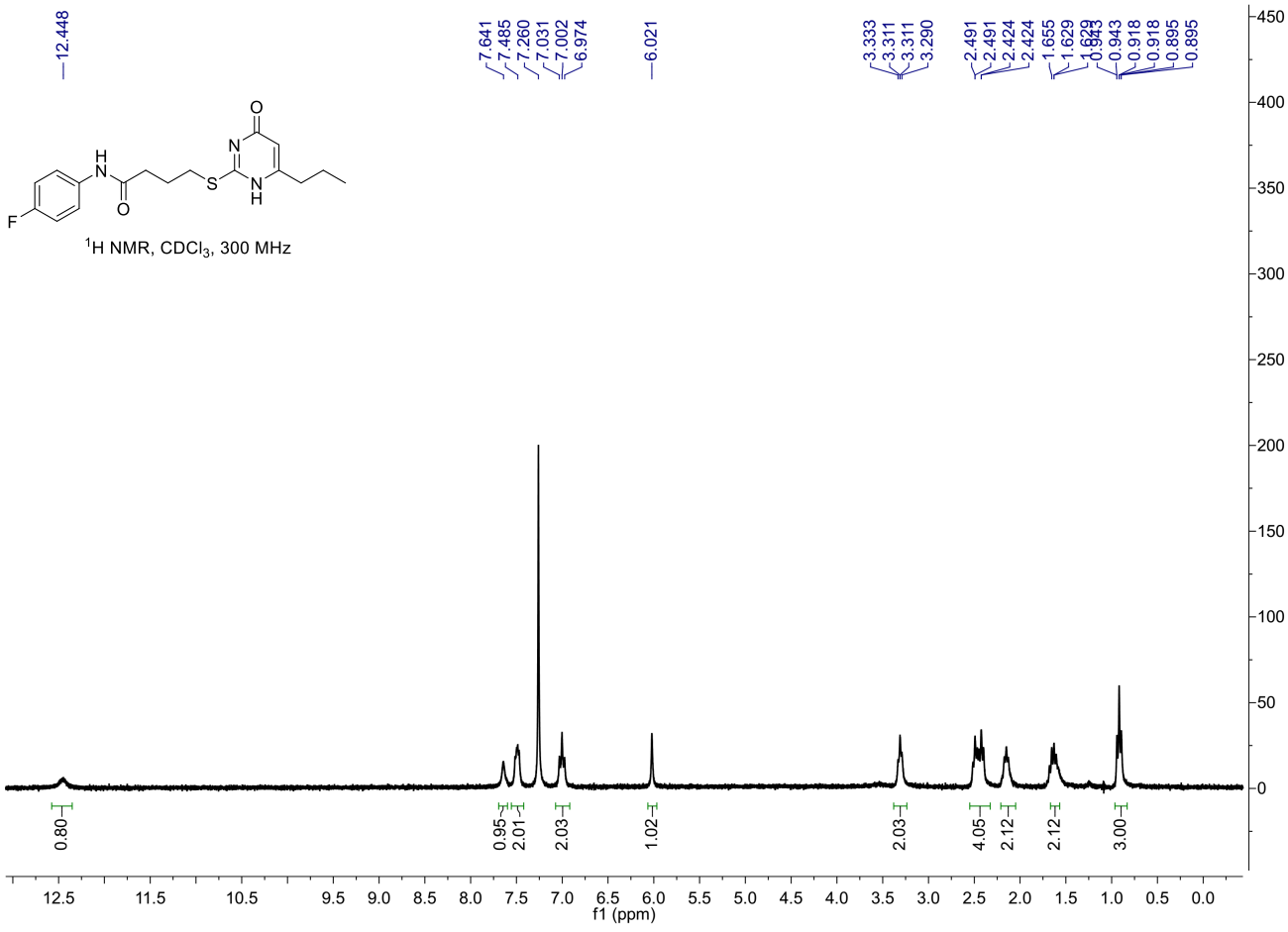

^{13}C NMR of compound 2c

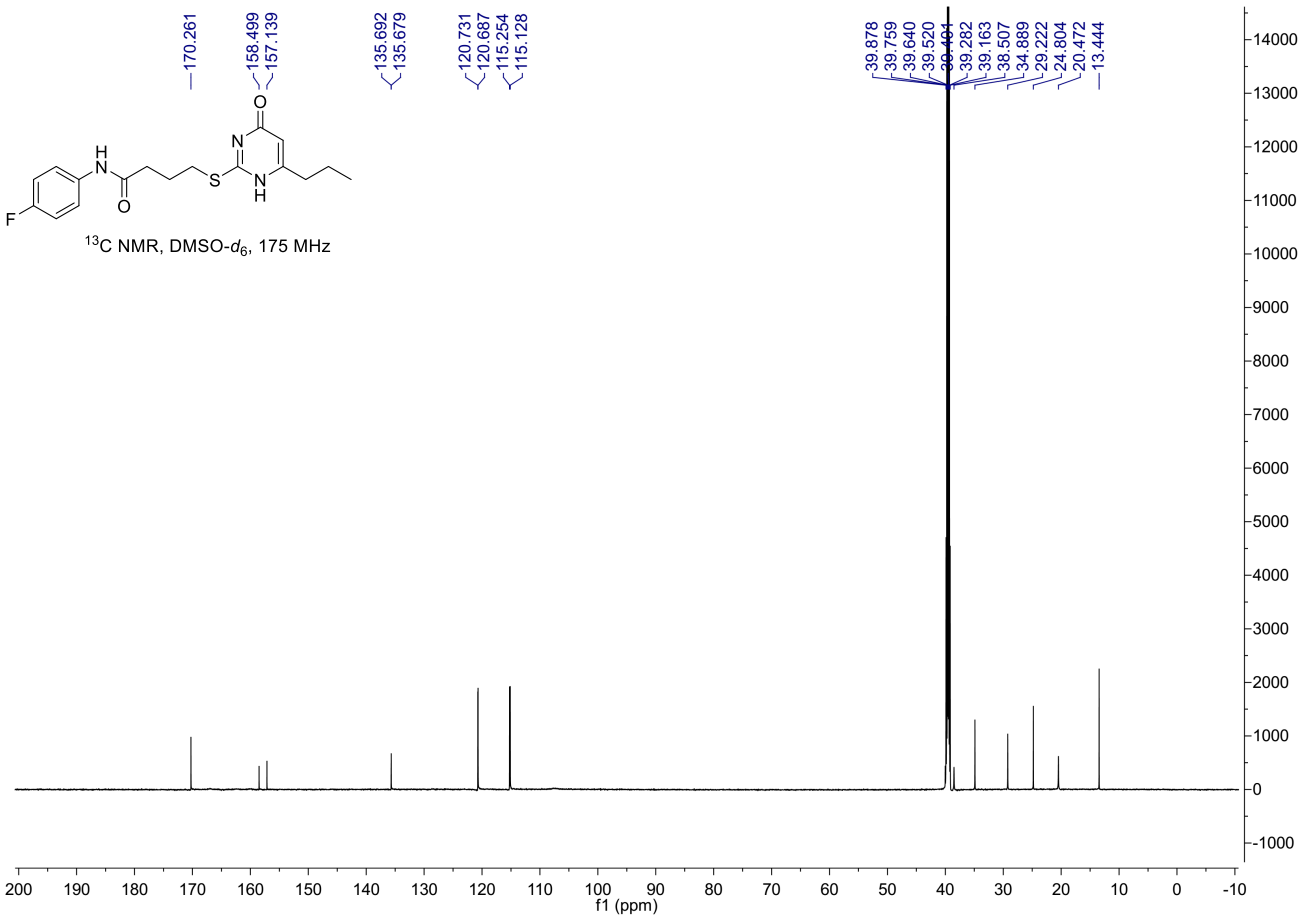

^{13}C NMR, DMSO-d_6, 175 MHz

^{19}F NMR of compound 2c

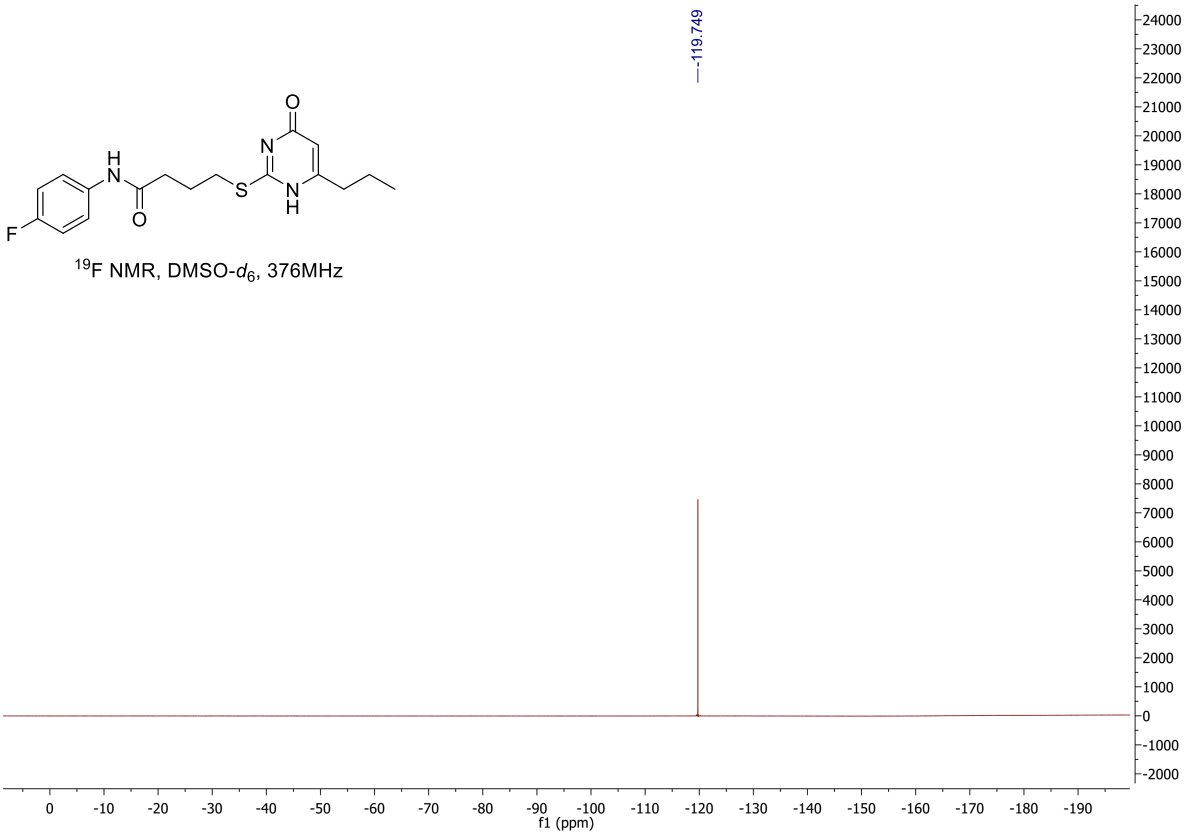

^{19}F NMR, DMSO-d_6, 376MHz

^{1}H NMR of compound 11

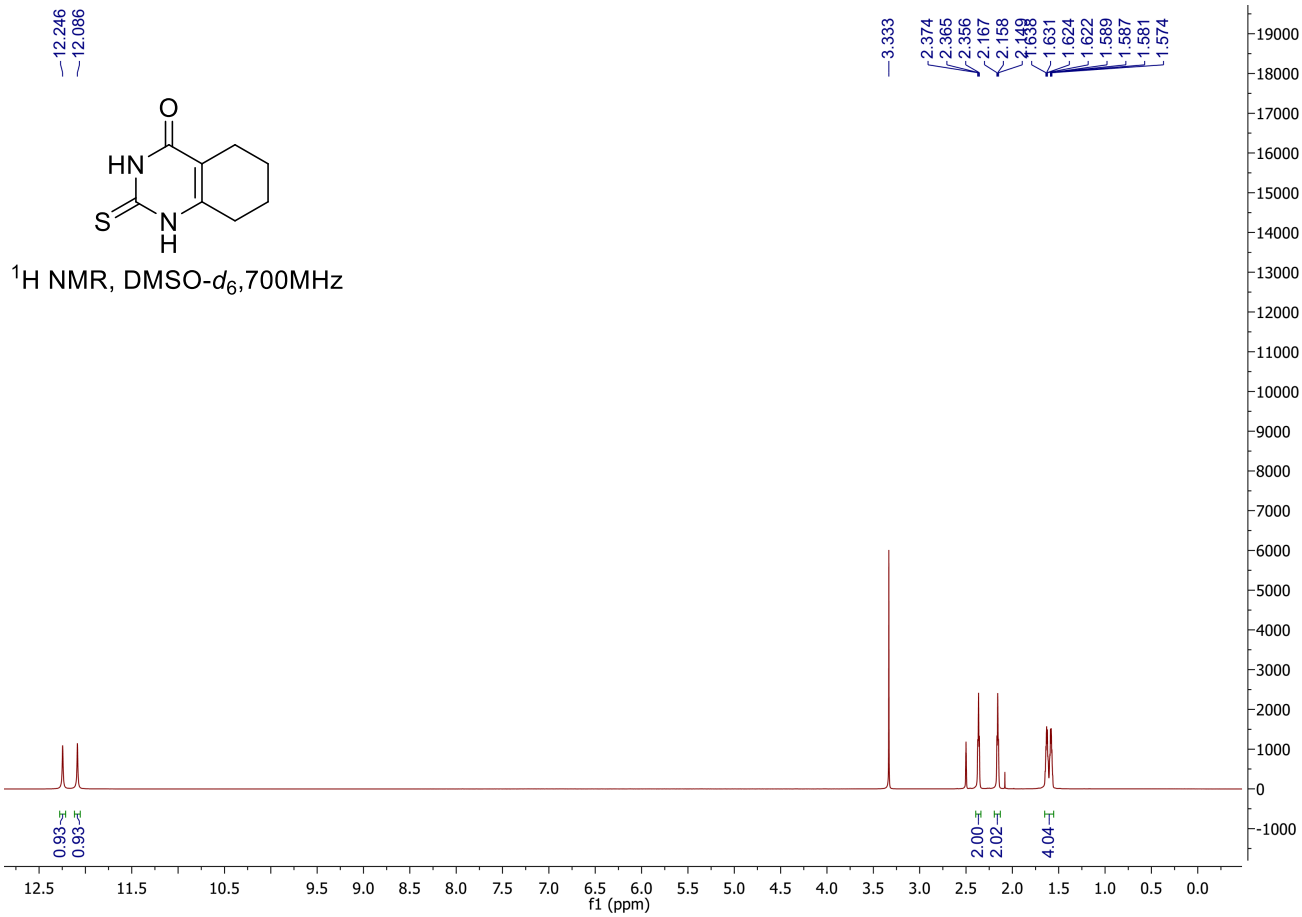

^{1}H NMR, DMSO-d_6,700MHz

^{13}C NMR of compound 11

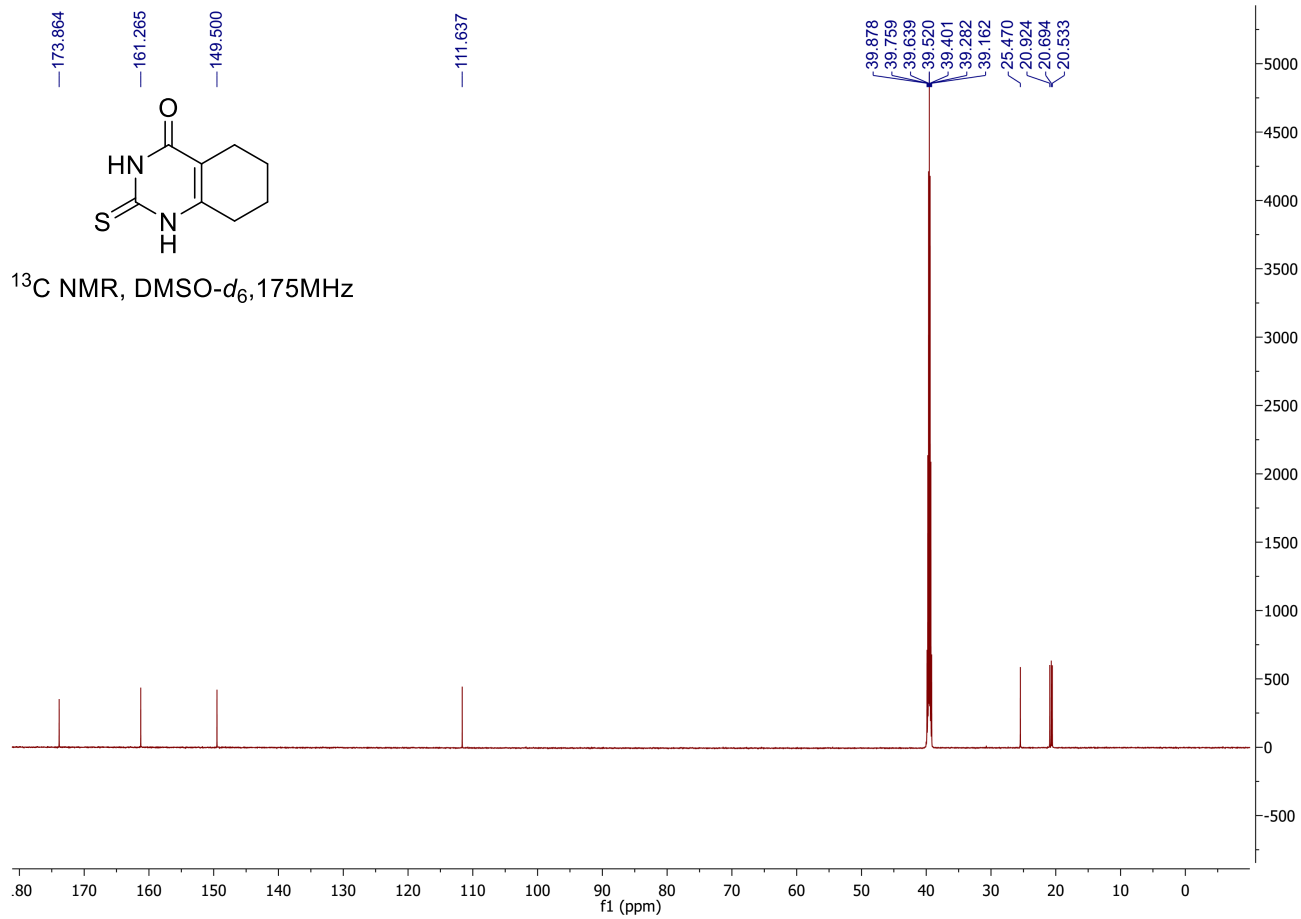

^{13}C NMR, DMSO-d_6,175MHz

^{1}H NMR of compound methyl 4-(4-oxo-3,4,5,6,7,8-hexahydroquinazolin-2-ylthio)butanoate

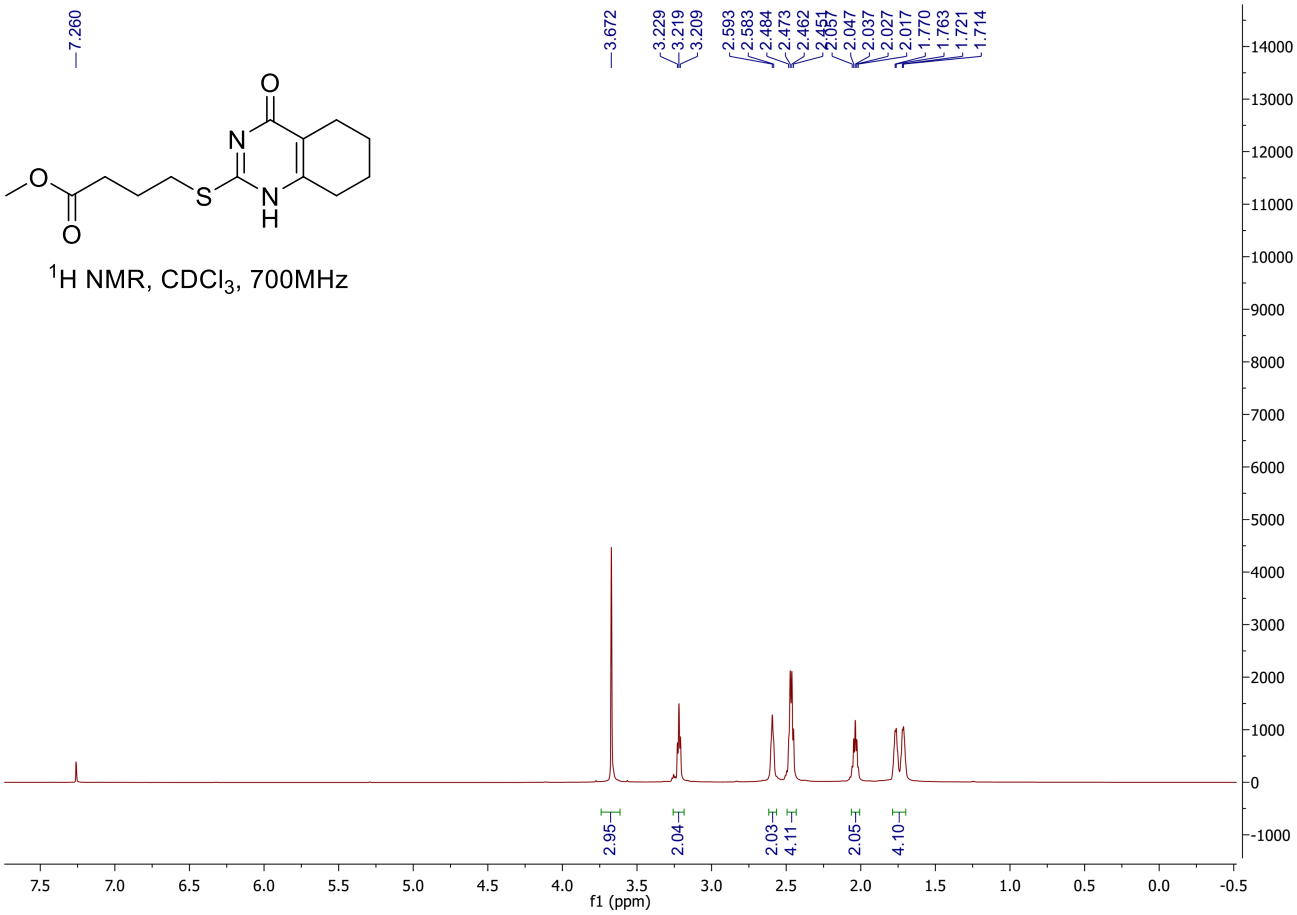

^{1}H NMR, $CDCl_3$, 700MHz

^{13}C NMR of compound methyl 4-(4-oxo-3,4,5,6,7,8-hexahydroquinazolin-2-ylthio)butanoate

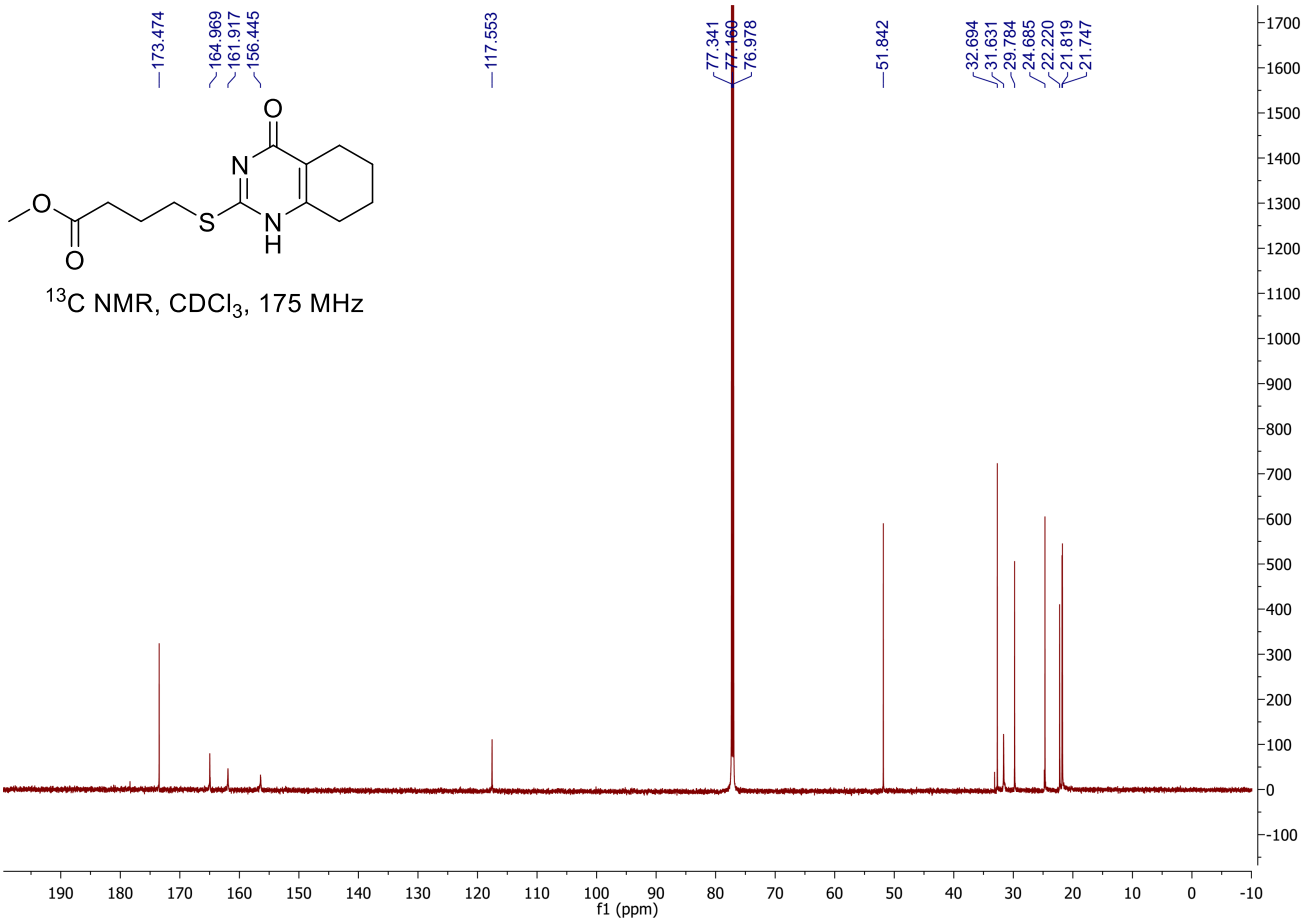

^{13}C NMR, $CDCl_3$, 175 MHz

^{1}H NMR of compound 12

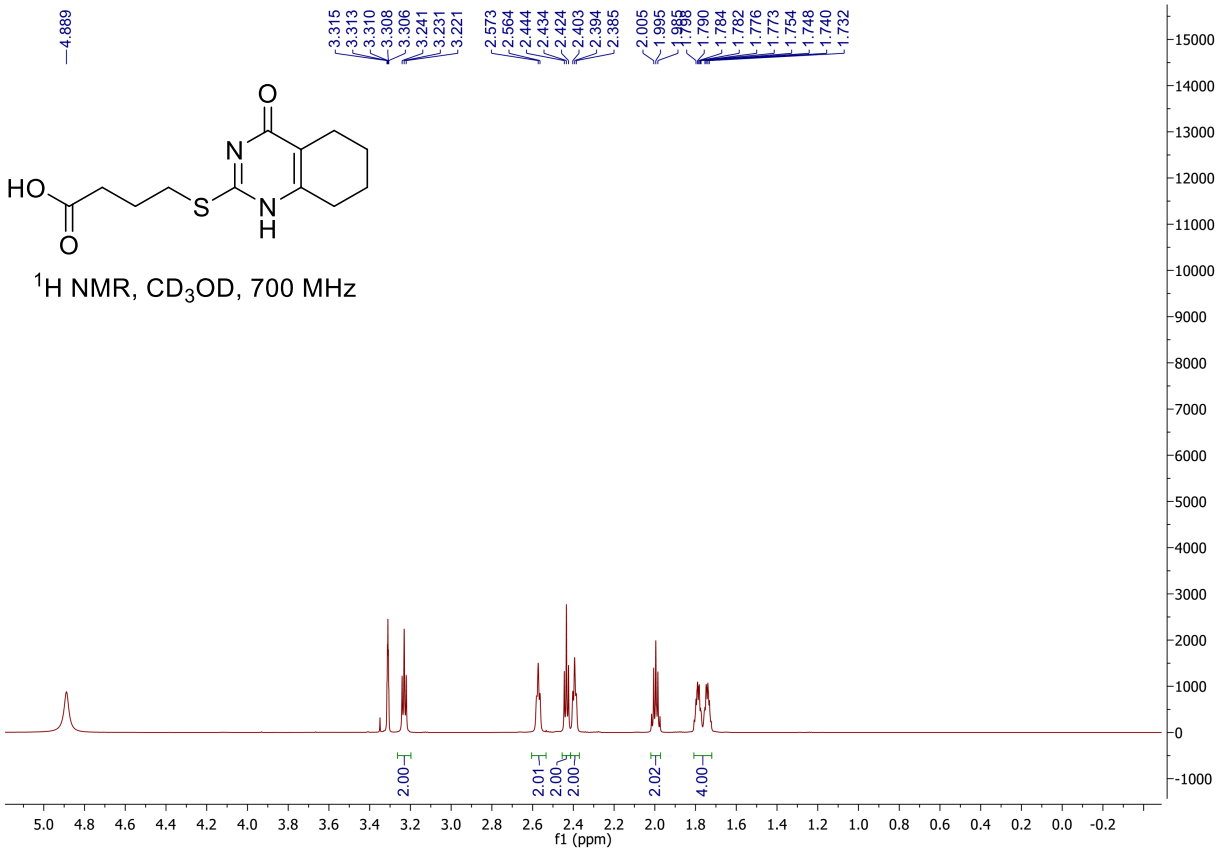

^{13}C NMR of compound 12

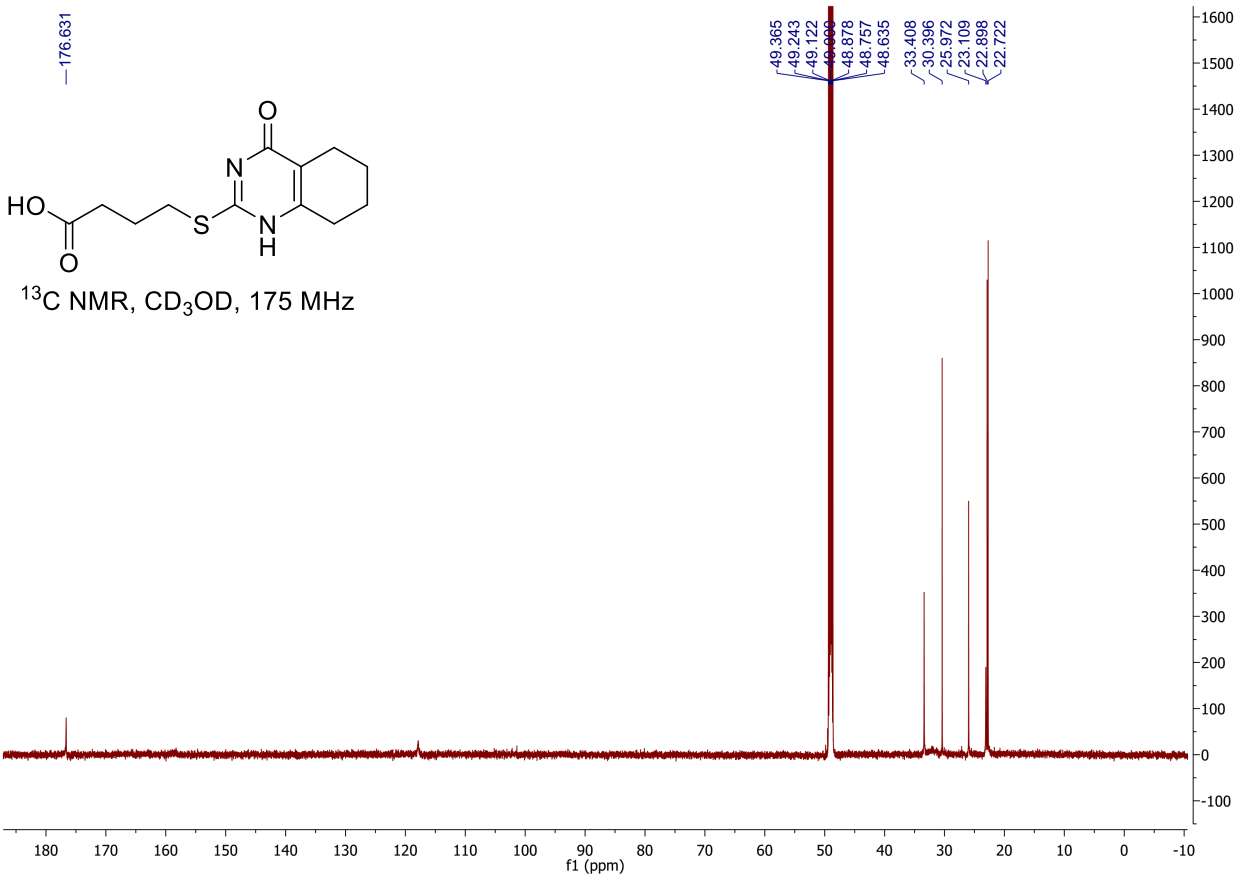

^{1}H NMR of compound 3a

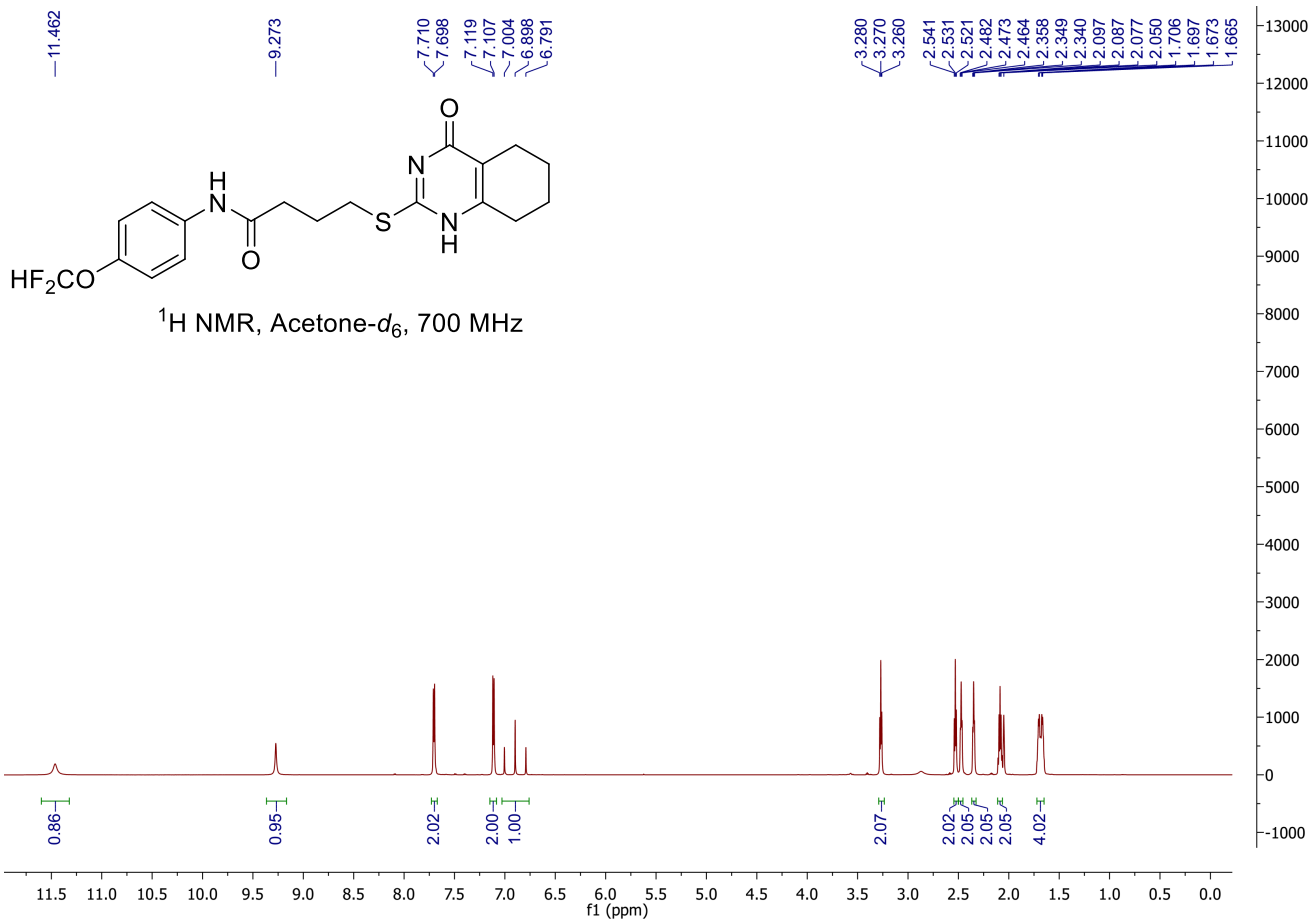

^{13}C NMR compound 3a

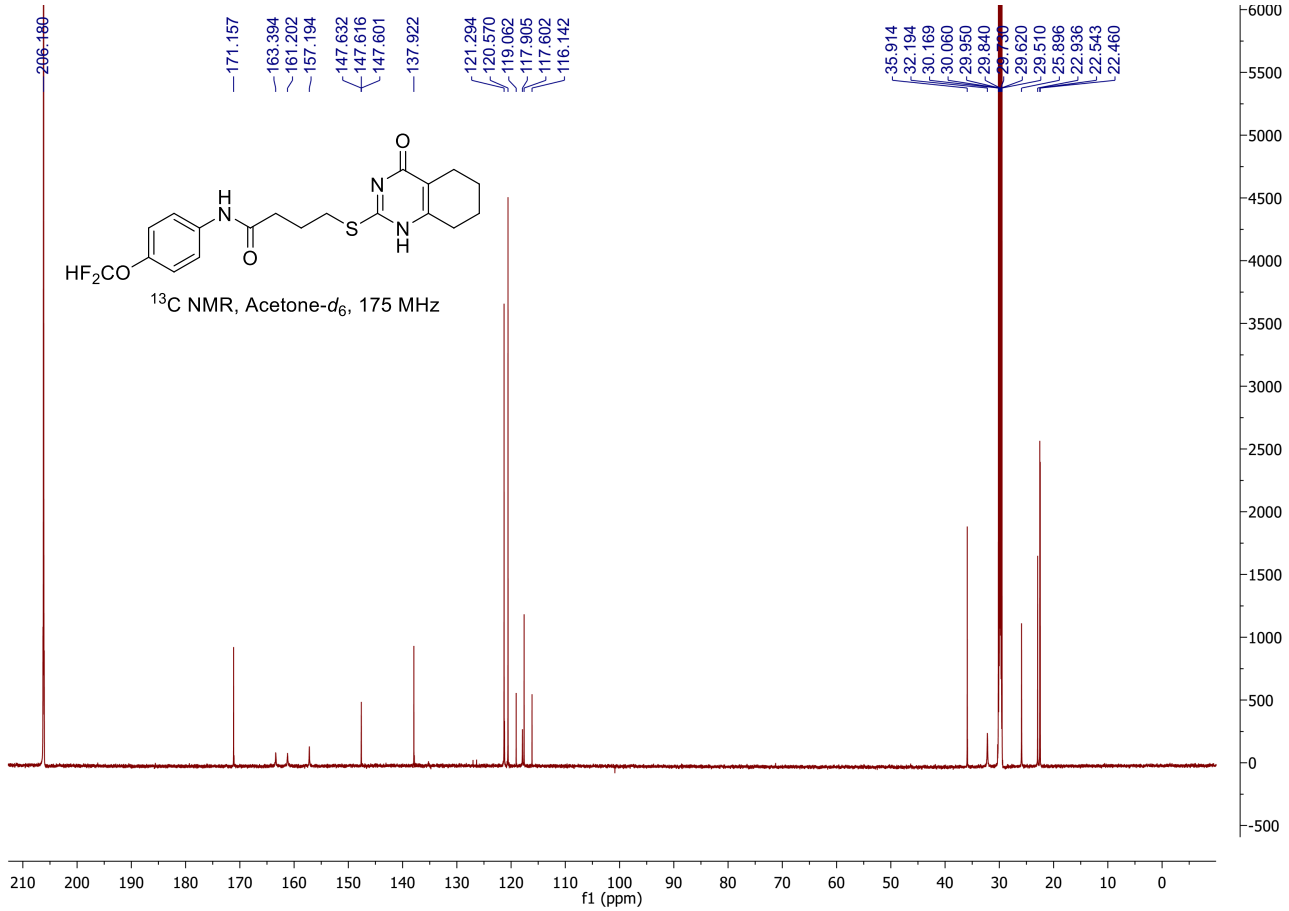

^{19}F NMR of compound 3a

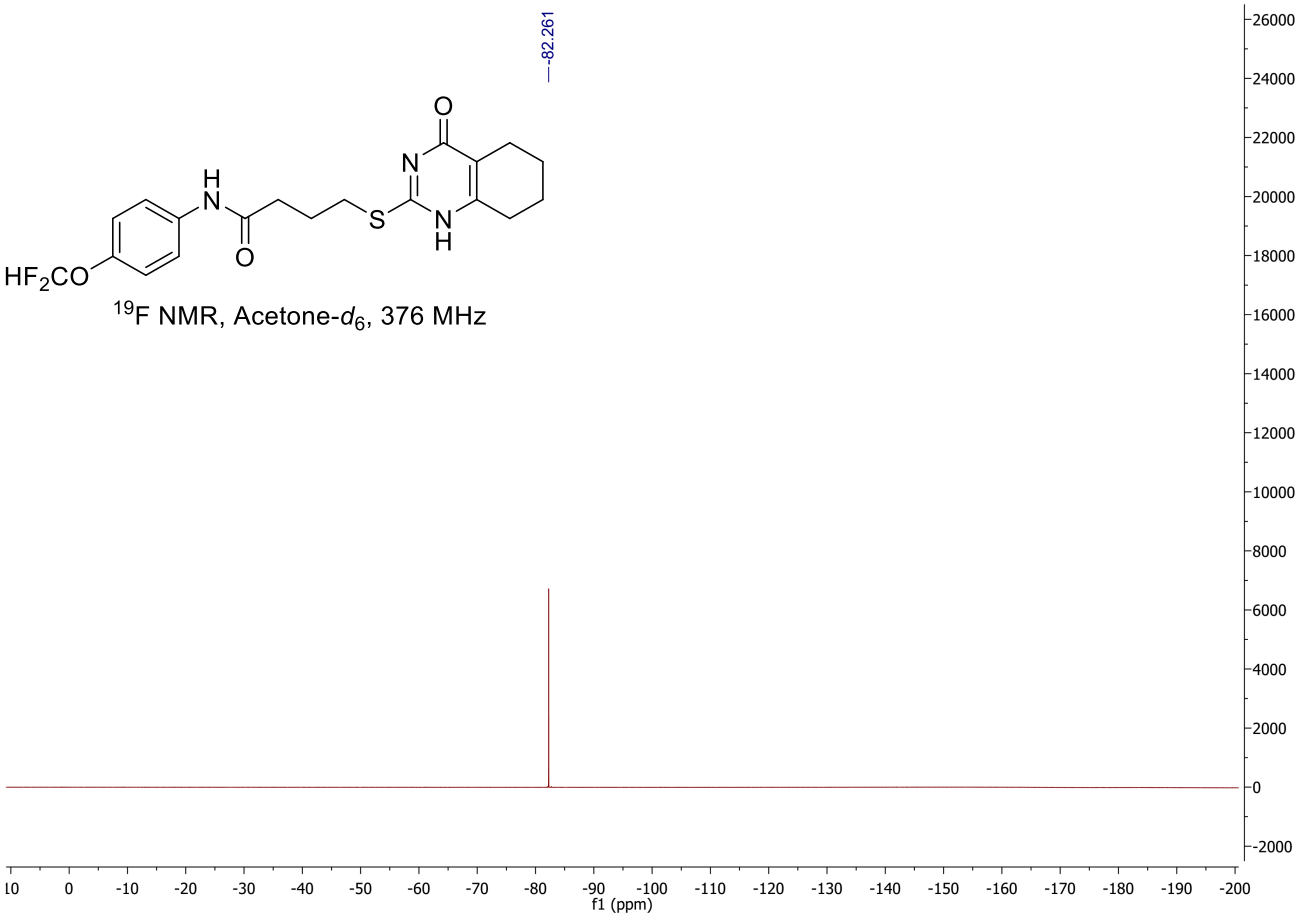

^{1}H NMR of compound 3b

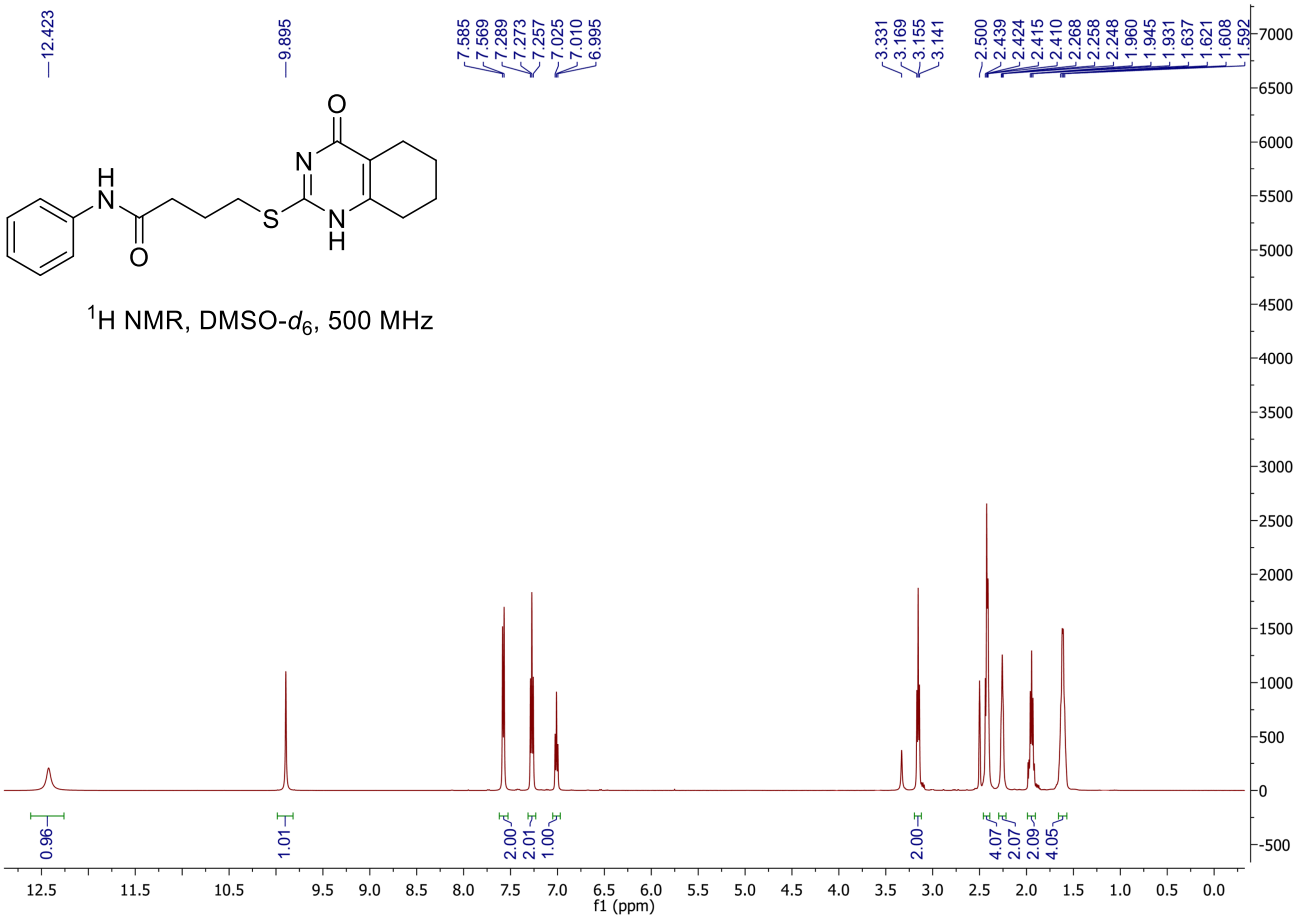

^{13}C NMR of compound 3b

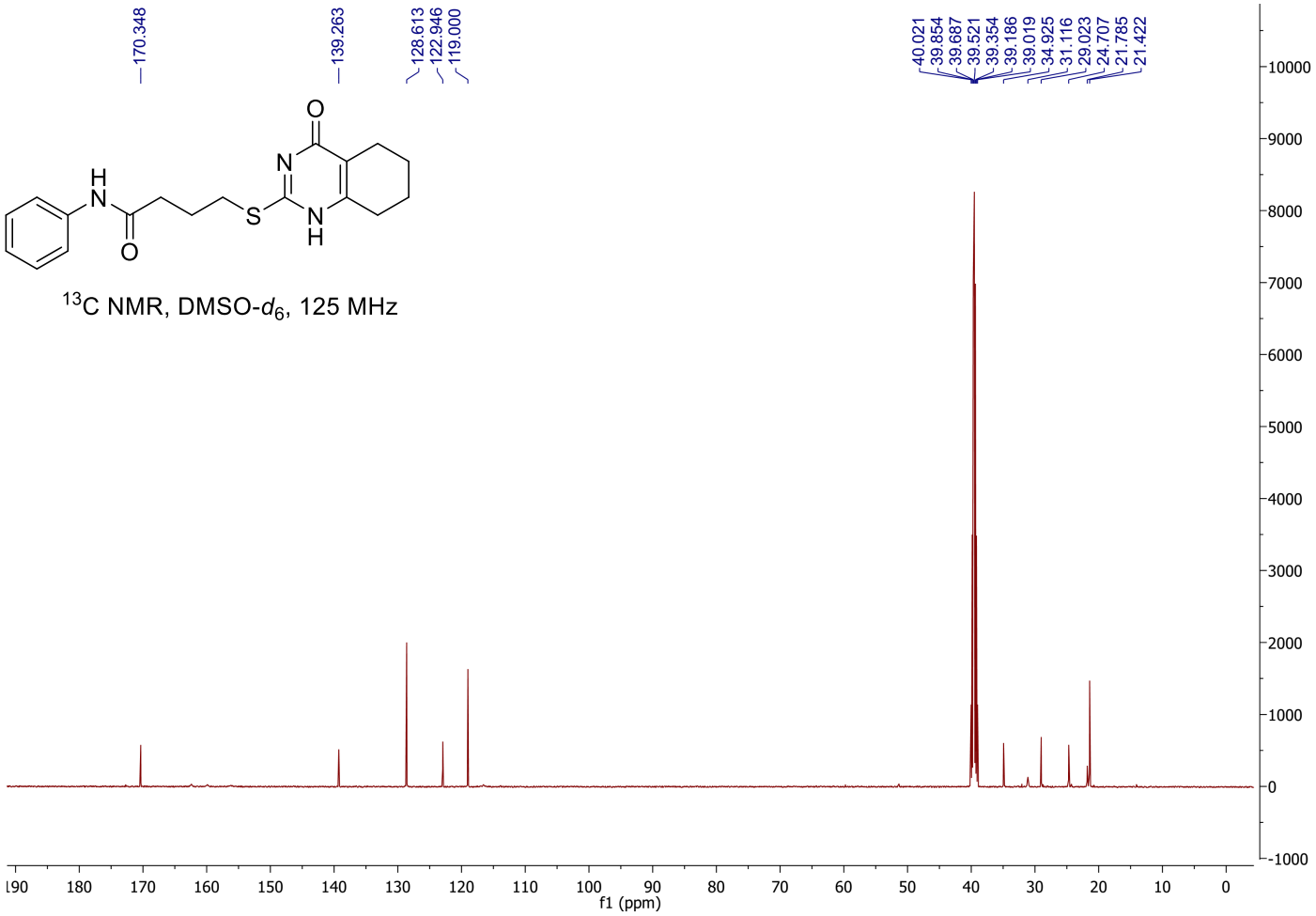

^{1}H NMR of compound 3c

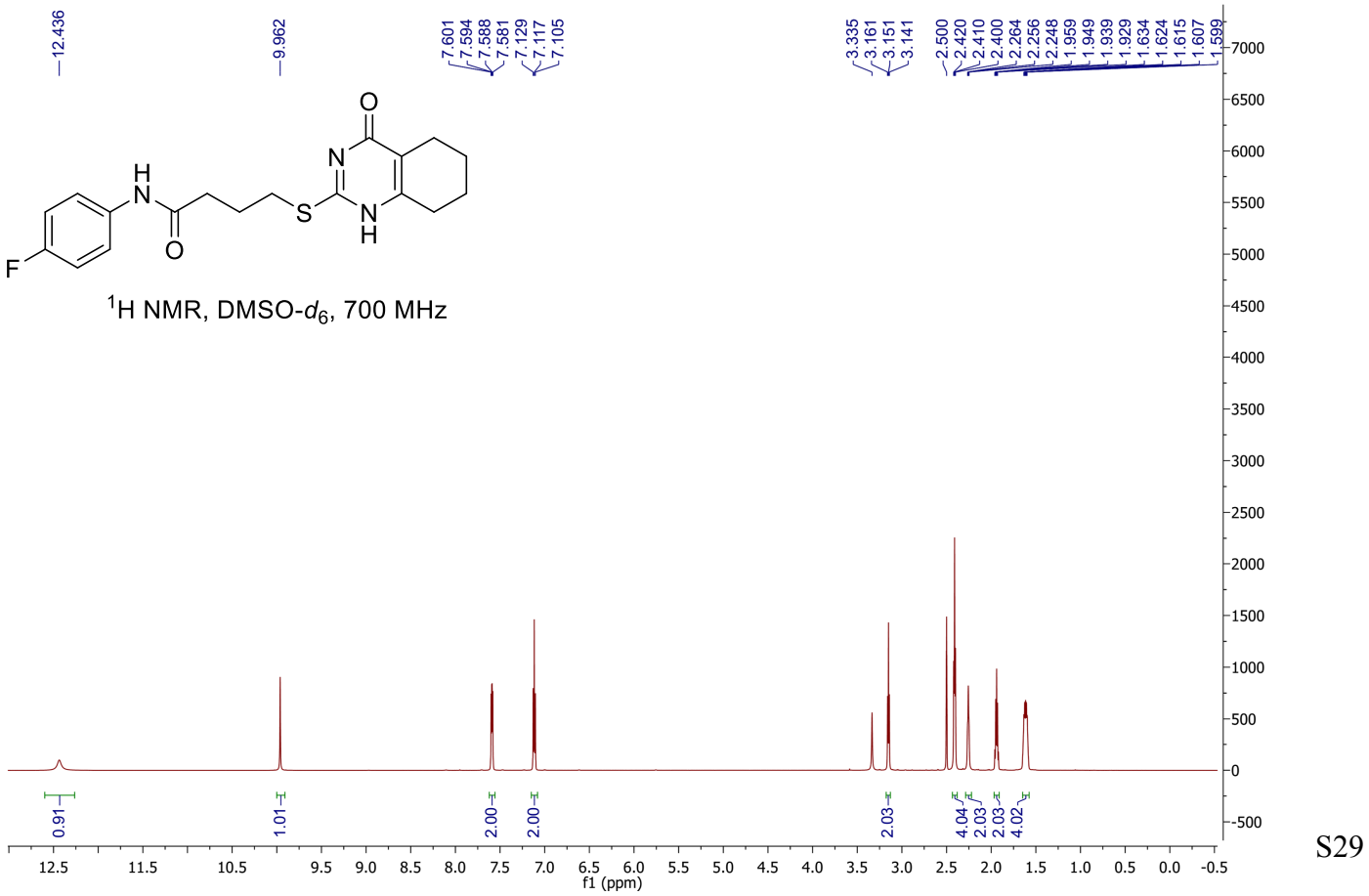

^{13}C NMR of compound 3c

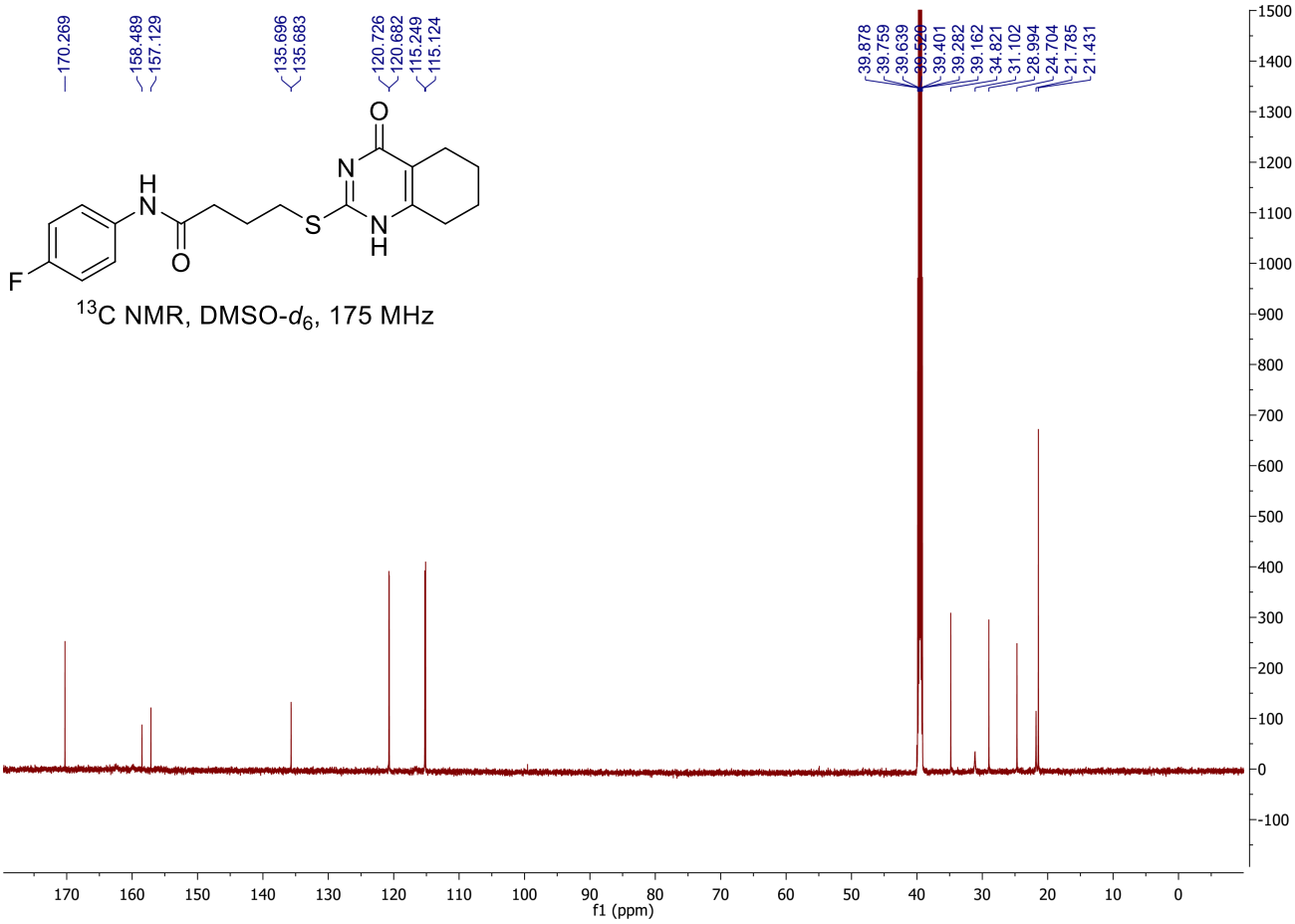

^{19}F NMR of compound 3c

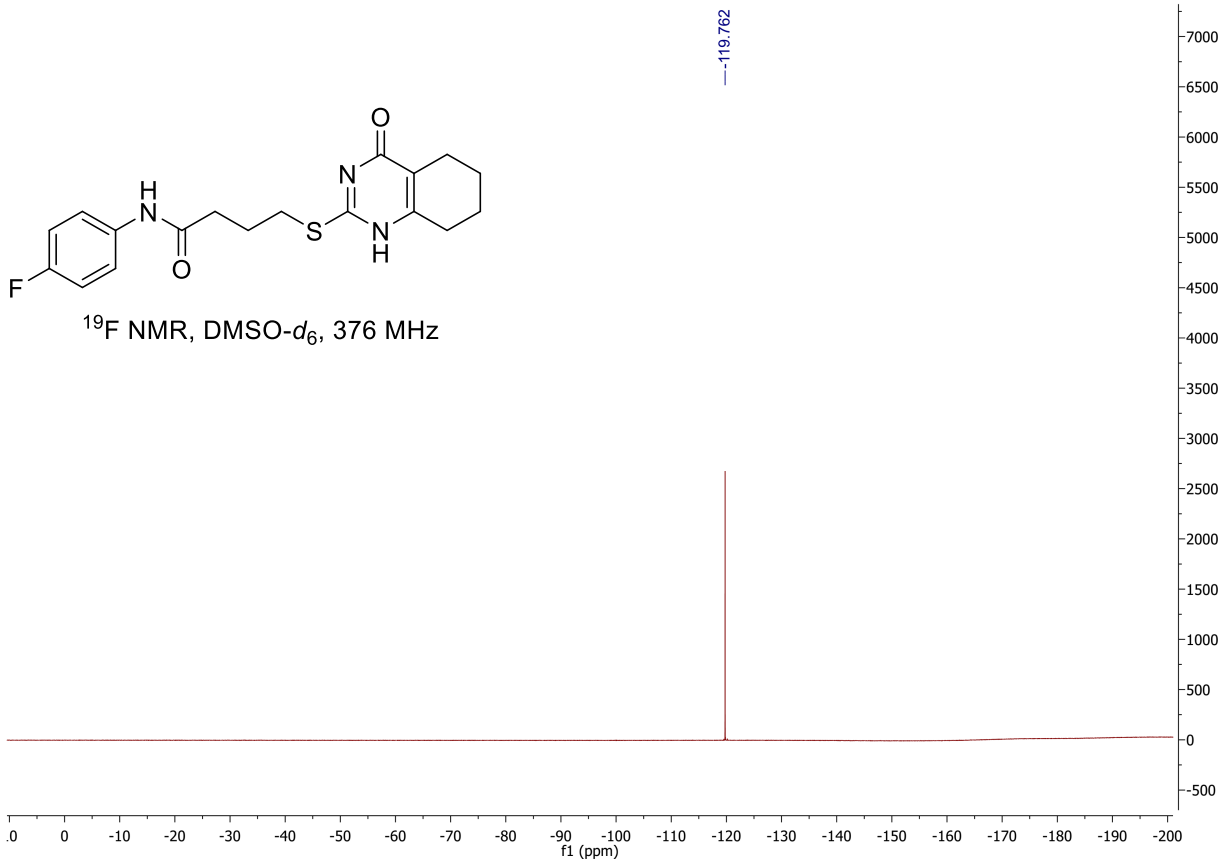

^{1}H NMR of compound 3d

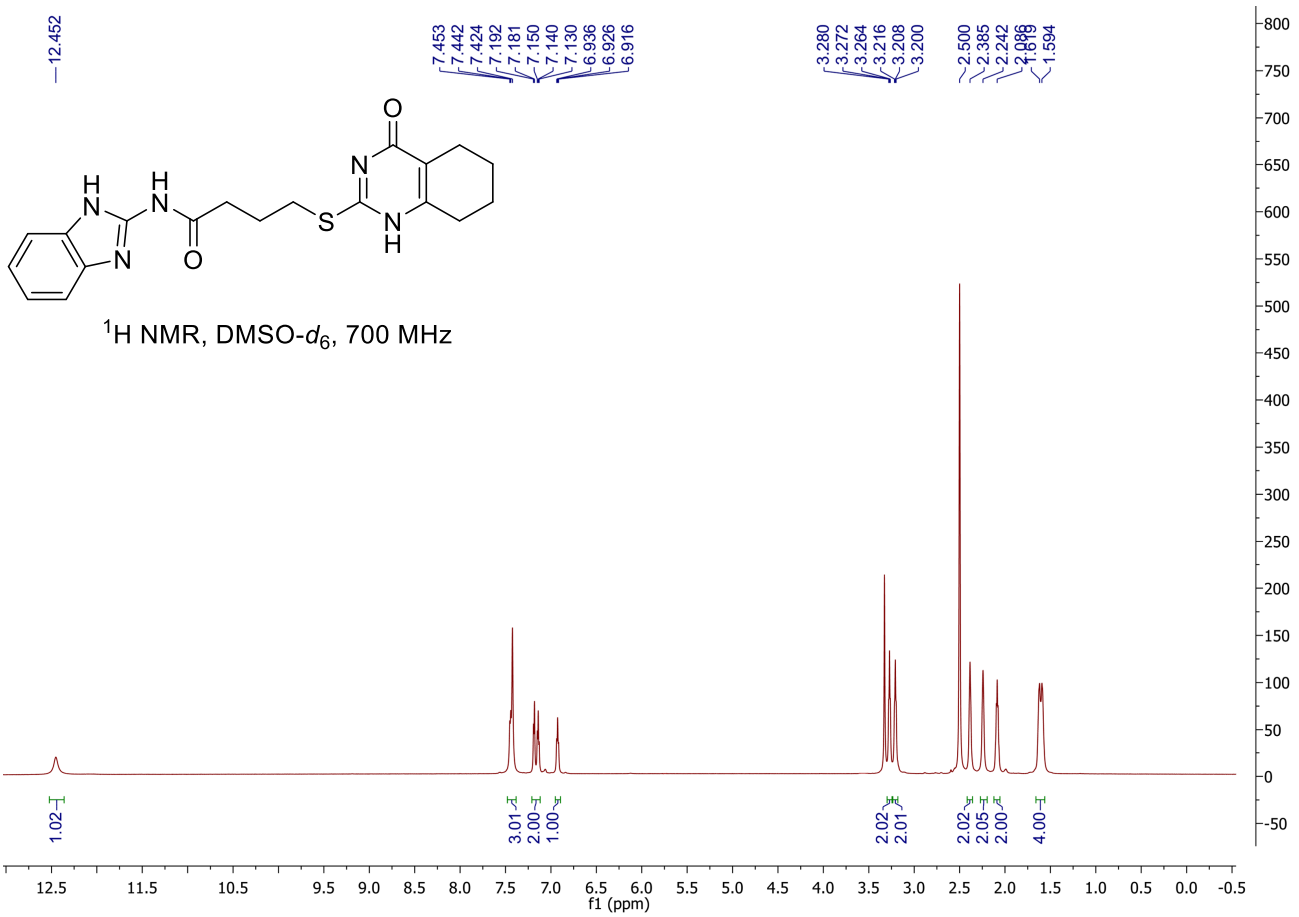

^{1}H NMR, DMSO-d_6, 700 MHz

^{13}C NMR of compound 3d

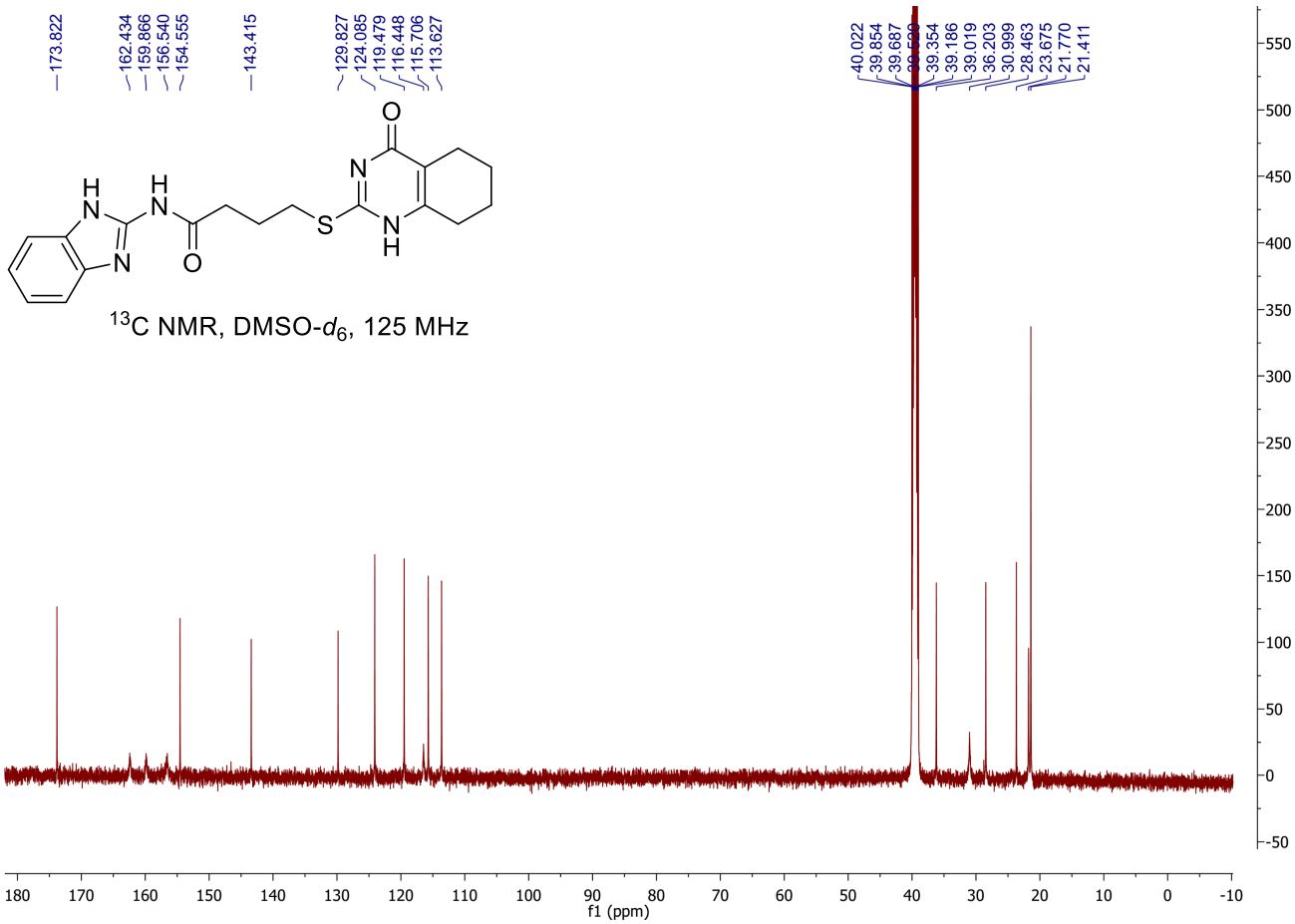

^{13}C NMR, DMSO-d_6, 125 MHz

^{1}H NMR of compound methyl 4-(4-oxo-3,4-dihydroquinazolin-2-ylthio)butanoate

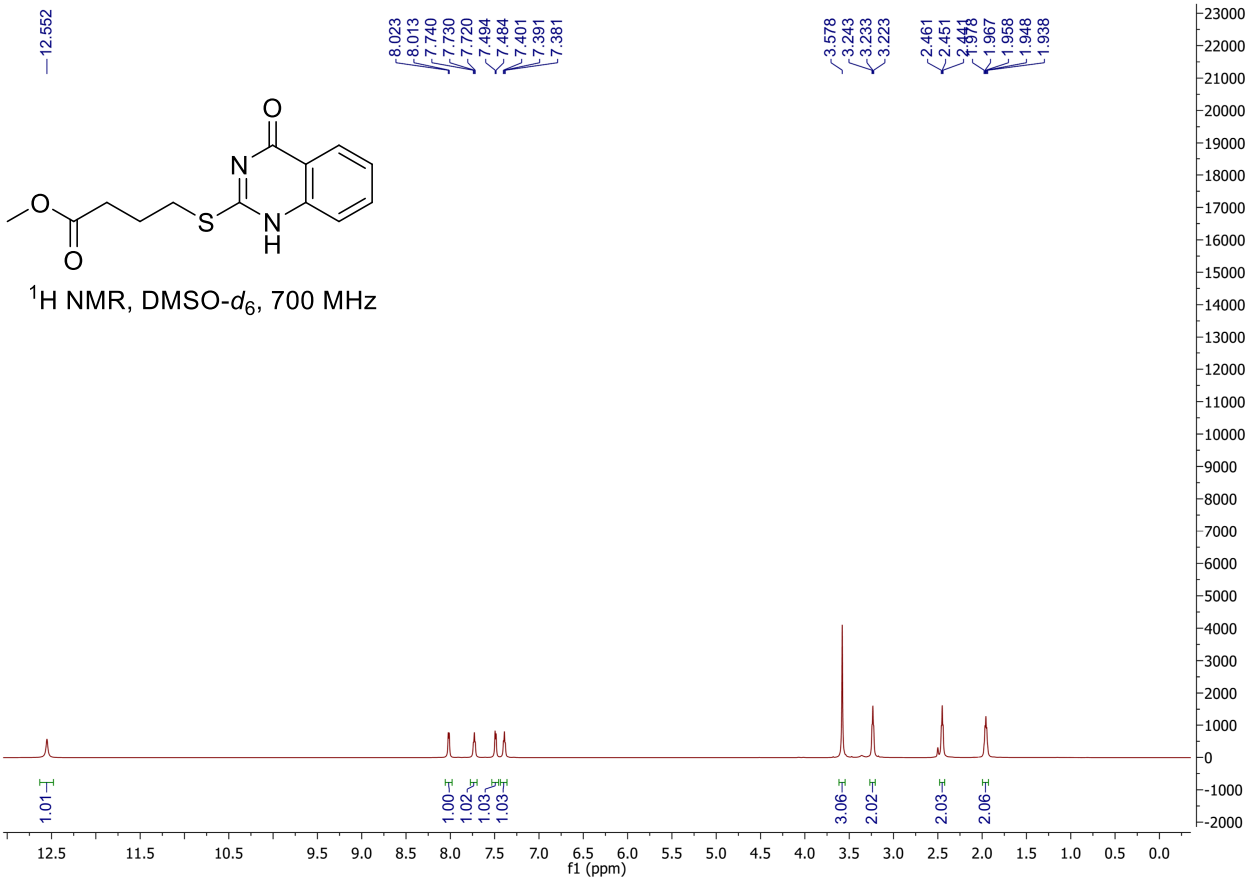

^{13}C NMR of compound methyl 4-(4-oxo-3,4-dihydroquinazolin-2-ylthio)butanoate

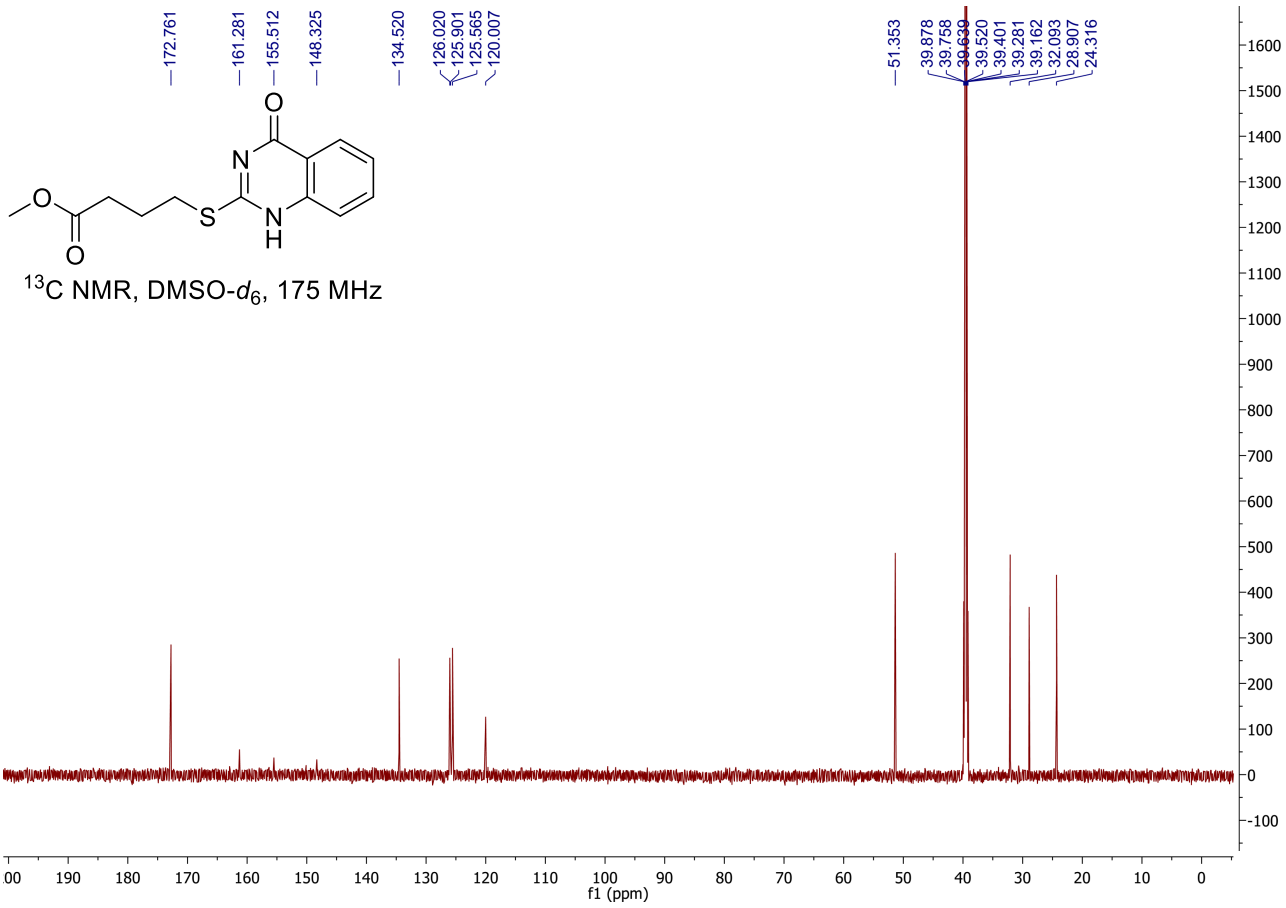

^{1}H NMR of compound 14

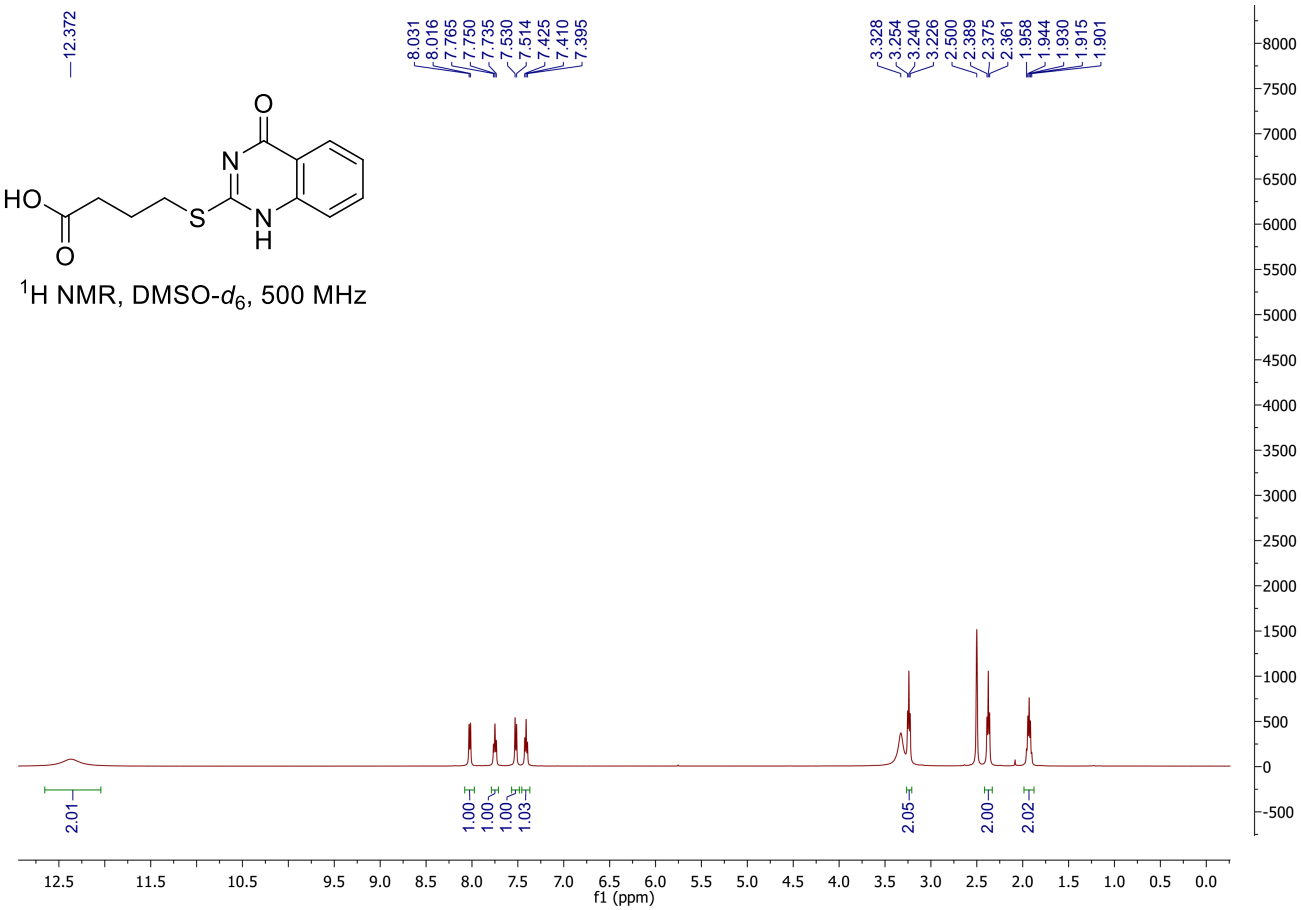

^{13}C NMR of compound 14

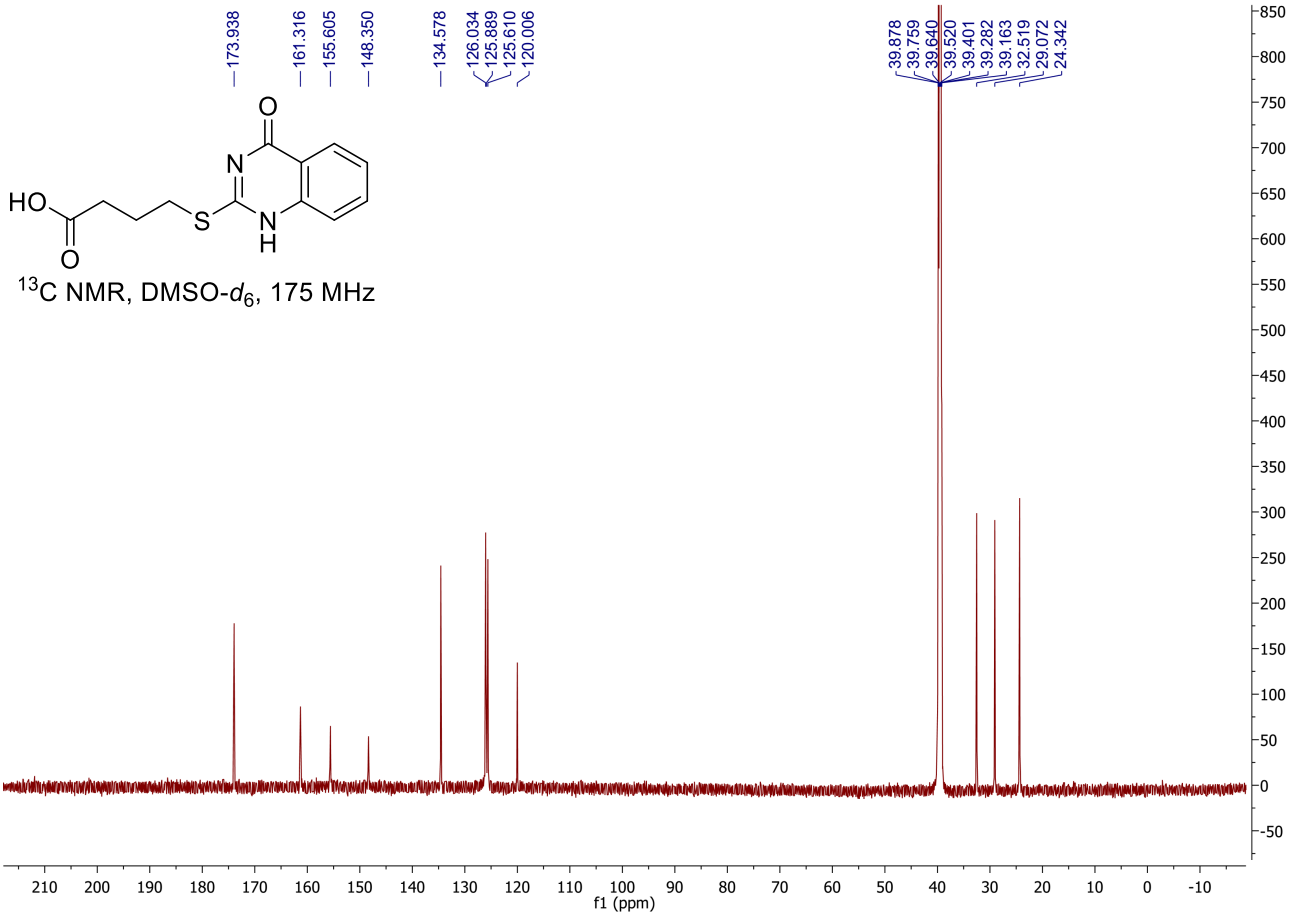

^{1}H NMR of compound 4a

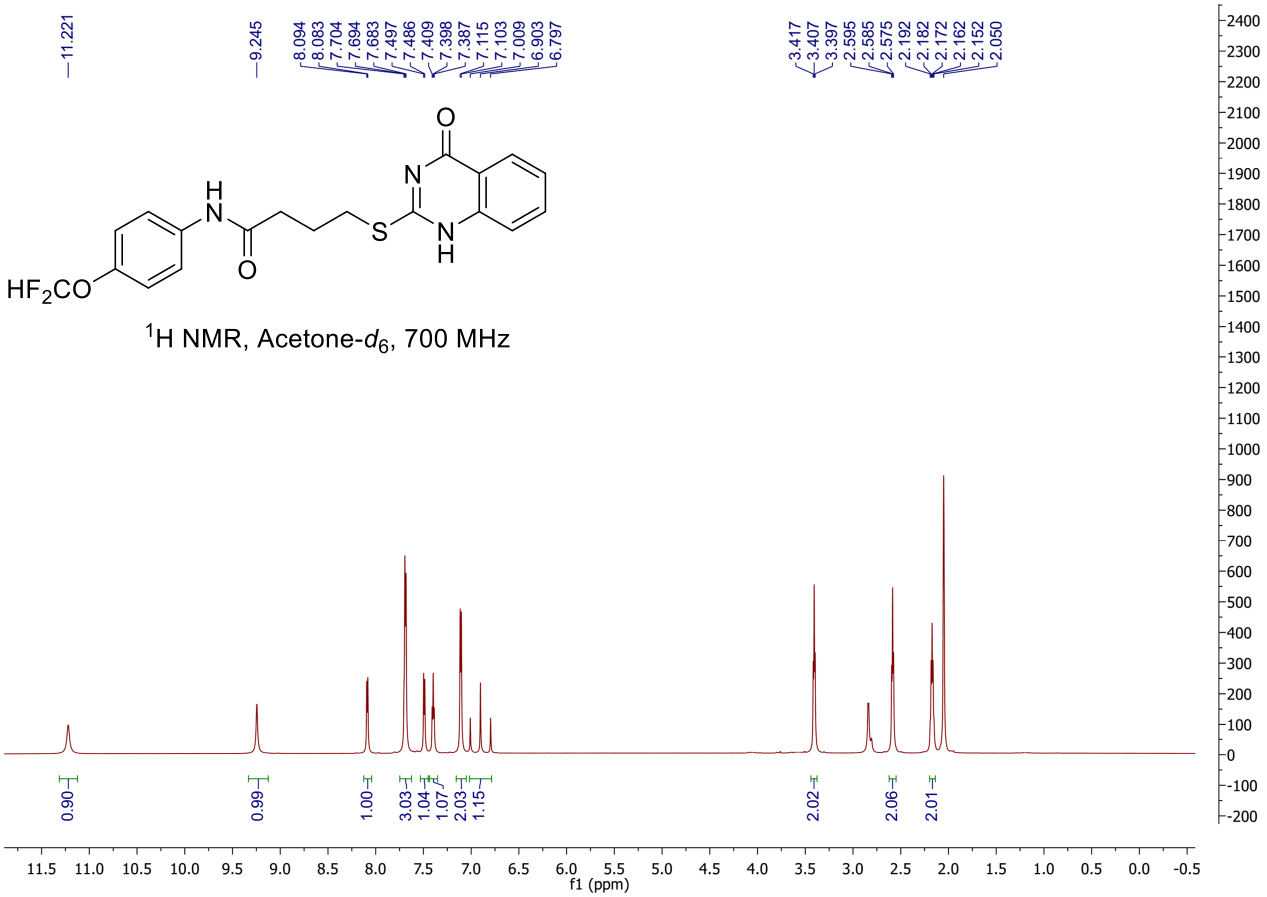

^{13}C NMR of compound 4a

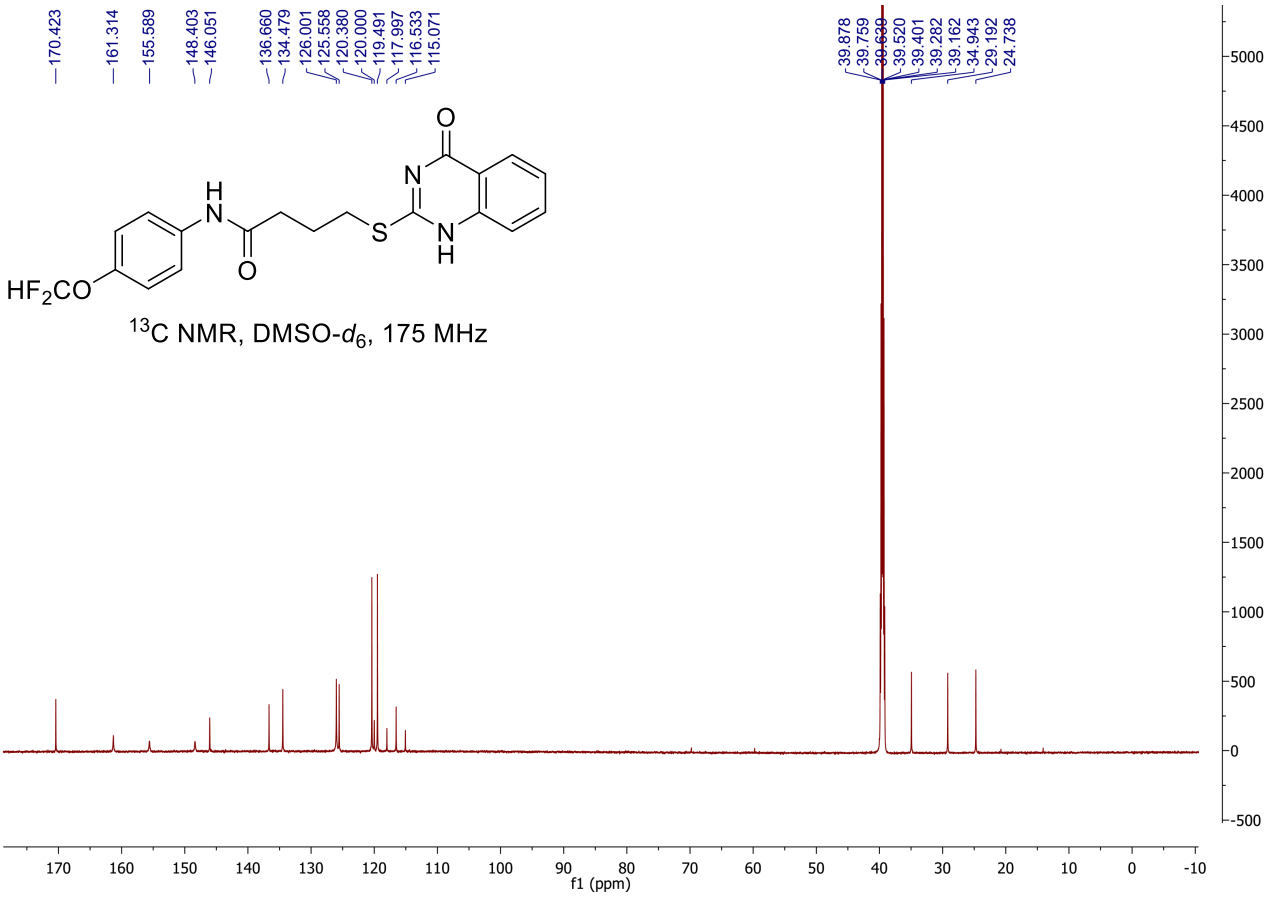

^{19}F NMR of compound 4a

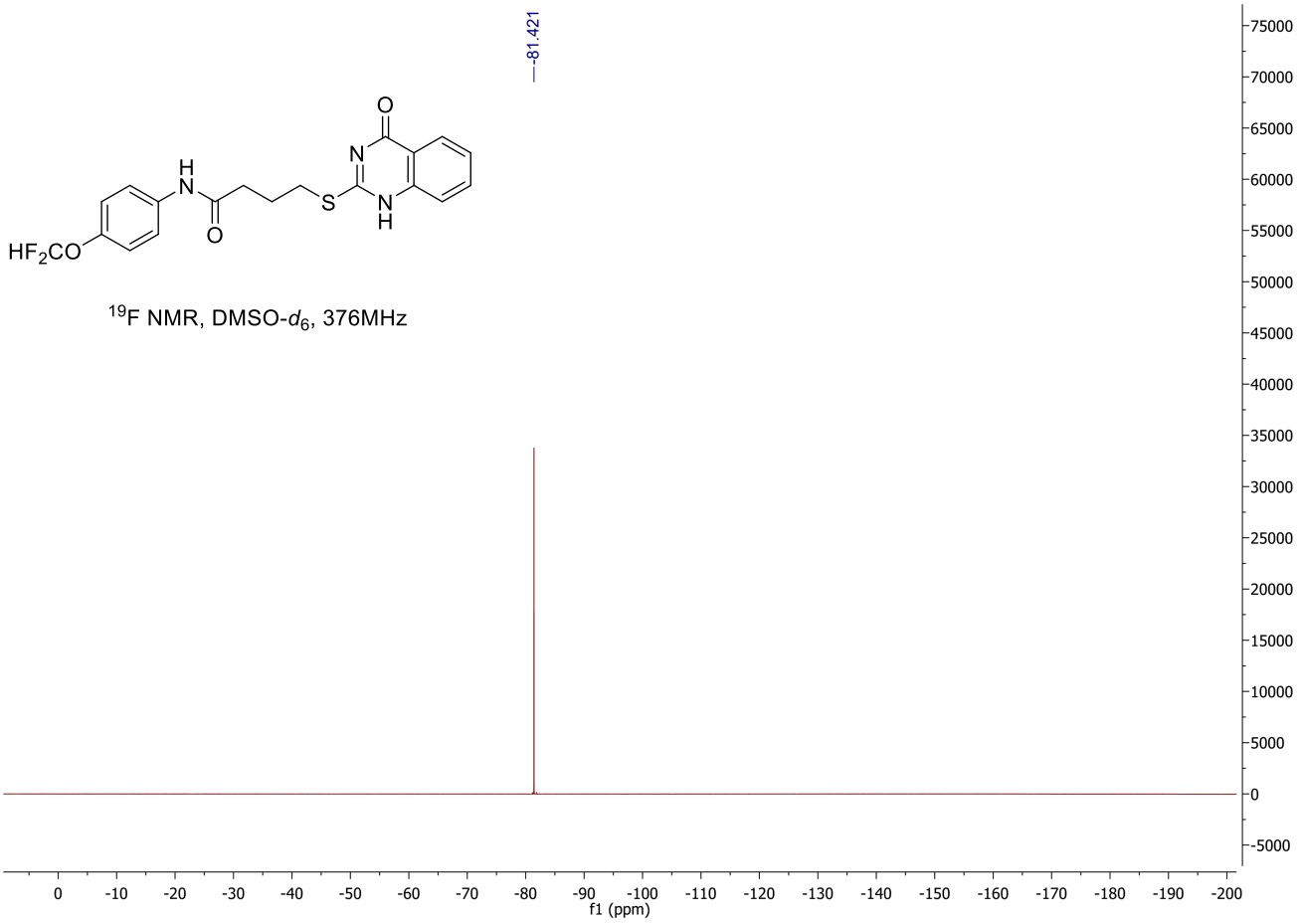

^{1}H NMR of compound 4b

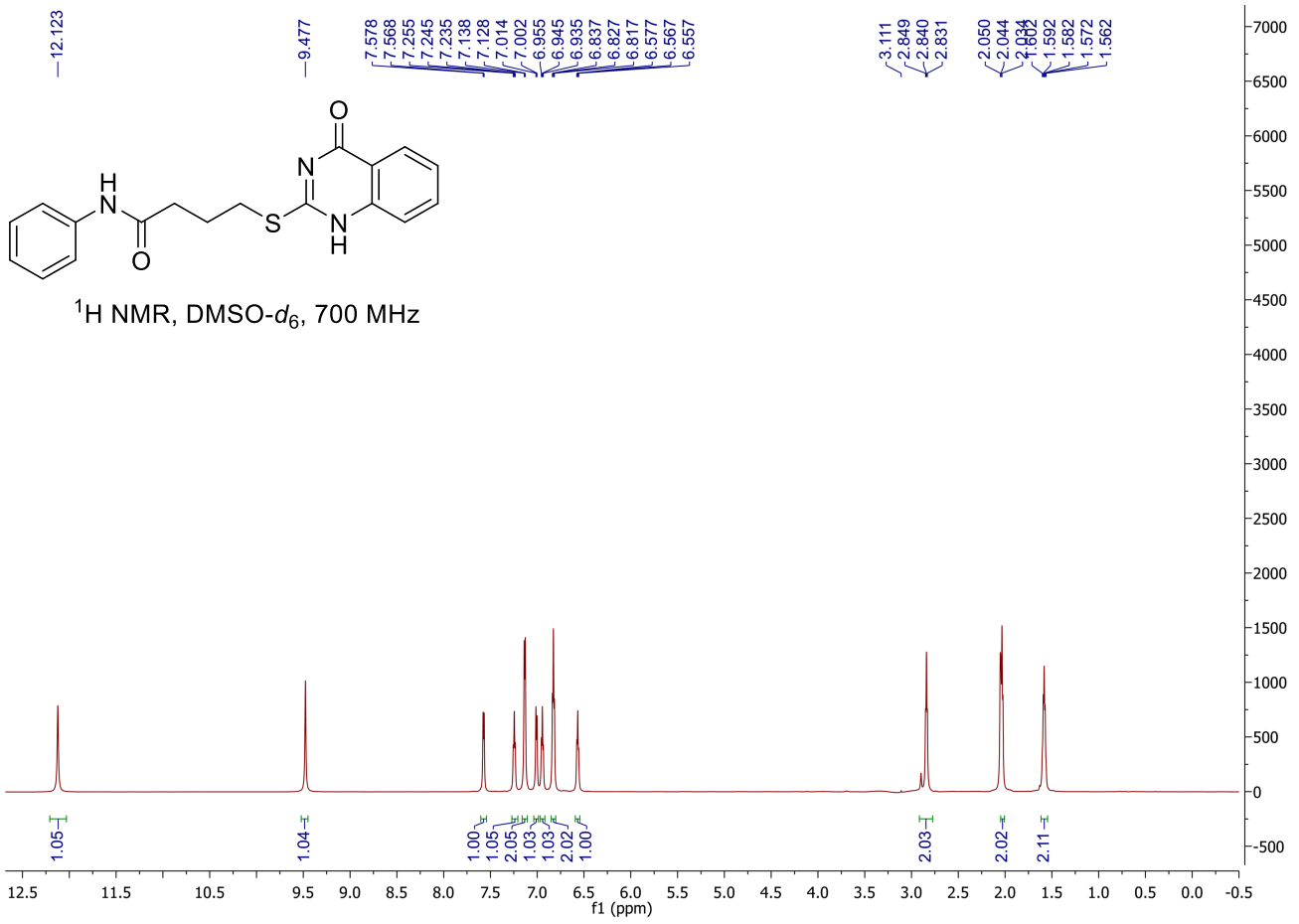

^{13}C NMR of compound 4b

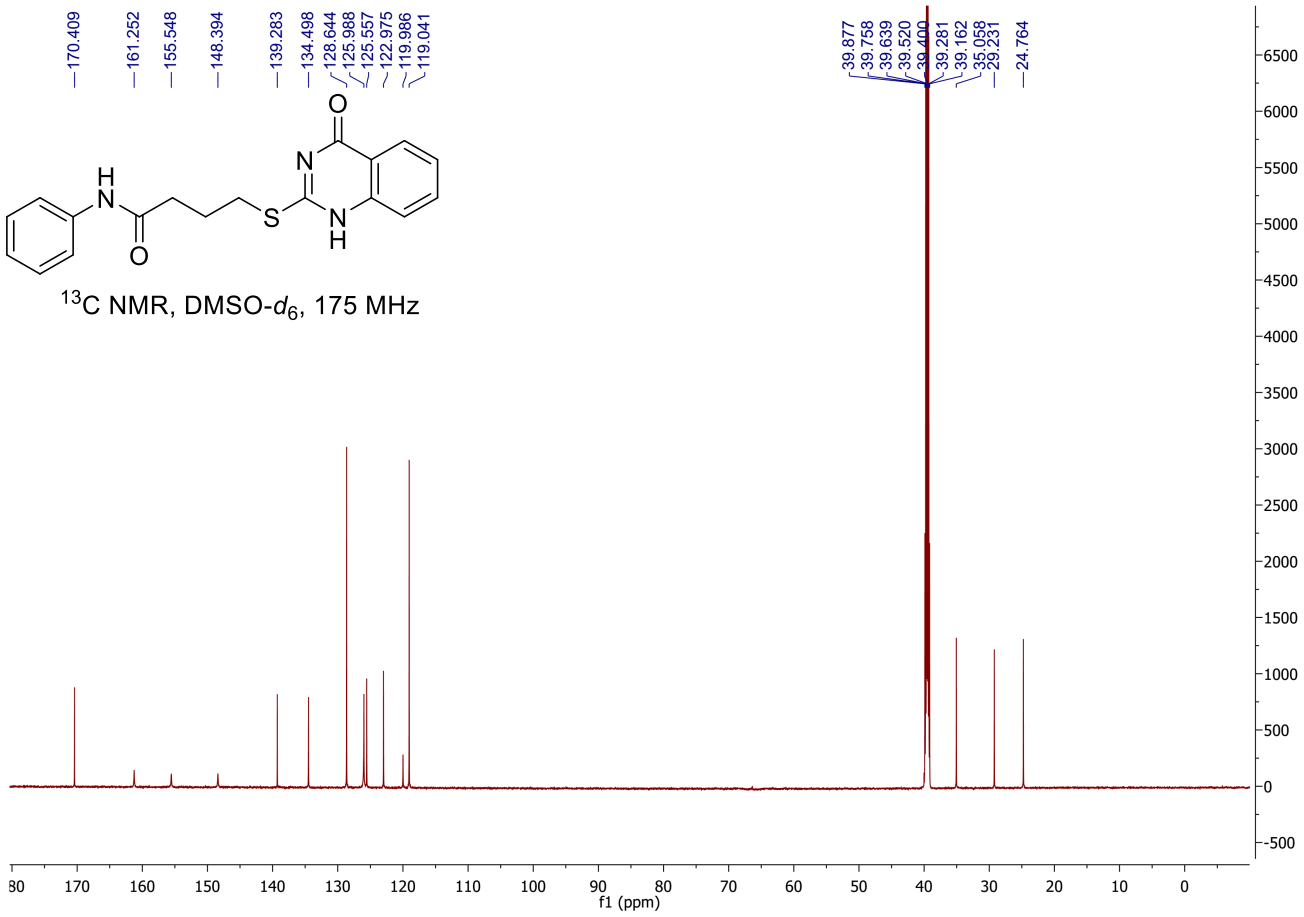

^{1}H NMR of compound 4c

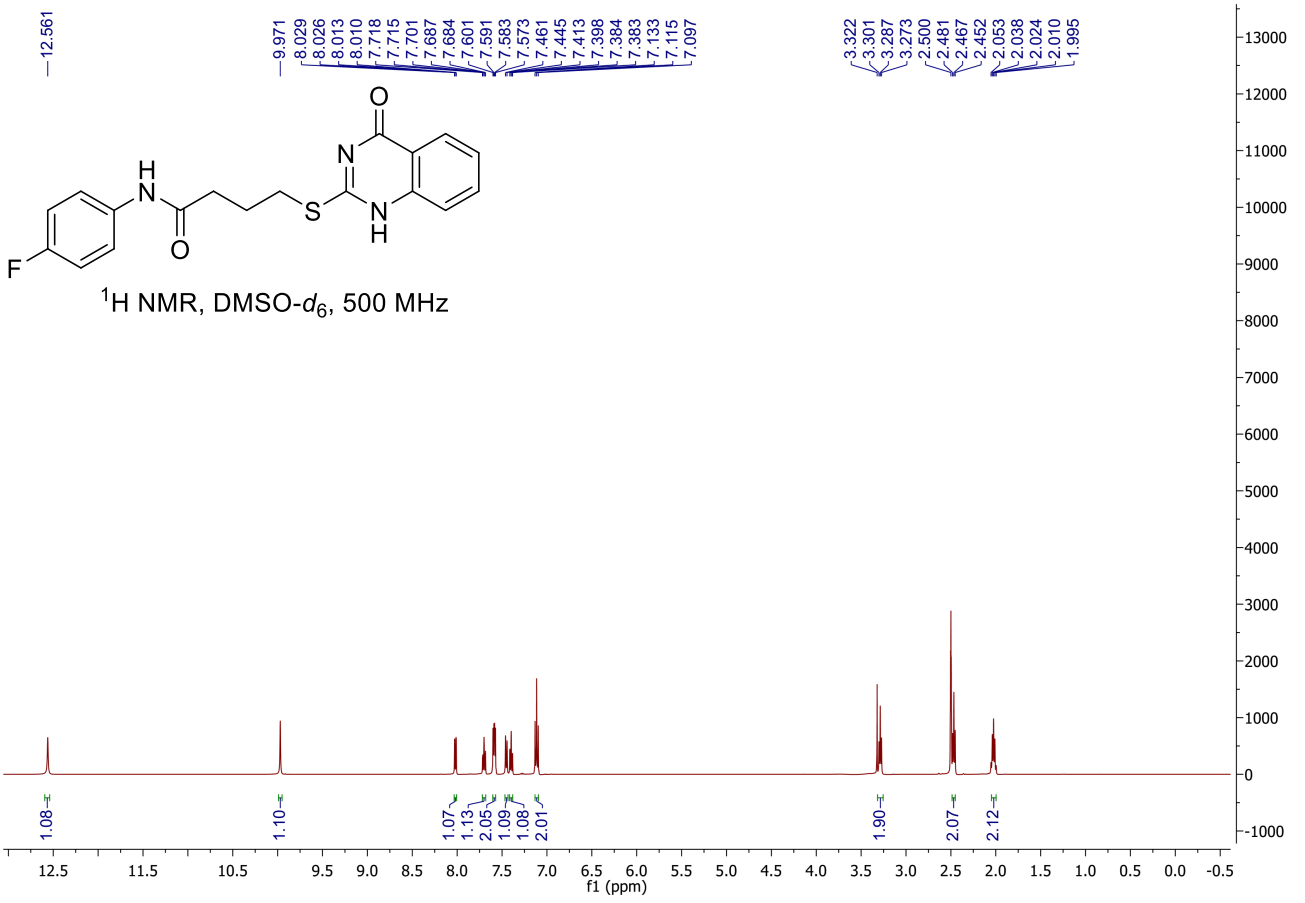

^{13}C NMR of compound 4c

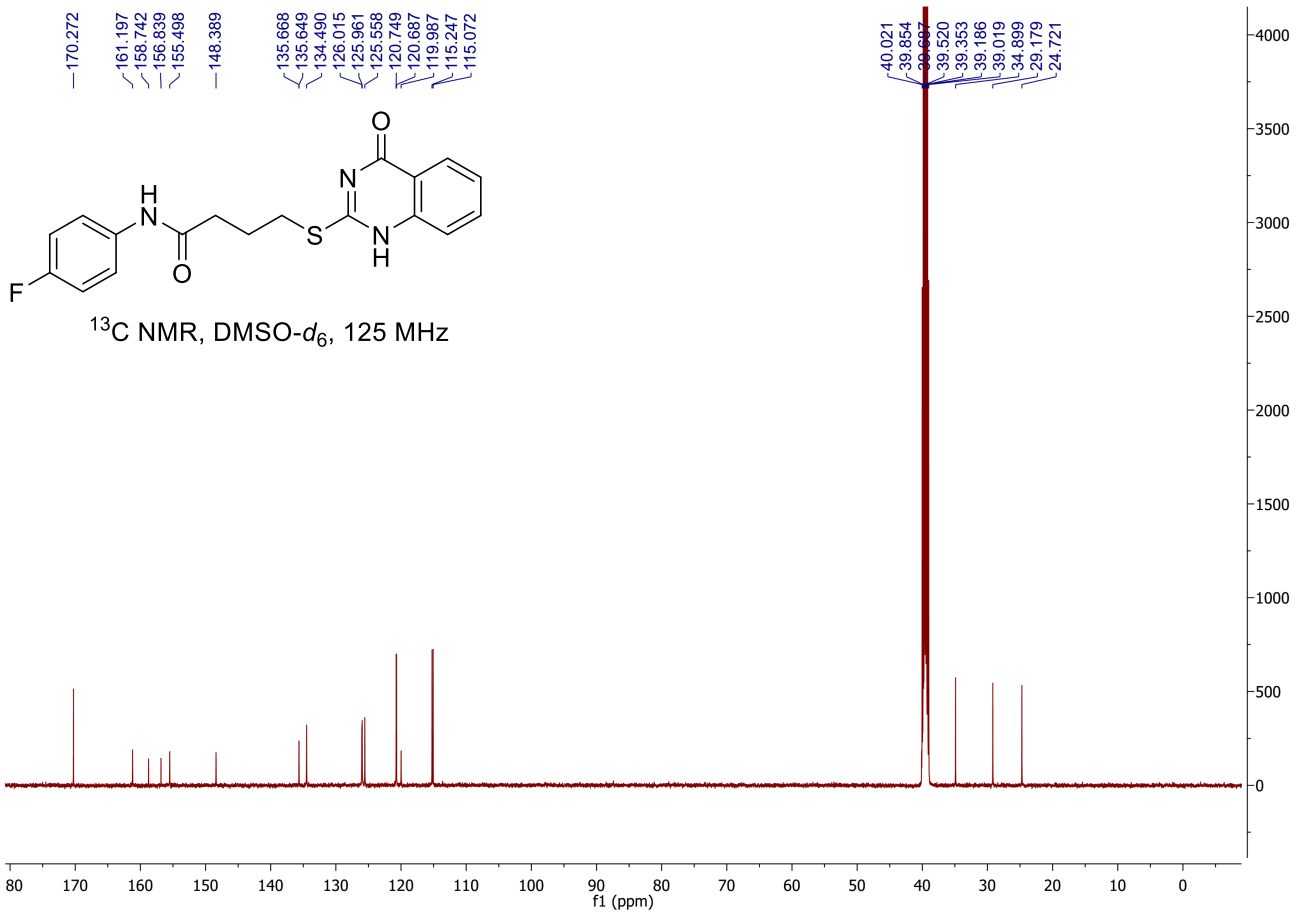

^{19}F NMR of compound 4c

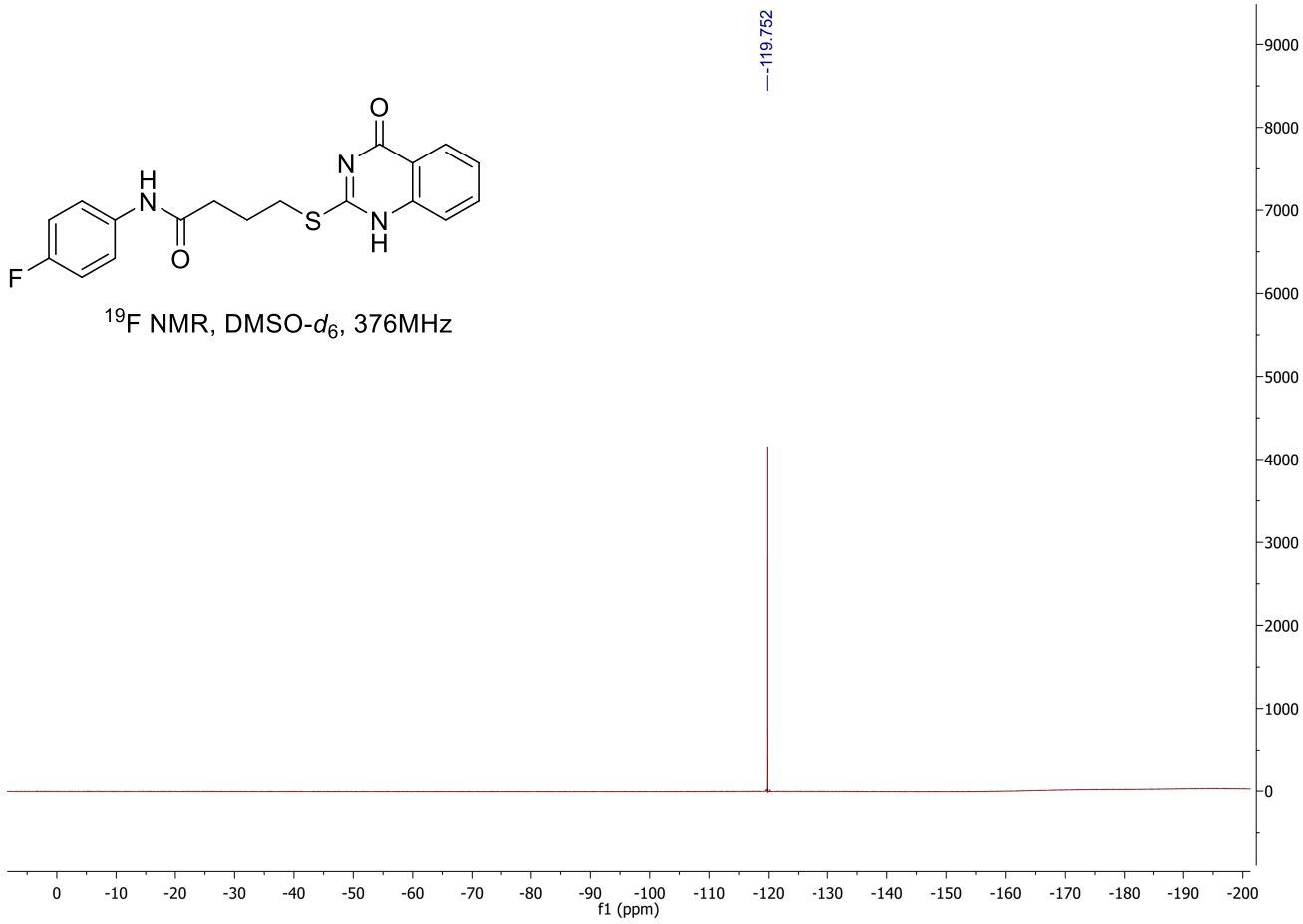

^{1}H NMR of compound 4d

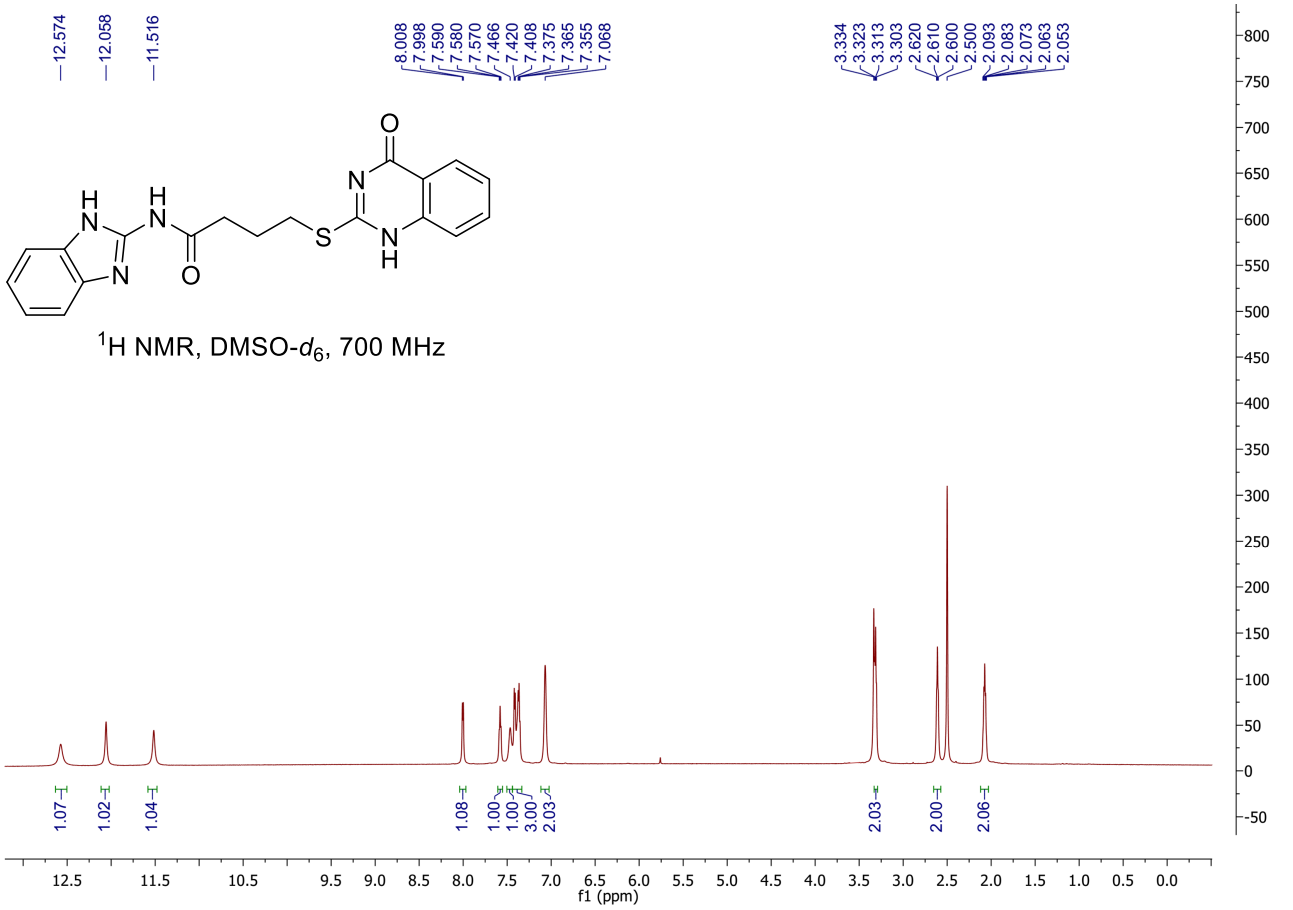

^{1}H NMR, DMSO-d_6, 700 MHz

^{13}C NMR of compound 4d

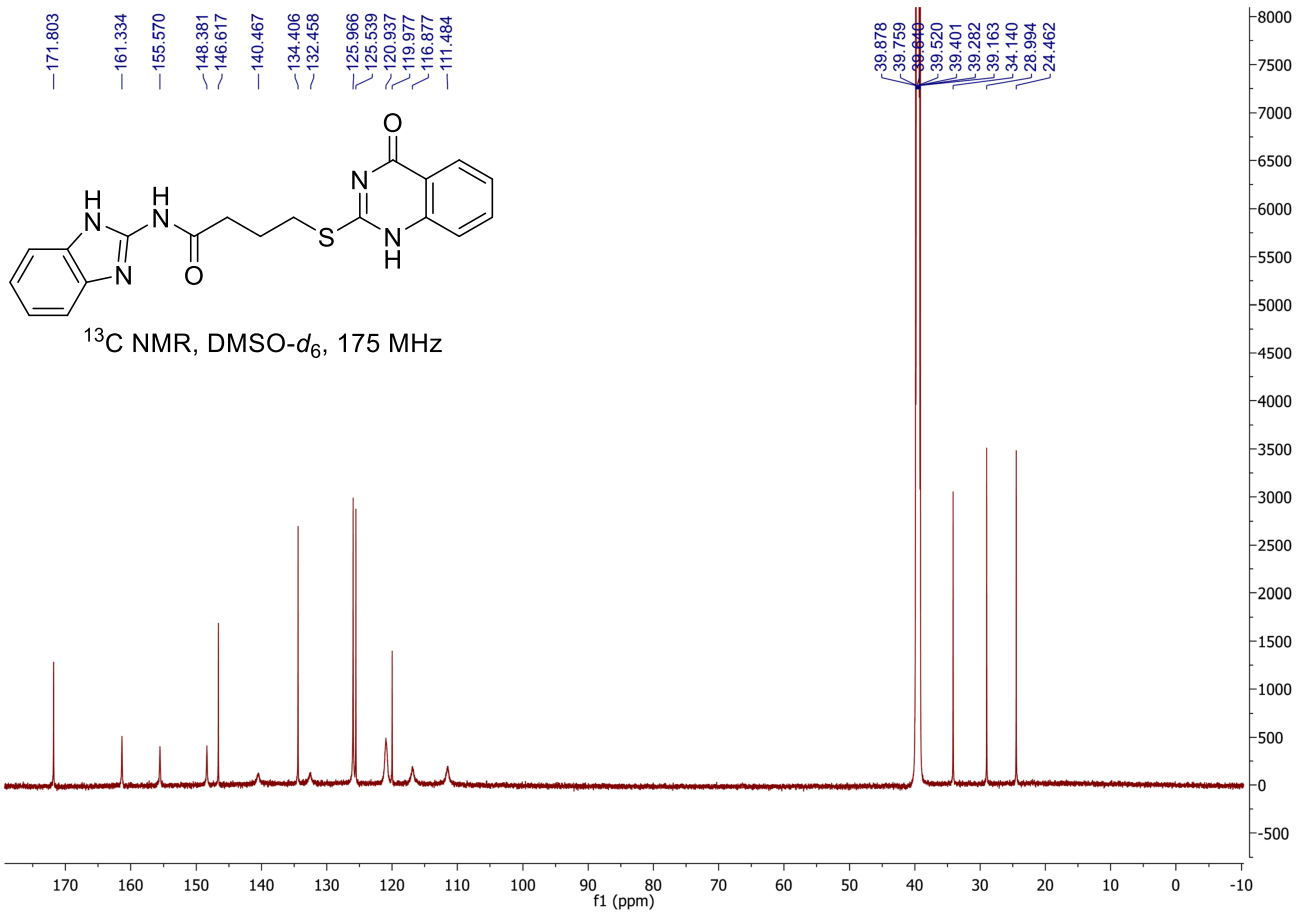

^{13}C NMR, DMSO-d_6, 175 MHz

^{1}H NMR of compound 4e

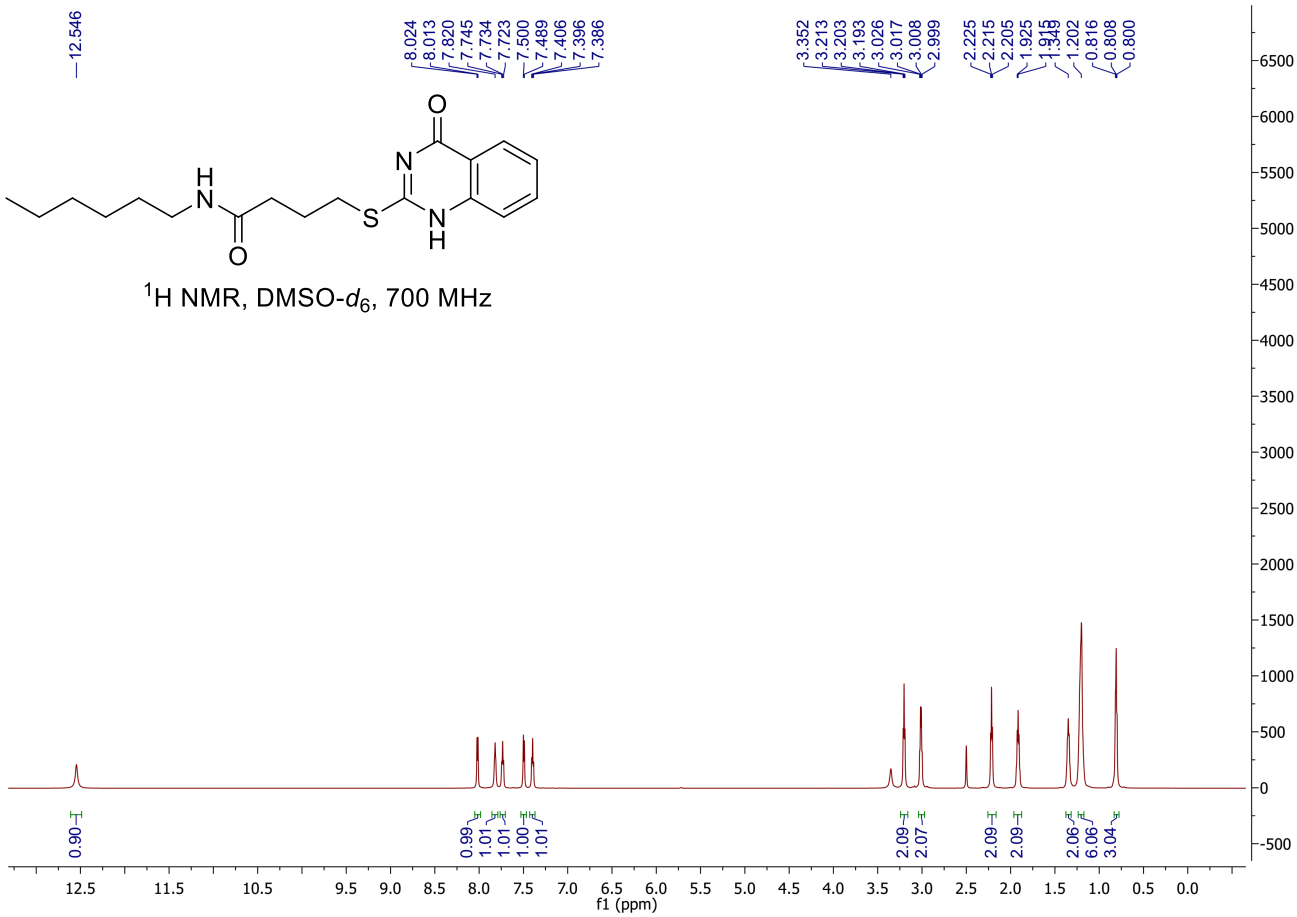

^{13}C NMR of compound 4e